



RESEARCH REPORT

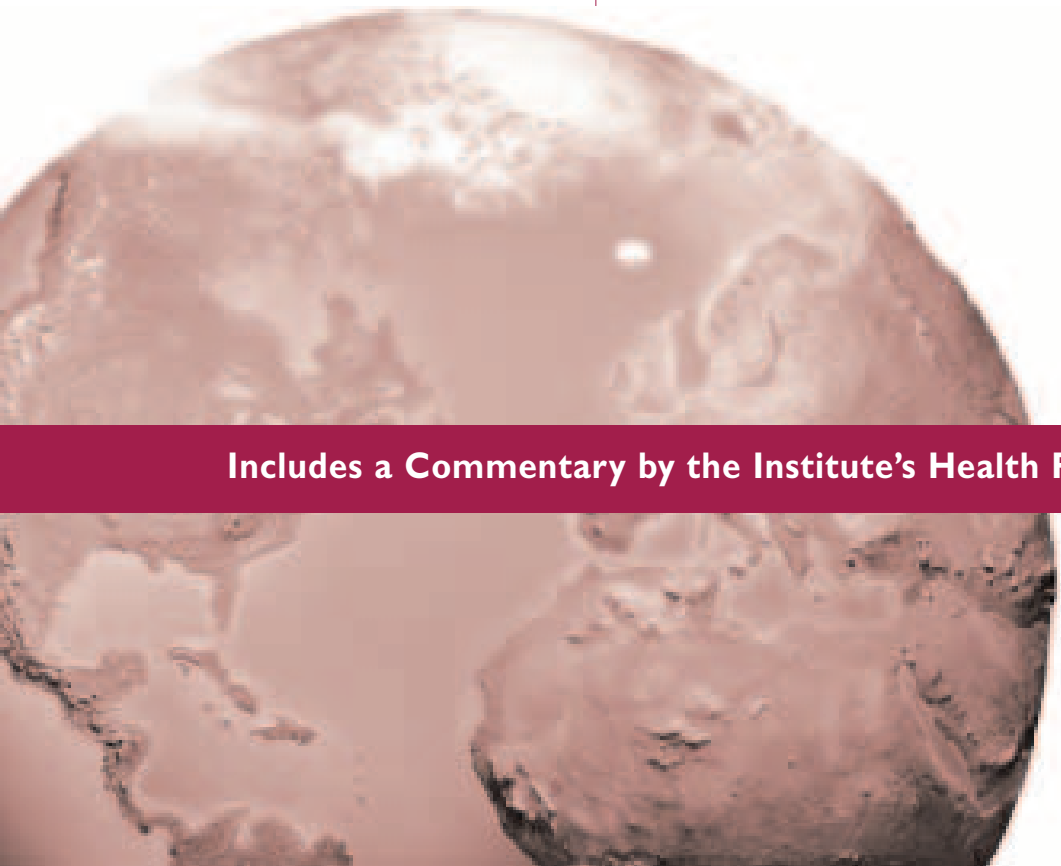
HEALTH
EFFECTS
INSTITUTE

Number 105
December 2001

**PREPRINT
VERSION**

Pathogenomic Mechanisms for Particulate Matter Induction of Acute Lung Injury and Inflammation in Mice

George D Leikauf, Susan A McDowell, Scott C Wesselkamper, Clay R Miller, William D Hardie, Kelly Gammon, Pratim P Biswas, Thomas R Korfhagen, Cindy J Bachurski, Jonathan S Wiest, Klaus Willeke, Eula Bingham, John E Leikauf, Bruce J Aronow, and Daniel R Prows



Includes a Commentary by the Institute's Health Review Committee



H E A L T H
E F F E C T S
I N S T I T U T E

The Health Effects Institute, established in 1980, is an independent and unbiased source of information on the health effects of motor vehicle emissions. HEI studies all major pollutants, including regulated pollutants (such as carbon monoxide, ozone, nitrogen dioxide, and particulate matter) and unregulated pollutants (such as diesel engine exhaust, methanol, and aldehydes). To date, HEI has supported more than 200 projects at institutions in North America and Europe and has published over 100 research reports.

Typically, HEI receives half its funds from the US Environmental Protection Agency and half from 28 manufacturers and marketers of motor vehicles and engines in the United States. Occasionally, funds from other public and private organizations either support special projects or provide resources for a portion of an HEI study. Regardless of funding sources, HEI exercises complete autonomy in setting its research priorities and in reaching its conclusions. An independent Board of Directors governs HEI. The Institute's Health Research and Health Review Committees serve complementary scientific purposes and draw distinguished scientists as members. The results of HEI-funded studies are made available as Research Reports, which contain both the Investigators' Report and the Review Committee's evaluation of the work's scientific quality and regulatory relevance.

HEI STATEMENT

Synopsis of Research Report 105

Genetic Differences in Induction of Acute Lung Injury and Inflammation in Mice

INTRODUCTION

Epidemiologic studies have indicated that small, short-term increases in the concentration of particulate matter (the complex and variable mixture of particles in the atmosphere) are associated with short-term increases in morbidity and mortality in the population. Some individuals appear to be more at risk than others. Genetic differences among individuals may be one reason for their differing responses to particulate matter, but this mechanism is currently not well understood. One likely explanation for genetically determined differences in susceptibility is that some genes are present in the population as slightly different variations or *alleles* of a basic gene; as a result, these genes are expressed at higher or lower levels in some individuals than others. Identifying such genetic polymorphisms in individuals with a particular disease may help to identify those who are at risk of developing the disease, or alternatively who may respond best to treatment. An initial step in understanding the role of genetic control in responses to particulate matter is to study responses in mice because multiple animals of identical genetic composition (strains) can be generated easily.

APPROACH

Dr George Leikauf and colleagues at the University of Cincinnati Medical Center hypothesized that the mouse response to high concentrations of inhaled nickel particles was under genetic control. Nickel has been shown to cause adverse effects at high concentrations in humans and in other species and is one of the important group of transition metals (which includes iron, copper, and vanadium) found in ambient air. The investigators sought to identify the genes involved in controlling the inflammatory and toxic effects of continuous exposure to nickel particles. The primary endpoint measured was an exposed mouse's survival time, or mean survival time for a group of

exposed mice, but other endpoints related to lung inflammation and injury were also measured. Leikauf and colleagues evaluated responses in different mouse strains; in first-generation offspring that resulted from crosses of different strains (F₁ mice); in backcross mice—that is, F₁ mice crossed with mice of one of the parental strains; and in mice expressing different levels of the human gene for transforming growth factor- α (TGF- α), a factor associated with responses to lung injury. In the latter case, the TGF- α gene had been inserted into the mouse genome as a transgene, generating a so-called transgenic mouse.

To identify the genes involved in the response to nickel, Leikauf and colleagues performed several complementary genetic and molecular analyses. The first was quantitative trait locus (QTL) analysis on backcross mice. This approach identified regions of individual chromosomes that were more or less closely associated with the trait or genetic characteristic of interest (namely, survival to nickel exposure). The second was haplotype analysis, which evaluated the contribution of one or several of these genetic regions to survival. The third was to use the novel microarray (or gene chip) technology; with this technique, the levels of expression of thousands of lung genes could be simultaneously evaluated during exposure to toxic levels of nickel.

RESULTS AND INTERPRETATION

Leikauf and colleagues showed convincingly that genetic factors play a key role in determining the acute response of mice to nickel toxicity. Initial experiments indicated that mice could be separated into susceptible or resistant strains according to how long they survived exposure to highly toxic levels of nickel sulfate particles (at the extremes were A strain [50 hours] and B6 strain [130 hours]). The A and B6 mouse strains showed a similar pattern of survival response to 2 other toxic agents, ozone and polytetrafluoroethylene, suggesting that similar mechanisms

may govern survival of exposure to all these agents. The investigators also found little correlation between some of the hallmark parameters of lung inflammation (increased protein level and percentage of neutrophils) and survival time in response to nickel exposure. This suggests that either lung inflammation per se or the inflammatory parameters evaluated in the study are not linked to survival.

Both QTL and haplotype analysis indicated that genes on 5 or 6 chromosomes, and a region on chromosome 6 in particular, were linked to survival to nickel exposure. The identified region on chromosome 6 contains genes for TGF- α , surfactant-associated protein B (SP-B), and aquaporin-1, genes that play a key protective role in lung responses to injury. Therefore, genes in this region are likely to be important in the response to nickel toxicity. Even after identifying a QTL or QTLs associated with a particular trait, however, definitively identifying the specific gene or genes responsible for the trait is a lengthy and complex task. The results of experiments in transgenic mice expressing human TGF- α also suggested the possible involvement of a mechanism involving both TGF- α and SP-B in survival: mice expressing the highest levels of the human TGF- α gene were the most resistant to nickel toxicity and showed the smallest decline in lung levels of SP-B.

Results from the microarray analysis indicated that a small fraction (about 200) of the more than 8,000 genes (examined in lung cells derived from either nickel-sensitive or nickel-resistant mice) changed their level of expression during exposure to nickel. The expression of some genes changed in both sensitive and resistant mice, whereas the expression of other genes changed only in sensitive mice or only in resistant mice. Genes whose levels of expression changed could be grouped functionally (for example, those involved in cellular metabolism and signal transduction) or temporally (those that showed steady or delayed increases or steady or delayed decreases in

expression levels). Some changes in expression were detected in genes of unknown function, indicating that some of these unidentified genes may be important in the response to nickel toxicity. The investigators enhanced the credibility of the findings from the microarray analysis by showing that selected genes with changed expression level (when analyzed by other methods) had similar patterns of change.

Generally, though, results from the microarray analysis could not be easily compared with those from the other genetic and molecular approaches because many genes of interest in inflammatory and injury responses were not present on the gene chip used. The use of microarrays has other limitations: It does not provide information about levels of proteins so it is not clear how detected changes in gene expression correlate with protein levels in the cell. In addition, the technique cannot distinguish in which cells, of the many found in the lung, gene expression changes are occurring. At least some of the gene expression changes detected at later times during the response to nickel probably occurred in cells that migrated into the lung as a consequence of the inflammatory response, rather than in lung cells per se.

Overall, Leikauf and colleagues have shown that mice respond to high toxic levels of inhaled nickel particles by altering gene expression. They have also preliminarily identified a small number of genes involved in susceptibility in this response. Similar genes may be involved in human responses to nickel particles in high concentrations. Additional studies are required to determine whether similar genes are involved in responses to low, ambient levels of nickel and other airborne pollutants. Further characterization of the genes involved in these responses will assist in efforts to understand the mechanisms by which pollutants act, characterize similarities and differences in gene expression among individuals' responses to a stimulus, and ultimately identify individuals who may be particularly susceptible to pollutant effects.



CONTENTS

Research Report 105

HEALTH
EFFECTS
INSTITUTE

Pathogenomic Mechanisms for Particulate Matter Induction of Acute Lung Injury and Inflammation in Mice

George D Leikauf, Susan A McDowell, Scott C Wesselkamper, Clay R Miller, William D Hardie, Kelly Gammon, Pratim P Biswas, Thomas R Korfhagen, Cindy J Bachurski, Jonathan S Wiest, Klaus Willeke, Eula Bingham, John E Leikauf, Bruce J Aronow, and Daniel R Prows

College of Medicine, University of Cincinnati, and Children's Hospital Medical Center, Cincinnati, Ohio

HEI STATEMENT

This Statement is a nontechnical summary of the Investigators' Report and the Health Review Committee's Commentary.

PREFACE

Background	1	Continuing Research	3
HEI's Particulate Matter Research Program	2	References	3

INVESTIGATORS' REPORT

When an HEI-funded study is completed, the investigators submit a final report. The Investigators' Report is first examined by three outside technical reviewers and a biostatistician. The Report and the reviewers' comments are then evaluated by members of the HEI Health Review Committee, who had no role in selecting or managing the project. During the review process, the investigators have an opportunity to exchange comments with the Review Committee and, if necessary, revise the report.

Abstract	5	Haplotype Analysis.	12
Introduction.	5	Nickel Retention	12
Specific Aims	5	Statistical Analyses and Quality Assurance.	13
Methods	7	Results	13
Experimental Design	7	Strain Phenotype Pattern	13
Atmosphere Generation and Characterization	8	Mode of Inheritance	13
High-Temperature Furnace System	9	Pulmonary Histopathology Induced by Nickel Sulfate.	14
Strain Selection and Tissue Preparation	9	Dose-Response Relationship	14
Bronchoalveolar Lavage	10	Pulmonary Protein and Leukocyte Infiltration in Lavage Fluid.	14
RNA Preparation.	10	Gene Expression in Lungs of B6 Mice	17
Fluorescent Labeling of Probes	10	Quantitative Trait Locus Analysis	20
Microarray Preparation.	10	Haplotype Analysis.	26
Hybridization.	10	Comparison of Microarray and Genomewide Scan	26
Temporal Clustering	10	Transgenic Mice	31
Northern Blotting and S1 Nuclease Protection Assays	11	Discussion	40
Phenotyping, DNA Preparation, and Genotyping	11	Strain Phenotype Patterns	40
Locus Number Estimation	12	Evaluation of Dose-Response Relations	40
Quantitative Trait Locus Mapping and Linkage Analysis	12		

Continued

Research Report 105

Relation Between Inflammation and Acute Lung Injury	41	Functional Genomic Evaluation of Positional Candidate Genes	45
Initial Evaluation of Particle Size and Chemical Speciation	41	Relation Between Lung Remodeling and Increased Susceptibility	46
Altered Regulation of Gene Expression in B6 Mice	42	Relation Between TGF- α and Surfactant-Associated Proteins	47
Nickel-Induced Acute Lung Injury—A Complex Quantitative Trait	43	Summary	48
Comparative Microarray of A and B6 Mice During Nickel Exposure	44	Acknowledgments	48
Combining Results of cDNA Microarrays and Quantitative Trait Locus Analyses	45	References	48
		About the Authors	56
		Other Publications Resulting from This Research	57
		Abbreviations and Other Terms	57

COMMENTARY Health Review Committee

The Commentary about the Investigators' Report is prepared by the HEI Health Review Committee and staff. Its purpose is to place the study into a broader scientific context, to point out its strengths and limitations, and to discuss remaining uncertainties and implications of the findings for public health.

Introduction	59	Microarray Analysis	65
Scientific Background	59	Genetic Determinants of Acute Lung Injury	65
Technical Evaluation	61	Functional Evaluation of Candidate Genes	66
Aims and Objectives	61	Discussion	66
Methods	62	Summary and Conclusions	69
Results	64	Acknowledgments	69
Genetic Basis of Susceptibility to Toxicants	64	References	70
Effects of Particle Size and Solubility	65		

RELATED HEI PUBLICATIONS

Publishing History: This document was posted as a preprint on www.healtheffects.org and then finalized for print.

Citation for whole report:

GD Leikauf, SA McDowell, SC Wesselkamper, CR Miller, WD Hardie, K Gammon, PP Biswas, TR Korfhagen, CJ Bachurski, JS Wiest, K Willeke, E Bingham, JE Leikauf, BJ Aronow, and DR Prows. 2001. Pathogenomic Mechanisms for Particulate Matter Induction of Acute Lung Injury and Inflammation in Mice. Research Report 105. Health Effects Institute, Boston MA.

When specifying a section of this report, cite it as a chapter of this document.

PREFACE

In 1994, HEI initiated a research program to investigate the complex issues associated with the health effects of exposure to particulate matter (PM*) in the air. This program was developed in response to growing concern about the potential public health significance of reported associations between daily fluctuations in levels of PM and changes in daily morbidity and mortality in time-series epidemiology studies. These results were questioned for a variety of reasons, including the lack of support from experimental studies and the lack of a mechanism to explain how such effects would occur. To address these issues, HEI undertook research initiatives in 1994, 1996, and 1998.

In 1994, the Particle Epidemiology Evaluation Project (Samet et al 1995, 1997) evaluated six of the time-series epidemiology studies that had reported effects of PM on mortality, and a program of epidemiology and toxicology studies were funded that aimed at understanding how PM might cause toxicity and what factors might affect susceptibility (RFA 94-2, "Particulate Air Pollution and Daily Mortality: Identification of Populations at Risk and Underlying Mechanisms"). In 1996, HEI issued RFA 96-1, "Mechanisms of Particle Toxicity: Fate and Bioreactivity of Particle-Associated Compounds", which sought studies that would improve our understanding of toxicologically relevant characteristics of ambient particles. In 1998, HEI issued RFA 98-1, "Characterization of Exposure to and Health Effects of Particulate Matter", which targeted a broad and ambitious set of research goals relating to both exposure assessment and health effects. In all, HEI has issued five requests for research on PM and funded 34 studies or reanalyses over the last 5 years.

This Preface provides general regulatory and scientific background information relevant to studies funded from RFA 98-1, including the study by Dr George Leikauf that is described in the accompanying Report and Commentary. This is one of 14 studies funded from RFA 98-1. The "HEI Program Summary: Research on Particulate Matter" (Health Effects Institute 1999) provides information on all PM studies funded since 1996.

BACKGROUND

Particulate matter is the term used to define a complex mixture of anthropogenic and naturally occurring airborne

particles. In urban environments, these particles derive mainly from combustion, including mobile sources such as motor vehicles and stationary sources such as power plants. The size, chemical composition, and other physical and biologic properties of PM depend on the sources of the particles and the changes the particles undergo in the atmosphere. The most commonly used descriptor of particles is size measured as *aerodynamic diameter*. On the basis of this parameter, ambient particles tend to fall into three size classes (often defined as modes): ultrafine or nuclei mode (particles less than 0.1 μm in diameter); fine or accumulation mode (particles between 0.1 and 2.5 μm in diameter), and coarse (particles larger than 2.5 μm in diameter). Fine and ultrafine particles are found primarily in emissions from combustion processes, whereas coarse particles are mostly generated by mechanical processes from a variety of noncombustion sources. Generally, the ultrafine and fine fractions are composed of carbonaceous material, metals, sulfate, nitrate, and ammonium ions. The coarse fraction consists of insoluble minerals and biologic aerosols, with smaller contributions from primary and secondary aerosols and sea salts (US Environmental Protection Agency [EPA] 1996).

A number of early epidemiologic studies indicated that human exposure to high concentrations of PM, such as London fog, had deleterious effects (such as an increased number of deaths) particularly in children, the elderly, and those with cardiopulmonary conditions (Firket 1931; Logan 1953; Ciocco and Thompson 1961; Gore and Shaddick 1968). Because of this apparent relation to increased mortality, the EPA has regulated the levels of ambient PM since 1971, when the Clean Air Act was first promulgated. This act authorized the EPA to set National Ambient Air Quality Standards (NAAQs) for a number of potentially harmful air pollutants (including PM) in order to protect the health of the population, particularly those people thought to be sensitive to the effects of pollution.

The first NAAQs for PM were based on controlling total suspended PM or particles up to 40 μm in diameter. In 1978, the standards were revised to regulate inhalable particles, or particles that can deposit in the respiratory tract and therefore have greater potential for causing adverse health effects. These particles measure 10 μm or smaller in aerodynamic diameter (PM_{10}). More recent epidemiologic studies, published in the early 1990s, indicated a relatively consistent association between short-term small increases in PM levels and increases in both morbidity and mortality from respiratory and cardiovascular diseases (reviewed by the

*A list of abbreviations and other terms appears at the end of the Investigators' Report.

Preface Table 1. Current National Ambient Air Quality Standards for Particulate Matter (Set in 1997)

Time Period	PM ₁₀	PM _{2.5}
Daily	150 µg/m ³	65 µg/m ³
Annual	50 µg/m ³	15 µg/m ³

Committee of the Environmental and Occupational Health Assembly, American Thoracic Society [Bascom et al 1996]).

Some studies also suggested that long-term exposure to low levels of PM is associated with adverse effects (Dockery et al 1993; Pope et al 1995). These latter studies also pointed to a possible role of fine particles (less than 2.5 µm in aerodynamic diameter [PM_{2.5}]). In 1997, the EPA decided that the evidence for the effects of fine particles was sufficient to promulgate a PM_{2.5} standard while retaining the PM₁₀ standard (US Environmental Protection Agency 1997) (see Preface Table 1). The next review of the PM NAAQS is scheduled to be completed by 2002.

HEI's PARTICULATE MATTER RESEARCH PROGRAM

The wealth of epidemiologic data published in the early 1990s suggested an association between PM and health effects, but aspects of these findings were not well understood. Problems involved uncertainties in the exposure estimates, confounding by weather or other factors, the role of copollutants, and the mechanisms by which particles may cause effects. Moreover, although the epidemiologic findings were consistent across different communities exposed to distinct mixtures and levels of pollutants, they were not well supported by either human exposure chamber studies or animal inhalation studies aimed at delineating the pathologic changes that might result in death. Failure of the experimental studies to provide support for the epidemiologic findings was attributed to insufficient statistical power, use of particles not representative of ambient particles, or use of animals not representative of the individuals susceptible to increased mortality.

By the mid 1990s, it became apparent that the research to advance our understanding of the association between exposure to particles and daily mortality found in the epidemiologic studies needed to focus on identifying (1) susceptible populations, (2) mechanisms by which particles may lead to increased mortality, and (3) characteristics of the particles responsible for the effects. It was recognized that both epidemiologic and experimental studies would be required. The HEI program from RFA-94 was aimed at

addressing these research needs. In 1994, HEI also initiated the Particle Epidemiology Evaluation Project to address the validity and replicability of key epidemiologic studies (Samet et al 1995, 1997). Out of that project evolved the National Morbidity, Mortality, and Air Pollution Study to continue the epidemiologic evaluation in a large number of cities across the US with varying levels of PM and other air pollutants (Samet et al 2000a,b). Subsequently, HEI funded studies under RFA 96-1 that would use fine and ultrafine particles to test specific hypotheses related to the role of particle constituents in PM toxicity.

With increased financial support from the EPA and industry, in January 1998 HEI requested applications targeting both exposure assessments and health effects. HEI held a workshop at the Offices of the National Research Council that brought together scientists and representatives of the EPA and the motor vehicle and oil industries to discuss research needs. Out of this discussion, RFA 98-1, "Characterization of Exposure to and Health Effects of Particulate Matter", was developed and issued. The exposure objectives included (1) characterizing personal exposure to particles in different indoor and outdoor microenvironments and in geographic locations that differ in the types and sources of particles, topography, and climate; and (2) improving particle characterization to increase the accuracy of exposure estimates in epidemiologic studies. The health effects objectives included (1) characterizing potential pathophysiologic effects caused by PM in sensitive subjects; (2) defining the relation between particle characteristics and dose, distribution, and persistence of particles in the respiratory tract; (3) identifying the kinds of particles or particle attributes that may cause toxicity; (4) investigating the diseases or conditions that affect sensitivity; and (5) delineating how copollutants affect or contribute to the physiologic response to particles. From this RFA, HEI funded a comprehensive set of exposure assessment and health effects studies.

Three exposure assessment studies were designed to investigate personal exposure to PM in potentially sensitive population subgroups in several US and European cities with diverse climatic and geographic features. These studies focused on (1) characterizing indoor concentrations of and personal exposure to PM_{2.5} for subjects in two European cities (Bert Brunekreef of Wageningen/Utrecht University); (2) characterizing exposure to PM_{2.5}, ozone, nitrogen dioxide, carbon monoxide, and sulfur dioxide in children, healthy seniors, and subjects with chronic obstructive pulmonary disease (Petros Koutrakis of Harvard School of Public Health); and (3) assessing personal exposure to PM_{2.5} and characterizing PM in terms of mass, functional groups, trace metals, polynuclear aromatic hydrocarbons, and elemental

and organic carbon (Barbara Turpin of Environmental and Occupational Health Sciences Institute). A fourth study aimed to validate a newly developed method for measuring the acidic component of ultrafine particles or PM_{0.1} (Beverly Cohen of New York University Medical Center).

Four human experimental and epidemiologic studies focused on several potentially important endpoints that may help elucidate the mechanisms of particle toxicity. The epidemiologic studies investigated the relation between PM levels and specific cardiac events: arrhythmias (Douglas Dockery of Harvard School of Public Health) and nonfatal myocardial infarctions (Annette Peters of GSF-Forschungszentrum für Umwelt und Gesundheit). The experimental studies investigated cardiovascular and pulmonary effects in healthy and asthmatic subjects exposed to ultrafine carbon particles (Mark Frampton of University of Rochester) and concentrated ambient particles (CAPs) from Los Angeles air (Henry Gong of Los Amigos Research and Education Institute).

Six animal studies addressed a number of hypotheses about susceptibility to and toxicity of particulate matter components using different health endpoints, animal models, and types of particles. These studies investigated (1) whether coexposure to CAPs from Boston air and ozone causes a synergistic amplification of asthmatic airway inflammation and hyperresponsiveness in juvenile mice with hypersensitive airways (Lester Kobzik of Harvard School of Public Health); (2) the genetic determinants of susceptibility to morbidity and mortality from nickel particles in inbred mouse strains (the study presented here; George Leikauf of University of Cincinnati); (3) whether exposing healthy rats to CAPs from New York City air causes changes in blood coagulation parameters that may be involved in thrombotic effects (Christine Nadziejko of New York University Medical Center); (4) the effects of particle size and composition on the lung inflammatory and histopathologic responses in old rats and rats with preexisting inflammation (Fletcher Hahn of Lovelace Respiratory Research Institute); (5) whether exposure to resuspended particles from Ottawa air samples causes changes in heart function and vascular parameters in adult rats (Renaud Vincent of Health Canada); and (6) the effects of CAPs from Detroit air on the airway epithelium in rats with preexisting hypersecretory airway disease (Jack Harkema of Michigan State University).

CONTINUING RESEARCH

Many of the key questions identified in the early 1990s are still relevant and many research projects continue to

address them. The research strategies have evolved, however, as results from completed studies have provided insights into which animal models and which endpoints may be the most helpful to evaluate. In addition, advances in exposure assessment and statistical methods have pointed to new approaches for conducting epidemiologic studies. In the past two years HEI has published several reports from its PM research program (Checkoway et al 2000; Gerde et al 2001; Godleski et al 2000; Goldberg et al 2000; Gordon et al 2000; Krewski et al 2000a,b; Lippmann et al 2000; Oberdörster et al 2000; Samet et al 2000a,b; Wichmann et al 2000). Many additional PM studies that are currently under review will be published in 2001 and 2002.

REFERENCES

- Bascom R, Bromberg PA, Costa DA, Devlin R, Dockery DW, Frampton MW, Lambert W, Samet JM, Speizer FE, Utell M. 1996. Health effects of outdoor air pollution. Part 1. *Am J Respir Crit Care Med* 153:3–50.
- Checkoway H, Levy D, Sheppard L, Kaufman J, Koenig J, Siscovick D. 2000. A Case-Crossover Analysis of Fine Particulate Matter Air Pollution and Out-of-Hospital Sudden Cardiac Arrest. Research Report 99. Health Effects Institute, Cambridge MA.
- Ciocco A, Thompson DJ. 1961. A follow-up on Donora ten years after: Methodology and findings. *Am J Pub Health* 15:155–164.
- Dockery DW, Pope CA III, Xu X, Spengler JD, Ware JH, Fay ME, Ferris BG, Speizer FE. 1993. An association between air pollution and mortality in six US cities. *N Engl J Med* 329:1753–1759.
- Firket J. 1931. The cause of the symptoms found in the Meuse Valley during the fog of December 1930. *Bull Acad R Med Belg* 11:683–741.
- Gerde P, Muggenburg BA, Lundborg M, Tesfaigzi Y, Dahl AR. 2001. Respiratory Epithelial Penetration and Clearance of Particle-Borne Benzo[a]pyrene. Research Report 101. Health Effects Institute, Cambridge MA.
- Godleski JJ, Verrier RL, Koutrakis P, Catalano P. 2000. Mechanisms of Morbidity and Mortality from Exposure to Ambient Air Particles. Research Report 91. Health Effects Institute, Cambridge MA.
- Goldberg MS, Bailar JC III, Burnett RT, Brook JR, Tamblyn R, Bonvalot Y, Ernst P, Flegel KM, Singh RK, Valois M-F. 2000. Identifying Subgroups of the General Population That May Be Susceptible to Short-Term Increases in Particulate Air

Pollution: A Time-Series Study in Montreal, Quebec. Research Report 97. Health Effects Institute, Cambridge MA.

Gordon T, Nadziejko C, Chen LC, Schlesinger R. 2000. Effects of Concentrated Ambient Particles in Rats and Hamsters: An Exploratory Study. Research Report 93. Health Effects Institute, Cambridge MA.

Gore AT, Shaddick CW. 1968. Atmospheric pollution and mortality in the county of London. *Br J Prev Soc Med* 12:104–113.

Health Effects Institute. 1999. Research on Particulate Matter (HEI Research Program Summary). Health Effects Institute, Cambridge MA.

Krewski D, Burnett RT, Goldberg MS, Hoover K, Siemiatycki J, Abrahamowicz M, White WH. 2000a. Part II: Sensitivity analyses. In: Reanalysis of the Harvard Six Cities Study and the American Cancer Society Study of Particulate Air Pollution and Mortality. A Special Report of the Institute's Particle Epidemiology Reanalysis Project. Health Effects Institute, Cambridge MA.

Krewski D, Burnett RT, Goldberg MS, Hoover K, Siemiatycki J, Jerrett M, Abrahamowicz M, White WH. 2000b. Part I: Replication and validation. In: Reanalysis of the Harvard Six Cities Study and the American Cancer Society Study of Particulate Air Pollution and Mortality. A Special Report of the Institute's Particle Epidemiology Reanalysis Project. Health Effects Institute, Cambridge MA.

Lippmann M, Ito K, Nádas A, Burnett RT. 2000. Association of Particulate Matter Components with Daily Mortality and Morbidity in Urban Populations. Research Report 95. Health Effects Institute, Cambridge MA.

Logan WPD. 1953. Mortality in London fog incident. *Lancet* i:336–338.

Oberdörster G, Finkelstein JN, Johnston C, Gelein R, Cox C, Baggs R, Elder ACP. 2000. Acute Pulmonary Effects of Ultrafine Particles in Rats and Mice. Research Report 96. Health Effects Institute, Cambridge MA.

Pope CA III, Thun MJ, Namboodiri MM, Dockery DW, Evans JS, Speizer FE, Heath CW. 1995. Particulate air pollution as a predictor of mortality in a prospective study of US adults. *Am J Respir Crit Care Med* 151:669–674.

Samet JM, Dominici F, Zeger SL, Schwartz J, Dockery DW. 2000a. The National Morbidity, Mortality, and Air Pollution Study. Part I: Methods and Methodological Issues. Research Report 94. Health Effects Institute, Cambridge MA.

Samet JM, Zeger SL, Birhane K. 1995. The association of mortality and particulate air pollution. In: Particulate Air Pollution and Daily Mortality: Replication and Validation of Selected Studies, The Phase I.A Report of the Particle Epidemiology Evaluation Project. Health Effects Institute, Cambridge MA.

Samet JM, Zeger SL, Dominici F, Curriero F, Coursac I, Dockery DW, Schwartz J, Zanobetti A. 2000b. The National Morbidity, Mortality, and Air Pollution Study. Part II: Morbidity, Mortality, and Air Pollution in the United States. Research Report 94. Health Effects Institute, Cambridge MA.

Samet JM, Zeger SL, Kelsall JE, Xu J, Kalkstein LS. 1997. Air pollution, weather, and mortality in Philadelphia. In: Particulate Air Pollution and Daily Mortality: Analysis of the Effects of Weather and Multiple Air Pollutants, The Phase I.B Report of the Particle Epidemiology Evaluation Project. Health Effects Institute, Cambridge MA.

US Environmental Protection Agency. 1996. Air Quality Criteria for Particulate Matter. Vol I. Document EPA/600/P-95/001. Office of Research and Development, Washington DC.

US Environmental Protection Agency. 1997. Revisions to the National Ambient Air Quality Standards for particulate matter: Final rule. *Fed Regist* 52:24634–24669.

Wichmann H-E, Spix C, Tuch T, Wölke G, Peters A, Heinrich J, Kreyling WG, Heyder J. 2000. Daily Mortality and Fine and Ultrafine Particles in Erfurt, Germany. Part I: Role of Particle Number and Particle Mass. Research Report 98. Health Effects Institute, Cambridge MA.

Pathogenomic Mechanisms for Particulate Matter Induction of Acute Lung Injury and Inflammation in Mice

George D Leikauf, Susan A McDowell, Scott C Wesselkamper, Clay R Miller, William D Hardie, Kelly Gammon, Pratim P Biswas, Thomas R Korfhagen, Cindy J Bachurski, Jonathan S Wiest, Klaus Willeke, Eula Bingham, John E Leikauf, Bruce J Aronow, and Daniel R Prows

ABSTRACT

To begin identifying genes controlling individual susceptibility to particulate matter, responses of inbred mouse strains exposed to nickel sulfate (NiSO₄*) were compared with those of mice exposed to ozone (O₃) or polytetrafluoroethylene (PTFE). The A strain was sensitive to NiSO₄-induced lung injury (quantified by survival time), the C3H/He (C3) strain and several other strains were intermediate in their responses, and the C57BL/6 (B6) strain was resistant. The strains showed a pattern of response similar to the patterns of response to O₃ and PTFE. The phenotype of A × B6 offspring (B6AF₁) resembled that of the resistant B6 parental strain, with strains exhibiting sensitivity in the order A > C3 > B6 = B6AF₁. Pathology was comparable for the A and B6 mice, and exposure to NiSO₄ at 15 µg/m³ produced 20% mortality in A mice. Strain sensitivity for the presence of protein or neutrophils in lavage fluid differed from strain sensitivity for survival time, suggesting that they are not causally linked but are controlled by an independent gene or genes. In the B6 strain, exposure to nickel oxide (NiO) by instillation (40 to 1000 nm) or inhalation (50 nm) produced no changes, whereas inhalation of NiSO₄ (60 or 250 nm) increased lavage proteins and neutrophils. Complementary DNA (cDNA) microarray analysis with 8,734 sequence-verified clones revealed a temporal pattern of increased oxidative stress, extracellular matrix repair,

cell proliferation, and hypoxia, followed by a decrease in surfactant-associated proteins (SPs). Certain expressed sequence tags (ESTs), clustered with known genes, suggest possible coregulation and novel roles in pulmonary injury. Finally, locus number estimation (Wright equation) and a genomewide analysis suggested 5 genes could explain the survival time and identified significant linkage for a quantitative trait locus (QTL) on chromosome 6, *Aliq4* (acute lung injury QTL4). Haplotype analysis identified an allelic combination of 5 QTLs that could explain the difference in sensitivity to acute lung injury between parental strains. Positional candidate genes for *Aliq4* include aquaporin-1 (*Aqp1*), SP-B, and transforming growth factor-α (TGF-α). Transgenic mice expressing TGF-α were rescued from NiSO₄ injury (that is, they had diminished SP-B loss and increased survival time). These findings suggest that NiSO₄-induced acute lung injury is a complex trait controlled by at least 5 genes (all possibly involved in cell proliferation and surfactant function). Future assessment of these susceptibility genes (including evaluations of human synteny and function) could provide valuable insights into individual susceptibility to the adverse effects of particulate matter.

INTRODUCTION

Epidemiologic studies have associated air pollution with respiratory morbidity and mortality (Logan 1953; Schwartz and Marcus 1990). Of the specific criteria pollutants measured, fine particulate matter (particles ≤ 2.5 µm in aerodynamic diameter) is often of the greatest concern, with mortality estimated to increase about 1% per increase in fine particle exposure of 10 µg/m³ (Fairley 1990; Schwartz 1992; Dockery et al 1993; Pope and Kanner 1993). Because the levels of pollution associated with adverse effects in epidemiologic studies are low compared with those shown to cause adverse effects in animals, we and others reasoned that individual susceptibility must play a major role in these responses (Kleeberger et al 1997b; Prows et al 1997, Leikauf et al 1998). Clinical studies have indicated varied responses to O₃-induced

* A list of abbreviations and other terms appears at the end of the Investigators' Report.

This Investigators' Report is one part of Health Effects Institute Research Report 105, which also includes a Preface, a Commentary by the Health Review Committee, and an HEI Statement about the research project. Correspondence concerning the Investigators Report may be addressed to Dr George D Leikauf, Department of Environmental Health, University of Cincinnati, PO Box 670056, Cincinnati OH 45267-0056.

Although this document was produced with partial funding by the United States Environmental Protection Agency under Assistance Award R82811201 to the Health Effects Institute, it has not been subjected to the Agency's peer and administrative review and therefore may not necessarily reflect the views of the Agency, and no official endorsement by it should be inferred. The contents of this document also have not been reviewed by private party institutions, including those that support the Health Effects Institute; therefore, it may not reflect the views or policies of these parties, and no endorsement by them should be inferred.

bronchoconstriction (McDonnell et al 1985). Similarly, inbred mouse strains vary in their sensitivity to developing O₃-induced acute lung injury, pulmonary inflammation, and increased protein in lavage fluid (Stokinger 1957; Goldstein et al 1973; Ichinose et al 1982; Gonder et al 1985; Kleeberger et al 1990, 1993, 1997a,b; Misra et al 1991; Rodriguez et al 1991; Kleeberger and Hudak 1992; Holroyd et al 1997, Prows et al 1997, 1999).

Less is currently known about the mechanisms of susceptibility to the effects of fine particulate matter, but several lines of evidence implicate macrophage activation, epithelial injury, and oxidative stress (Bingham et al 1972; Pryor et al 1990; Camner and Johansson 1992; Stohs and Bagchi 1995; Pritchard et al 1996). For example, ultrafine particles, such as those generated from PTFE, can induce acute lung injury (Pryor et al 1990; Johnston et al 1998; Oberdörster et al 1998). Fine particulate matter can be enriched in water-soluble transition metals that undergo reduction-oxidation with biological macromolecules to induce oxidative stress. In other studies, the water-soluble metals (vanadium, chromium, nickel, and iron) released from residual oil fly ash, a particulate matter surrogate, may have been responsible for acute lung injury and inflammation (Costa and Dreher 1997; Dreher et al 1997; Dye et al 1997). In vitro studies identified the active components of this mixture as vanadium, chromium, and nickel, with vanadium being the most active (Pritchard et al 1996; Kodavanti et al 1998a,b). In studies in vivo, however, the converse was true: for example, nickel was the most biologically active metal in surrogate particulate matter (Pritchard et al 1996; Costa and Dreher 1997; Kodavanti et al 1998a,b). Other in vivo studies with intratracheal instillation of residual oil fly ash found differences in response among rat strains, suggesting genetic susceptibility may play a role in individual responsiveness to inhaled particulate matter (Kodavanti et al 1997).

Of the transition metals enriched in the fine fraction of ambient particulate matter in the workplace, nickel compounds are particularly pernicious (National Institute for Occupational Safety and Health [NIOSH] 1977; International Agency for Research on Cancer [IARC] 1990; National Toxicology Program [NTP] 1996). Nickel exists in soluble forms (eg, NiSO₄) and insoluble forms (eg, NiO and elemental nickel) that enter the environment primarily via high-temperature combustion, electroplating, and smelting processes (Nriagu 1980; Senior and Flagan 1982; Milford and Davidson 1987; IARC 1990; NTP 1996). In mainstream cigarette smoke, nickel is present in concentrations (0.2 to 0.51 µg/cigarette) greater than those of other metal ions including copper, cadmium, and iron (0.19, 0.07 to 0.350, and 0.042 µg/cigarette, respectively) (IARC 1986). Nickel

concentrations in particulate matter are 0.0006 to 0.078 µg/m³ in rural areas and as high as 0.328 µg/m³ in urban areas in the United States (Milford and Davidson 1987; Schroeder et al 1987). Nickel concentrations in stack effluent from municipal solid waste incinerators, oil combustors, and coal combustors can be even higher and have been measured at 0.26 to 5.18 µg/m³ (Biswas and Wu 1998).

Nickel concentrations in ambient air are highest near industrial sources. In the United States, the number of local nickel sources (more than 2000 facilities) is 3 times the number of cadmium, chromium, and cobalt sources combined (total of 650 facilities) (Leikauf et al 1995). Inventories of nickel released into the air exceed 1.0 billion lb/year (as compared with the sum of 0.3 billion lb/year for the other 3 metals combined). The US Environmental Protection Agency (EPA) estimates that as many as 160 million people live within 12.5 miles of sources emitting nickel with a median concentration of 0.05 µg/m³ (NTP 2001). Ambient air concentrations near nickel production sites are not measured routinely, but nickel levels ranged from 0.001 to 0.732 µg/m³ in Ontario, Canada (Chan and Lusi 1986), with recorded maximal concentrations of 4.4, 2.3, and 6.1 µg/m³ measured in 1980, 1986, and 1988, respectively (Brecher et al 1989; Dobrin and Potvin 1992; Ontario Ministry of the Environment 1992). In the United States, the EPA estimates that 720,000 people live near primary nickel sources that produce levels as high 15.8 µg/m³ (NTP 2001). These levels have to be viewed with caution because chemical speciation and particle size analyses are not available. In contrast, speciation data are more readily obtained in occupational environments where exposures for soluble nickel have averaged 260 to 760 µg/m³ with short-term peaks exceeding 2000 µg/m³ (NIOSH 1977; Haber et al 2000). Occupational levels of insoluble nickel have ranged from 200 to 10,000 µg/m³ (NIOSH 1977; Haber et al 2000).

The respiratory tract is the primary tissue affected by inhaled nickel compounds, with the insoluble forms (eg, nickel subsulfide and NiO) being carcinogenic and the soluble forms (eg, NiSO₄, nickel chloride, and nickel acetate) being acutely toxic to the lung. Nickel carbonyl is a gaseous form of nickel (produced by combining nickel with carbon monoxide). Like NiSO₄, nickel carbonyl can deliver ionic nickel (Ni²⁺) to the alveolus (Hackett and Sunderman 1968) and has been associated with numerous incidences of acute lung injury and death among welders (Shi 1986; Barceloux 1999).

Previous NiSO₄ inhalation studies have noted both acute respiratory effects (macrophage activation, alveolar proteinosis, neutrophil accumulation, and epithelial disruption) and chronic respiratory effects (interstitial monocytic and

macrophage infiltrates and fibrosis) in F344/N rats and B6C3F₁ mice (Benson et al 1988, 1995; Dunnick et al 1988, 1995; NTP 1996). Exposure of B6C3F₁ mice to nickel at 1600 µg/m³ (6 hours/day, 5 days/week) produced 100% mortality within 12 days. Long-term occupational exposures have been associated with increased deaths from respiratory disease and asthma when concentrations exceeded the current standard for soluble nickel of 100 µg/m³ (NIOSH 1977; Cornell and Landis 1984; Malo et al 1985; Shirakawa et al 1990; Bright et al 1997).

SPECIFIC AIMS

The purpose of this study was to examine whether host (genetic) factors contribute to increased individual susceptibility to the acute effects of NiSO₄. The specific hypothesis addressed by this study was that individual susceptibility to lung injury induced by nickel particles is a heritable trait. To test this hypothesis during the 18-month research period funded by HEI, 2 specific aims were proposed. The first specific aim was to examine the molecular mechanisms of toxicity of fine transition metal particles. Mice were exposed to NiSO₄ aerosol with a mass median aerodynamic diameter (MMAD) of 0.2 µm, and acute lung injury was assessed by determining pulmonary pathology, inflammation, and gene expression. Interstrain differences in pulmonary responses were compared by exposing selected strains of inbred mice to fine NiSO₄ aerosol and measuring survival time as an indicator of acute lung injury, protein content of bronchoalveolar lavage (BAL) fluid, and pulmonary inflammation. Gene expression was assessed using a cDNA microarray. Strain phenotype patterns were also assessed for acute lung injury produced by exposure to 2 known irritants, ultrafine PTFE and O₃. After the identification of resistant and sensitive (polar) mouse strains, offspring of the respective polar strains were exposed to fine NiSO₄ aerosol to assess the likely mode of trait inheritance. From the initial findings, mean survival time (MST) was measured in a sensitive mouse strain (A) and a resistant mouse strain (B6), and in the F₁ progeny of these two strains.

The second specific aim was to begin to evaluate the genetic determinants of acute lung injury. A QTL analysis of a selected phenotype (survival time) was performed using a genomewide scan for linkage in backcross mice generated from the polar strains A and B6.

METHODS

EXPERIMENTAL DESIGN

To begin investigating the genetic determinants of irritant-induced acute lung injury, 7 inbred mouse strains were continuously exposed to NiSO₄, PTFE, or O₃. Two strains with polar responses to acute lung injury, a sensitive A strain and a resistant B6 strain, were identified. To investigate the mode of inheritance of susceptibility to NiSO₄-induced acute lung injury, the survival times of offspring from a cross of the resistant and sensitive inbred mouse strains (B6AF₁) and backcrosses were determined. To investigate the pathology associated with NiSO₄-induced acute lung injury, A and B6 mice were exposed, histological sections were microscopically examined, and the lung wet weights and dry weights were determined. To evaluate the levels of NiSO₄ that produce acute lung injury, groups of the sensitive A strain mice were exposed to concentrations ranging from 15 to 150 µg/m³.

Previously, Kleeberger and colleagues (1990, 1997b) reported that pulmonary protein and inflammatory cells present in lavage fluid varied between B6 (sensitive) and C3 (resistant) mice exposed to O₃ for 48 hours. Protein and polymorphonuclear leukocyte (PMN) levels were therefore measured in the lavage fluid of B6, C3, and A strain mice, and the first-generation progeny of the sensitive B6 and resistant C3 mouse strains (B6C3F₁) after 48 hours of exposure to NiSO₄. Submicrometer combustion aerosols were also generated in a controlled manner for use in evaluating inflammatory cells and protein in lavage fluid from B6 mice. The formation of submicrometer Ni²⁺ species in a high-temperature furnace was investigated using systematic manipulation of pyrolysis temperature, residence time, and dilution air to obtain different submicrometer sizes of NiO and NiSO₄ aerosols. After intratracheal instillation of or inhalation (whole-body) exposure to nickel, the effects of particle size and solubility were evaluated.

To investigate differential gene expression during the initiation and progression of acute lung injury, lung messenger RNA (mRNA) was isolated initially from B6 mice after exposure to NiSO₄ aerosol for 0 (control), 3, 8, 24, 48, or 96 hours. Polyadenylated mRNA was isolated, reverse transcribed, and fluorescently labeled. Samples from exposed mice (Cy5-labeled) were competitively hybridized against samples from unexposed, control mice (Cy3-labeled), onto microarrays containing 8,734 murine cDNAs. To assess the temporal patterns of gene expression, genes were clustered according to similarities in expression over time. To evaluate the pathophysiology of changes in gene expression, genes were categorized according to

function. More conventional Northern blot and S1 nuclease protection assays were performed to quantify the expression changes of selected genes observed in microarray analysis. Next, the levels of gene expression for lung mRNA from the nickel-exposed A strain mice were compared with those from B6 mice at 3, 8, 24, and 48 hours of exposure.

Finally, we investigated the genetic determinants of the quantitative trait (survival time) by performing a genome scan of backcross offspring derived from the polar strains (B6AF₁ crossed with the A strain). The genomewide scan employed microsatellite markers (simple sequence length polymorphisms [SSLPs]) distributed throughout the mouse genome to map chromosomal regions with linkage to the susceptibility phenotype. Polymerase chain reaction (PCR) was used to quickly identify segments of the mouse genome that harbor genetic loci linked to the survival phenotype. This was conducted with female F₁ mice and male parental strain and the complementary mating pattern to determine whether the trait is sex linked or imprinted. Hepatic DNA was isolated from 307 backcross mice, and initial mapping was conducted with 77 SSLPs distributed at distances of 20 to 30 cM throughout the genome. Regions of interest, defined as those with lod scores (equal to the likelihood of linkage divided by the likelihood of no linkage) of 1.5 or higher, were examined by denser mapping of SSLPs. Phenotype and genotype data were initially analyzed using the MAPMAKER/QTL software program (Lincoln et al 1992b). Subsequently, threshold levels of significance for linkage assessment (ie, significant lod scores for identifying QTLs) were determined by evaluation of 10,000 permutations of the original data set using QTL Cartographer (Basten et al 1994, 1997). The QTL results were analyzed by the *simultaneous search* method of MAPMAKER/QTL to identify possible gene–gene interactions and determine the overall degree of genetic variance predicted by the QTLs. These findings were then compared with the gene expression results as determined by cDNA microarray analysis.

Mice were handled in accordance with protocols approved by the Institutional Animal Care and Use Committee of the University of Cincinnati Medical Center and of the Children's Hospital Research Foundation.

ATMOSPHERE GENERATION AND CHARACTERIZATION

Nickel aerosols were generated by two methods. Most inhalation studies described in this report were conducted by exposure to an aqueous aerosol of NiSO₄. Continuous aerosol exposures (up to 2 weeks) of inbred mice included fine NiSO₄ (particle alone), ultrafine PTFE (particle and gas mixture), and O₃ (gas alone). Mice were exposed to

NiSO₄ or O₃ in stainless steel cages placed inside a 0.32-m³ stainless steel inhalation chamber. Nickel sulfate aerosol (MMAD, 0.22 μm; geometric SD (σ_g) = 1.85) was generated from a solution of NiSO₄ hexahydrate (NiSO₄ •6H₂O, Sigma, St Louis MO) using a modified Collison 3-jet nebulizer (3.5 L/min) (BGI, Waltham MA) placed inside a glass tube (internal diameter [ID], 24 mm). Decreasing the distance from the jets to the wall decreased the size of the primary droplet formed by the nebulizer. This modification, along with empirical selection of the solution concentration, enabled the generation of a submicrometer aerosol, as measured in the inhalation chamber after dilution with HEPA filtered air.

The particle number concentration and particle size were determined using a differential mobility analyzer consisting of an electrostatic classifier (model 3071A, Thermo-Systems [TSI], St Paul MN), a condensation nucleus counter (model 3022A, TSI), and scanning mobility particle sizer (SMPS) fast-scanning software (TSI). The chamber nickel concentration was determined using the dimethylglyoxime method (Ferguson and Banks 1951). Samples of the chamber atmosphere were collected with 2 midjet impingers (Ace Glass, Vineland NJ) placed in series, each containing 10 mL of distilled water (flow rate, 11.3 L/min; sampling time, 22.1 minutes; volume sampled, 250 L). Collected samples were mixed with a solution containing 1 M HCl, 0.2 M Br⁻, 12 M NH₄OH (Fisher, Fair Lawn NJ), 1% dimethylglyoxime (Sigma), and 95% ethanol. Absorbance was measured at 445 nm (model DU-64, Beckman, Fullerton CA). Resulting nickel concentrations are expressed as micrograms per cubic meter to enable direct comparisons between different nickel aerosols described in the scientific literature. Using this method, the limit of detection for nickel was 0.5 μg/m³. During nickel exposures, mice were supplied with food and water. For initial assessment of acute lung injury in mice, nickel exposures (\pm SD) were 150 \pm 15 μg/m³. Ozone (10.0 \pm 0.1 ppm) was generated from 100% ultradry oxygen (Matheson, Columbus OH) using an ultraviolet ozonator (model V1-0, OREC, Phoenix AZ). Chamber samples from the animal's breathing zone were drawn through PTFE tubing and analyzed continuously with an O₃ detector (model 1008-PC, Dasibi, Glendale CA). This instrument was calibrated against an EPA transfer standard.

For PTFE exposures, mice were placed in stainless steel cages inside a 0.05-m³ Plexiglas chamber and exposed continuously to PTFE particles, 10⁷/cm³ (30 L/min). A PTFE powder (0.75 g) (Fluon, ICI Chemicals and Polymers, Bayonne NJ) was placed in a ceramic furnace tube (ID, 2.5 cm) and heated to 420° \pm 5°C with a Lindberg Hevi-Duty furnace (Sola Basics Industries, Watertown WI). At this temperature, ultrafine particles (MMAD, 0.02 μm) and

hydrofluoride gas are released (Oberdörster et al 1998). Airflow through the heated tube was 5.0 L/min, and diluting airflow was 25 L/min. Particle size and concentration were determined with an electrical aerosol analyzer (model 3030, TSI).

HIGH-TEMPERATURE FURNACE SYSTEM

In addition to generation of fine NiSO_4 by the above-described method, in a few tests aerosols were generated by combustion. To simulate the process by which nickel-containing particles are generated during oil combustion, a laboratory-scale furnace (model HTF55342C, Lindberg/Blue M, Asheville NC) with a horizontal alumina reactor tube (Type AD-998C, Coors Ceramic Company, Golden CO) was used to produce an adjustable temperature (ambient to 1200°C). The temperature was stable within 10% of the set point for a length of 55 cm. Airflow through the furnace was controlled using a combination of flow meters (Dwyer Instruments, Michigan City IN) calibrated to a primary standard (Gilibrator II, Gilian Instrument Corp, Clearwater FL). Aerosol was fed into the furnace by nebulizing (model 3076, TSI) a 0.35 M aqueous nickel nitrate, $\text{Ni}(\text{NO}_3)_2 \cdot 6\text{H}_2\text{O}$ or NiSO_4 solution (Sigma) made with distilled, particle-free water, using dry, particle-free air at 3.0 L/min and 300 kPa. Excess water was removed from the aerosol using a diffusion dryer (model 206200, TSI) filled with anhydrous calcium sulfate (WA Hammond Drierite Company, Xenia OH). Furnace temperatures were systematically varied to establish the temperature at which chemical changes occurred in the aerosol.

Aerosol size characteristics were measured by a SMPS (model 3934, TSI) using an electrostatic classifier (model 3071A, TSI), in series with a condensation nucleus counter (model 3022A, TSI), externally controlled by fast-scanning software (Version 1.1, TSI). Aerodynamic diameter data were converted to mass concentrations using the technique of Sioutas and colleagues (1999). X-ray diffractometry of powder collected on 47-mm glass-fiber filters was used to determine crystalline structure (model D/Max 2100 H, Cu $K\alpha$ radiation, Rigaku). To simulate the pyrolysis of nickel in a furnace environment, we used aerosolized nickel nitrate, prepared by making a 0.35 M solution using particle-free distilled H_2O and nickel nitrate hexahydrate [$\text{Ni}(\text{NO}_3)_2 \cdot 6\text{H}_2\text{O}$, ICDD number 47-1049]. Because the sulfur content of fuel oil can affect speciation, and therefore particle size distributions, the use of nickel nitrate allowed the behavior of NiO to be observed in the absence of sulfur, indicative of fuel oil with no residual sulfur.

To examine the effect of nickel aerosol solubility, insoluble NiO powder was generated by pyrolysis of nickel nitrate at 800°C and segregated according to size (40, 130, 300, and 1000 nm). Nickel oxide powder obtained by both of these

techniques was captured on preweighed PTFE filters (pore size, 2 μm ; Gelman, Ann Arbor MI), measured gravimetrically, and sonicated in sterile Dulbecco phosphate-buffered saline without Ca^{2+} or Mg^{2+} , pH 7.2 (GibcoBRL, Grand Island NY) for 10 minutes before intratracheal instillation. For whole-body inhalation experiments, NiO or NiSO_4 aerosols were produced in the furnace and introduced into a 40-L whole-body exposure chamber. Nickel oxide aerosol was produced by pyrolysis of nickel nitrate at 800°C; NiSO_4 was aerosolized directly at 50°C. Control animals were exposed to dry, particle-free air passing through an 800°C furnace. Mixing inside the chamber was thorough, as demonstrated by uniform aerosol size and concentration measurements taken at 6 locations within the chamber. Particle size distributions inside the chamber were measured by the SMPS at 3-hour intervals during the exposure. Oxides of nitrogen concentrations measured using a chemiluminescence analyzer (model 42H, Thermo Environmental Instruments, Franklin MA) were 0.09 ppm for nitric oxide (NO) and less than 0.1 ppm for nitrogen dioxide. Dry bulb temperature inside the chamber was constant at $24^\circ \pm 0.5^\circ\text{C}$; relative humidity inside the chamber was adjusted to 40% using vaporized distilled H_2O .

STRAIN SELECTION AND TISSUE PREPARATION

All inbred mouse strains (A, AKR, C3, B6, CBA, DBA/2, FVB/N, and specific F_1 crosses and backcrosses) were purchased from the Jackson Laboratory (Bar Harbor ME). To examine lung pathology, NiSO_4 -exposed mice were obtained at death and control mice were injected with pentobarbital sodium (50 mg/kg body weight; Nembutal, Abbott Laboratories, North Chicago IL) and exsanguinated. A cannula (ID, 0.58 mm) was inserted into the trachea, and the lungs were instilled in situ (30 cm H_2O) with phosphate-buffered formaldehyde (pH 7.1), removed, and immersed in fixative for 24 hours. The left lung was washed with phosphate-buffered saline, dehydrated through a series of graded ethanol solutions (30% to 70%), and processed into paraffin blocks (Hypercenter XP, Shandon Scientific, Pittsburgh PA). Paraffin-embedded tissues were divided into 5- μm sagittal sections and stained with hematoxylin and eosin.

To obtain tissue for determination of lung wet weight, lung dry weight, and lung wet-to-dry weight ratio, the chest cavity was opened and the heart-lung block was removed. The lungs were rinsed with phosphate-buffered saline, trimmed of heart, connective tissue, and esophagus, and blotted dry with gauze, and the wet weights were recorded. Lungs were then dried in a plastic desiccator containing silica gel (Sargent-Welch, Skokie IL) for 2 weeks before dry weights were recorded.

BRONCHOALVEOLAR LAVAGE

Mice were exposed for up to 72 hours and killed by exsanguination (after intraperitoneal administration of pentobarbital sodium at 50 mg/kg body weight). The lungs were lavaged 3 times with 1 mL of Hanks balanced salt solution (GibcoBRL), without Ca^{2+} or Mg^{2+} , and with D-glucose (pH 7.2). Individual samples of BAL fluid were pooled and immediately placed on ice (4°C). Aliquots (250 μL each) of lavage fluid were cytocentrifuged (Cytospin 3, Shandon Scientific), and the cells were stained with Diff-Quick (Baxter Diagnostics, McGraw Park IL) for differential cell analysis. Differential cell counts were performed by identifying at least 300 cells. The pooled lavage fluid was then centrifuged (500g, 4 minutes, 4°C), and the supernatant was decanted. The cell pellet from each lavage was resuspended in 1 mL of Hanks balanced salt solution. Total cell counts were determined with a hemocytometer. The total protein concentration in the supernatant was measured using the method of Bradford (1976) with bovine serum albumin (BSA) as a standard (Bio-Rad Laboratories, Hercules CA).

RNA PREPARATION

Total RNA was isolated from lung homogenized (using Tissumizer, Tekmar Co, Cincinnati OH) in 3 mL of TRIZOL (GibcoBRL) and recovered by acid phenol extraction. Polyadenylated mRNA was isolated by binding total RNA to poly-T oligonucleotides covalently linked to polystyrene-latex particles and then eluted with low-salt buffer (Qiagen, Valencia CA).

FLUORESCENT LABELING OF PROBES

Polyadenylated mRNA was pooled from 3 mice at selected times throughout NiSO_4 exposure and fluorescently labeled with 5' Cy5-labeled random 9mers during reverse transcription. Polyadenylated mRNA was pooled from 3 unexposed, control mice and tagged with 5' Cy3-labeled random 9mers during reverse transcription (Operon Technologies, Alameda CA). For each reverse transcription reaction, 200 ng of polyadenylated mRNA was incubated for 2 hours at 37°C with 200 units of Moloney murine leukemia virus (M-MLV) reverse transcriptase (GibcoBRL), 4 mM dithiothreitol, 1 U RNase Inhibitor (Ambion, Austin TX), 0.5 mM deoxyribonucleoside triphosphates (dNTPs), and 2 μg of labeled 9mers in a 25- μL volume with enzyme buffer supplied by the manufacturer. The reaction was terminated by a 5-minute incubation at 85°C. For cohybridization, paired Cy3 and Cy5 reactions were combined and purified with a TE-30 column (Clonetech, Palo Alto CA), brought to 90 μL with $d\text{H}_2\text{O}$, and precipitated with 2 μL of glycogen at 1 mg/mL, 60 μL of 5 M ammonium acetate, and 300 μL of ethanol.

After centrifugation, the pellet was resuspended in 24 μL of hybridization buffer (5 \times SSC, 0.2% sodium dodecyl sulfate [SDS], 1 mM dithiothreitol).

MICROARRAY PREPARATION

Sequences used for the microarray were PCR products purified by gel filtration with Sephacryl-400 (Amersham Pharmacia Biotech, Piscataway NJ), dried, and resuspended in $d\text{H}_2\text{O}$. Each cDNA was fixed to the surface of modified glass slides, and arraying was performed by robotics (Incyte Pharmaceuticals, Palo Alto CA). The microarray was then washed 3 times in $d\text{H}_2\text{O}$ at room temperature, treated with 0.2% I-Block (Tropix, Bedford MA), dissolved in 1 \times Dulbecco phosphate-buffered saline at 60°C for 30 minutes, and rinsed in 0.2% SDS for 2 minutes followed by three 1-minute washes in $d\text{H}_2\text{O}$.

HYBRIDIZATION

Each paired Cy3 and Cy5 probe solution was resuspended by incubation at 65°C for 5 minutes with mixing, applied to an array, covered with a 22-mm² glass coverslip, and placed in a sealed chamber. After hybridization at 60°C for 6.5 hours, slides were washed in 3 consecutive solutions of decreasing ionic strength. The Cy3 and Cy5 channels were simultaneously scanned with independent lasers at 10- μm resolution. The detected fluorescent light was optically filtered, and photon multiplier tubes were used to translate photons into an analog electrical signal. To adjust for differences in probe labeling efficiency, the balance coefficient (ratio of total Cy3 to total Cy5 fluorescence signals) was derived for each microarray: for A mice, the ratios were 0.89, 0.98, 0.66, and 1.35, for the 3-, 8-, 24-, and 48-hour microarrays, respectively; for B6 mice, 1.05, 1.14, 0.83, and 0.88, for the 3-, 8-, 24-, 48-, and 96-hour microarrays, respectively. The differential expression level for each cDNA was normalized to the balance coefficient of each microarray to give a balanced differential expression value for each cDNA. The criteria for inclusion of a cDNA in the analysis were that the fluorescent signal from the cDNA exceeded a signal-to-background ratio of 2.5 and that the cDNA covered more than 40% of its grid location on the microarray.

TEMPORAL CLUSTERING

To assess temporal patterns, differentially expressed genes were grouped according to similarities in expression. The gene similarity metric (uncentered correlation), as described by Eisen and colleagues (1998), was used for identifying temporal clusters of genes. Genes with a balanced differential expression greater than 1.7-fold at 2 or more exposure times were included in the B6 strain analysis. Genes with a

balanced differential expression greater than 1.7 in either strain at any exposure time were used in the comparison of A and B6 mice. Balanced differential expression values were assigned pseudocolors; cells representing increased expression levels relative to control were colored red, and those representing decreased expression levels relative to control were colored green. Black was assigned to missing values, and additional annotations were generated from Unigene_Mm042799 (National Center for Biotechnology Information, Bethesda MD). The sequences of ESTs lacking homology with known genes were analyzed. A Basic Local Alignment Search Tool (BLAST) search against the nonredundant GenBank, EMBL, DDBJ, and PDB sequence databases was performed for each EST, and homology with known genes was assessed by the score generated. To assess physiologic significance, differentially expressed genes were evaluated according to function with the aid of the hierarchy component of GEMTools (Incyte Pharmaceuticals).

NORTHERN BLOTTING AND S1 NUCLEASE PROTECTION ASSAYS

To assess further the increased expression of the metallothionein-1 and heme oxygenase-1 genes as observed with the microarray analysis, Northern blot analysis was performed. Using a method previously described (Dalton et al 1994), mouse metallothionein-1 and rat heme oxygenase-1 cDNAs were used as the templates for ^{32}P -labeled riboprobes (hybridization buffer was $3\times$ SET where $1\times$ SET is 150 mM NaCl, 30 mM Tris-HCl, pH 7.8, 2 mM EDTA), 0.1% SDS, 0.2% Ficoll, 0.2% polyvinylpyrrolidone, 0.2% BSA, 250 mg/mL yeast transfer RNA; 65°C , 16 hours). Blots were washed in $1\times$ SSC, 0.1% SDS, followed by $0.3\times$ SSC, 0.1% SDS, at 65°C , and quantified by phosphorimaging (Molecular Dynamics PhosphorImager, ImageQuant, Sunnyvale CA). Each blot was subsequently probed using a γ - ^{32}P -labeled oligonucleotide to 28S ribosomal RNA (rRNA) (hybridization buffer was $5\times$ SET, 0.1% Ficoll, 0.1% polyvinylpyrrolidone, 0.1% BSA, 0.5% SDS, 0.05 mg/mL denatured salmon sperm DNA, 0.004 mg unlabeled 28S rRNA oligonucleotide; 42°C ; 3 hours) (Barbu and Dautry 1989). Blots were washed in $2\times$ SET, 0.1% SDS, at room temperature, followed by $0.5\times$ SET, 0.1% SDS, at 42°C , and quantified by phosphorimaging.

To assess further the decrease in SP gene expression observed with the microarray analysis, S1 nuclease protection assays were performed. Using a method described previously (Bachurski et al 1995), S1 probes specific for murine SP-A, SP-B, and SP-C, and ribosomal protein L32 for comparison, were linearized, end-labeled with γ - ^{32}P -adenosine triphosphate (γ - ^{32}P -ATP), combined, and hybridized (16 hours, 55°C) with the same total lung RNA

used for the microarray analysis. Single-stranded regions were digested away from protected fragments by S1 nuclease (110 U, GibcoBRL) in the presence of excess unlabeled salmon sperm DNA (1 hour, room temperature). The protected fragments were electrophoresed through 6% polyacrylamide gels containing 8 M urea and quantitated by phosphorimaging (ImageQuant).

PHENOTYPING, DNA PREPARATION, AND GENOTYPING

Mice were continuously exposed by inhalation to nickel at $150\ \mu\text{g}/\text{m}^3$ to induce acute lung injury and death. The mice used in these studies were obtained from the Jackson Laboratory (Bar Harbor ME) and included male and female A and B6 as well as B6AF₁ and AB6F₁ (both termed F₁ subsequently) control mice, and backcross mice ($n = 307$), generated from F₁ \times A ($n = 162$) and A \times F₁ ($n = 145$) matings. Mice were acclimated for approximately 1 week prior to nickel exposure and maintained in a virus-free and pathogen-free environment with a light cycle of 12 hours on and 12 hours off. Six exposures were performed throughout the year, with groups ranging from 30 to 67 mice/exposure. All exposures also contained at least 2 control mice (one A and one B6 of either sex), approximately equal numbers of each backcross mating scheme (A \times F₁ and F₁ \times A), and males and females of each group. Survival time was recorded to within a 5% error for each animal. After death, the liver was removed from each mouse, immediately frozen in liquid nitrogen, and stored at -70°C for subsequent genotype studies.

Genomic DNA was isolated using a DNA extraction kit (Wizard DNA, Promega, Madison WI). Samples were analyzed for purity (A_{260}/A_{280}), and DNA concentrations (A_{260}) were quantitated using a Beckman DU-64 spectrophotometer. A fraction of each DNA sample was diluted to 10 ng/ μL for use in microsatellite analysis. Polymerase chain reactions were performed to genotype backcross progeny for microsatellite markers located throughout the mouse genome. Primer pairs were chosen on the basis of known polymorphisms between the A and B6 strains and purchased from Research Genetics (Huntsville AL). Polymerase chain reactions were performed in 15- μL reactions in 96-well plates (MJ Research, Watertown MA) using a 4-block thermocycler (model PTC-225, MJ Research). The final concentration for each reaction was 10 mM Tris-HCl (pH 8.3), 50 mM KCl, 1.5 mM MgCl₂, 0.2 mM of each dNTP (Promega), $1\times$ RediLoad (Research Genetics, Huntsville AL), and 0.132 μM of each microsatellite primer. This reaction mixture was added to 100 ng of genomic DNA (10 μL) and 0.6125 U of *Taq* DNA polymerase (GibcoBRL). The final mixtures were initially

denatured at 94°C for 3 minutes, followed by 35 to 37 cycles of 94°C for 30 seconds, 55°C for 45 seconds, and 72°C for 30 seconds. A final elongation step at 72°C for 7 minutes was followed by refrigeration (4°C) until genotyping by gel analysis. The PCR products were differentiated on agarose gels (GibcoBRL) and visualized by ethidium bromide staining. The agarose concentration used (2.5% to 6%) depended on the size of the allelic variants and had a resolution of about 4% to 5% difference in size between A and B6 alleles.

LOCUS NUMBER ESTIMATION

To estimate the number of independent genes segregating with the response to nickel-induced acute lung injury, the following formula of Sewall Wright was used: $n = (P_2 - F_1)^2 / 4(V_{N_2} - V_{F_1})$, where n is the estimated number of segregating loci; P_2 and F_1 are the MSTs of A and B6AF₁ mice, respectively; and V_{N_2} and V_{F_1} are computed variances of the ($F_1 \times A$) backcross and F_1 cohorts, respectively (Silver 1995). This estimate assumes that the genes are unlinked, and that each gene is semidominant and contributes equally to the phenotype.

QUANTITATIVE TRAIT LOCUS MAPPING AND LINKAGE ANALYSIS

To identify chromosomal regions linked to nickel-induced acute lung injury, backcross progeny derived from crossing sensitive A and resistant B6 strains of mice were phenotyped, genotyped, and analyzed for evidence of QTLs. Initially, 307 backcross mice were genotyped for 77 microsatellite markers distributed at intervals of 20 to 30 cM across the genome. After generation of a linkage map (MAPMAKER/EXP version 3.0b; Lander et al 1987), all phenotype data (ie, survival times) and genotype data were analyzed for linkage using MAPMAKER/QTL version 1.1b (Paterson et al 1991; Lincoln et al 1992a,b) and QTL Cartographer model 3 (Basten et al 1994, 1997) computer programs. Initial analysis of the phenotype distribution indicated skewness; log transformation produced a normal distribution. Regions with lod scores greater than 1.6 were subsequently typed for additional microsatellite markers. To identify other loci explaining lesser portions of the genetic variance, the major locus was fixed to remove its variance, and the genome was rescanned to determine any additional linkages. After identification of each additional locus, the combined loci were sequentially fixed to further determine suggestive linkages. To look for suggestion of epistatic interactions between the putative QTLs, the backcross data set was examined using Epistat (Chase et al 1997) and the *cumulative search* function of MAPMAKER/QTL (Lincoln et al 1992b).

HAPLOTYPE ANALYSIS

To gain insight into the contribution of each QTL and combination of QTLs to the overall survival phenotype, haplotype analysis was performed. This procedure directly quantifies a difference in survival time (in hours) associated with a particular haplotype. For this analysis, each QTL was assumed to be fully penetrant and located at the microsatellite marker nearest to the peak lod score for the identified QTL regions (ie, *D1Mit213*, *D6Mit183*, *D8Mit65*, *D9Mit299*, *D12Mit112*, and *D16Mit152*). Mean survival times for groups of mice with the same haplotype (ie, sensitive alleles) at each QTL or combination of QTLs were calculated and then compared with the MSTs of mice with the opposing haplotype (ie, resistant alleles) to determine the contributions of these QTLs to the overall phenotype.

NICKEL RETENTION

Mice that express human transforming growth factor- α (hTGF- α) in the lung have varied lung remodeling. To compare the amount of nickel retention between nontransgenic and hTGF- α transgenic mice, lungs were obtained before or 72 hours after exposure to NiSO₄ at 70 $\mu\text{g}/\text{m}^3$; lung wet weights were determined; and then the lungs were dried. Each sample was placed in a 1.25-mL vial and sent to the University of Wisconsin Nuclear Reactor Laboratory for neutron activation analysis. Vials with known amounts of NiSO₄ standards or lung samples from exposed mice were passed through the nuclear reactor and irradiated for 4 hours (using an irradiation position designated as Whale 8). Beginning 375 hours later, each vial was counted for 2 hours at 0 cm (vertical axis) with a 170-cm³ intrinsic germanium detector (GEM-40190, Ortec Products, PerkinElmer Instruments, Wellesley MA) coupled to a multichannel analyzer (PC-based unit, Ortec Products). Peak areas were computed using a basic program compiled at the University of Wisconsin Nuclear Reactor Laboratory, NAACALC. Flux calculations were based on nickel content in known standards, and samples had less than 0.20% counter dead times.

STATISTICAL ANALYSES AND QUALITY ASSURANCE

To evaluate resistance to acute lung injury caused by NiSO₄, PTFE, or O₃, survival times were determined and are presented here as the means \pm SEs. Differences between means were assessed using an analysis of variance (ANOVA) followed by a Student-Newman-Keuls multiple comparison test of significance. To assess NiSO₄-induced changes in lung wet-to-dry weight ratios and in protein or PMNs in lavage fluid, values are presented as the means \pm SEs. Statistical analysis was performed using a 2-way ANOVA followed by a Student-Newman-Keuls test of significance. The factors for each analysis were

strain (A vs C3 vs B6C3F₁ vs B6) and exposure (exposed vs control). Analysis of cDNA microarray data was based on experiments performed by the manufacturer (Incyte Pharmaceuticals), which showed that 99% of the cDNAs displayed differential expression less than 1.4-fold for a single sample hybridized against itself (Braxton and Bedilion 1998). Genes were considered differentially expressed if the change was greater than 1.7-fold in this study. For S1 nuclease protection assays, samples were normalized to L32 and means were compared by 1-way ANOVA followed by the Dunnett test for multiple comparisons. Comparison of 2 means of multiple groups were evaluated by ANOVA in conjunction with the Student-Neuman-Keuls test for comparisons among all the groups or by the Dunnett test when the comparison of treated groups with a control group was of most concern. Sigma Stat (San Rafael CA) was used to analyze group variances and to determine statistical differences. Values were considered different when a level of significance (*P* value) less than 0.05 was obtained.

The data values were limited to 3 significant figures based on the most limiting measurements. Group values are expressed as the means \pm SEs. Animals were obtained solely from Jackson Laboratory to enable others to reproduce these genetic analyses and to provide for uniformity. Each shipment was given a unique number to allow for tracking of individual groups. Within a test, permanent markers were used for labeling samples from each individual animal as steps progressed through the study (eg, livers for DNA analysis). Spectrophotometers were autocalibrated before each use. Standard curves generated in each analysis were compared with historical analyses for spectrophotometer analysis of proteins. Balances and micropipettes were routinely calibrated. Data were recorded in ink in bound scientific notebooks. Copies of recordings were retained in chronological order. Computer programs for data analysis were used and backups were kept on separate disks.

RESULTS

STRAIN PHENOTYPE PATTERN

The survival times of 7 inbred mouse strains were used to quantitate acute lung injury induced by continuous exposures. After exposure to NiSO₄, the A strain was sensitive and the B6 strain was resistant to acute lung injury (Figure 1). Other strains, FVB/N, CBA, AKR, DBA/2, and C3, varied in sensitivity. The strain phenotype pattern observed with fine NiSO₄ was similar to that of the other 2 irritants tested, ultrafine PTFE and O₃ (Figure 1). The survival times decreased with each irritant (NiSO₄ >

PTFE > O₃); nonetheless, the pattern of a sensitive A strain and resistant B6 strain was consistent across the irritants. Of the 3 more common strains, the relative susceptibility for this trait followed the order A > C3 > B6.

MODE OF INHERITANCE

To determine whether resistance or sensitivity is recessive or dominant, the first-generation offspring of a cross of the resistant B6 strain mice with the sensitive A strain mice (B6AF₁) were exposed to NiSO₄. These mice were resistant, with survival times resembling those of the resistant B6 parental strain (Figure 2). Exposure to ultrafine

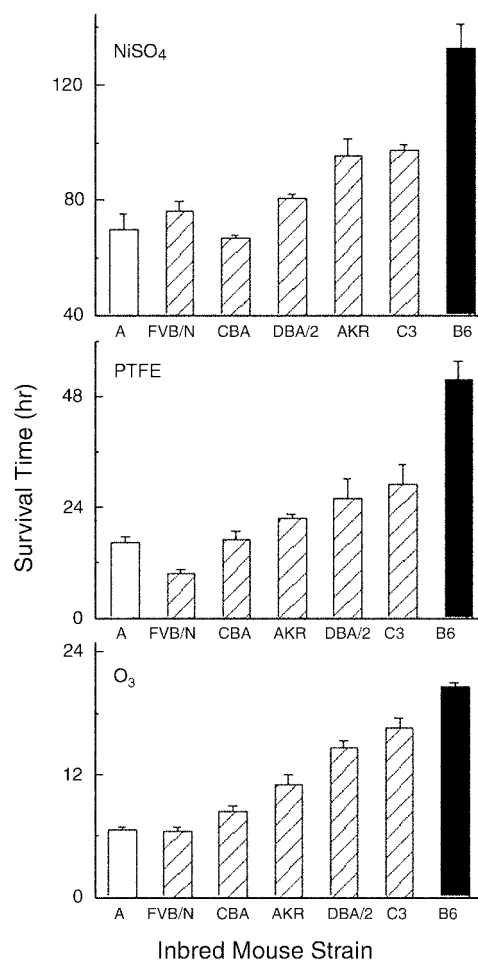


Figure 1. Survival times of 7 inbred strains of mice during continuous exposure to fine NiSO₄, ultrafine PTFE, and O₃. Mice were exposed continuously to NiSO₄ at 150 $\mu\text{g}/\text{m}^3$ (MMAD, 0.2 μm ; $\sigma_g = 1.9$), PTFE particles at $10^7/\text{cm}^3$, or 10 ppm O₃, and the time of death was recorded. The white bar shows the mean response for the A mouse strain; the hatched bars show means for strains with intermediate responses; the black bar shows the mean response for the resistant B6 strain. Values are means \pm SE ($n = 6$ to 27 mice/strain for NiSO₄, $n = 6$ to 15 mice/strain for PTFE, and $n = 9$ to 60 mice/strain for O₃).

PTFE or O_3 resulted in similar effects, with the B6AF₁ mice having survival times resembling those of the B6 parental strain (Figure 2). For each irritant, the response of the A strain was significantly less than that of the B6 strain, which was not significantly different from the B6AF₁ response. These findings suggest that resistance is inherited as a dominant trait, or that susceptibility is recessive.

PULMONARY HISTOPATHOLOGY INDUCED BY NICKEL SULFATE

Acute lung injury in the sensitive A strain and resistant B6 strain was evaluated by light microscopic observations and by measuring lung wet-to-dry weight ratios. The exposure-induced changes in pulmonary histology were comparable between the sensitive A strain and resistant B6 strain. When compared with corresponding control mice (Figures 3A and 3B), exposed mice had greater perivascular distention (Figures 3C and 3D) and focal loss of epithelial integrity, alveolar congestion, and alveolar hemorrhage, with luminal erythrocytes (Figures 3E and 3F). No strain differences between A and B6 mice were observed. At the time of death (MST \pm SE = 67 \pm 2 and 120 \pm 3 hours for A and B6 mice, respectively), lung wet-to-dry weight ratios of exposed mice increased significantly over those of their respective controls (Figure 4). No statistical difference was observed between control A and B6 mice or between exposed A and B6 mice at death, indicating the amount of lung edema at death was comparable between the two strains. Together with the results of lung histopathology, these findings indicate that the two strains succumbed to comparable acute lung injury, but varied in their innate ability to stave off those events that curtail survival time.

DOSE-RESPONSE RELATIONSHIP

Having found that A mice were sensitive, we then obtained dose-response information for this strain. Groups of 10 mice (5 males and 5 females) were continuously exposed for up to 14 days, and 100% mortality was observed at fine NiSO₄ aerosol concentrations of 150 and 60 $\mu\text{g}/\text{m}^3$ (Figure 5). At lower NiSO₄ concentrations of 30 and 15 $\mu\text{g}/\text{m}^3$, the A mice exhibited 60% and 20% mortality, respectively. The lethal dose of NiSO₄ producing 50% mortality (LD₅₀) was estimated to be 27 $\mu\text{g}/\text{m}^3$.

PULMONARY PROTEIN AND LEUKOCYTE INFILTRATION IN LAVAGE FLUID

Compared with nonexposed control mice, the A, B6, and C3 mice had greater levels of protein recovered by

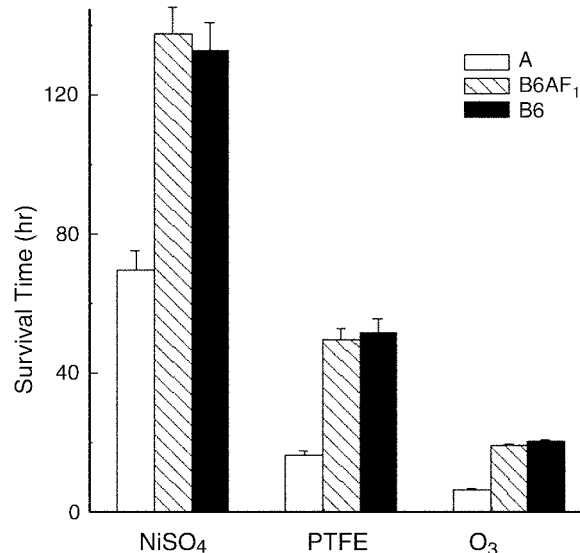


Figure 2. Survival times of A, B6AF₁, and B6 inbred mice during continuous exposure to fine NiSO₄, ultrafine PTFE, or O₃. Mice were exposed continuously to NiSO₄ at 150 $\mu\text{g}/\text{m}^3$ (MMAD, 0.2 μm ; $\sigma_g = 1.9$), PTFE particles at $10^7/\text{cm}^3$, or 10 ppm O₃. The white bars show the mean responses for the A (parental) mouse strain; the hatched bars show the mean responses for the offspring (B6AF₁), a cross of the parental strains (B6 and A); the black bars show the mean responses of the B6 (parental) mouse strain. With each irritant the A strain response was significantly less than the B6 or B6AF₁ responses; the B6 and B6AF₁ responses did not differ significantly. (Values are means \pm SE; $n = 6$ to 59 mice/strain for each irritant.) Statistical analysis was performed using a 2-way ANOVA followed by a Student-Newman-Keuls test of significance. Statistical significance for all comparisons of means was accepted at $P < 0.05$.

lavage after a 48-hour exposure to fine NiSO₄ aerosol. The amount of protein induced by exposure varied between strains. The response of the B6 strain was greatest with a mean value higher than that of the C3 or A strains (Figure 6). Of the 3 strains tested, susceptibility to lavage protein followed the order B6 > C3 \geq A. The cross of the sensitive B6 and the resistant C3 strains produced offspring (B6C3F₁) with a resistant phenotype, resembling the resistant C3 parental strain.

The PMNs and macrophages (monocytes) recovered in lavage after 48 hours of exposure are presented in Table 1. Relative to each strain's nonexposed control values, the A, B6, and C3 mice each had small, but significant increases in the percentage of PMNs recovered in lavage fluid. Again, the A and B6 strains had comparable responses, and the C3 strain was less responsive. Of the 3 strains tested, susceptibility to lavage PMNs followed the order A \geq B6 > C3. Cross of the sensitive B6 strain and resistant C3 strain produced offspring (B6C3F₁) that possessed a resistant phenotype (ie, their response was significantly less

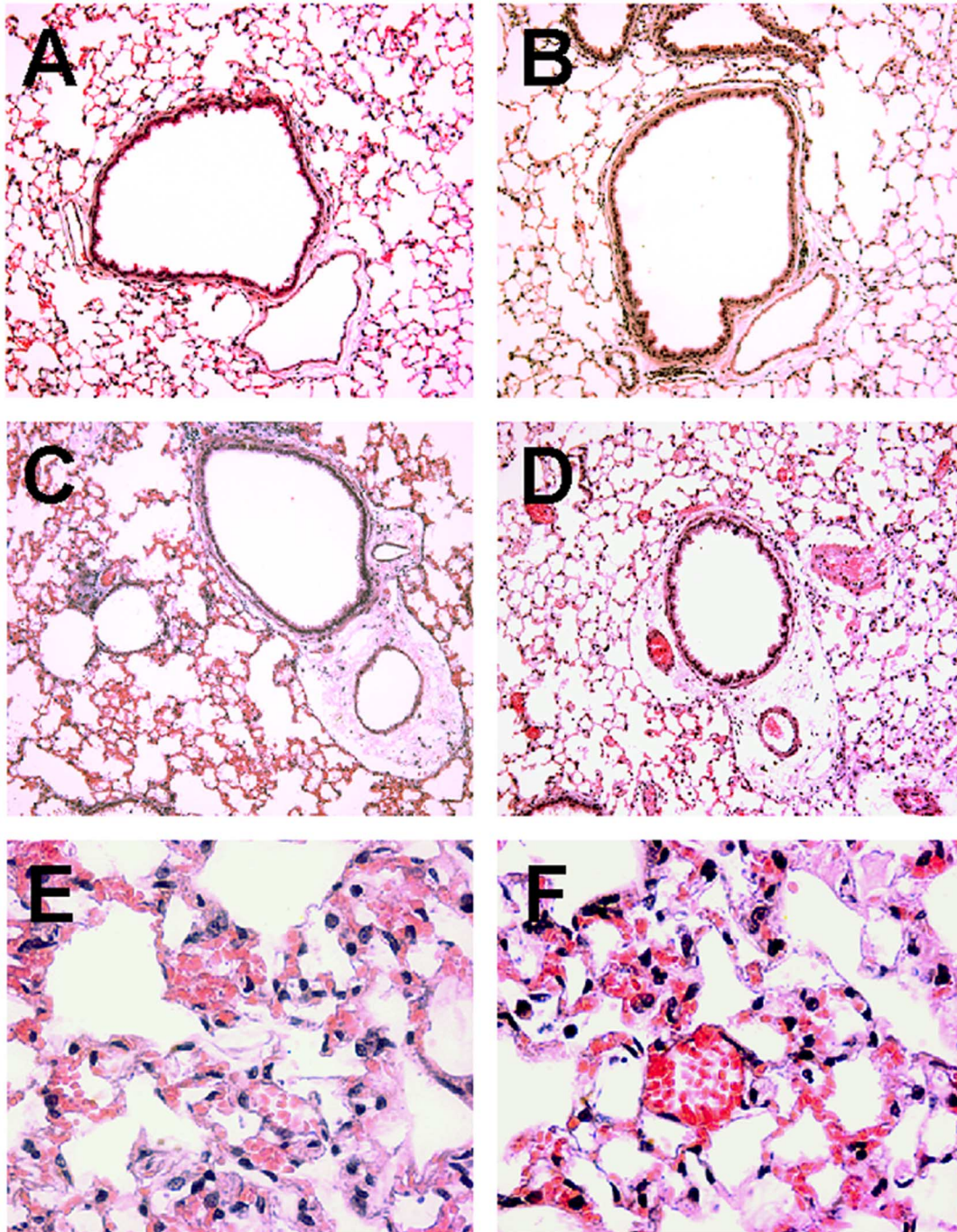


Figure 3. Lung histology of A and B6 inbred mice exposed continuously to filtered air or to fine NiSO₄ aerosol. Tissues from control mice or mice exposed to NiSO₄ (150 µg/m³) were fixed with phosphate-buffered formaldehyde solution, embedded in paraffin, stained with hematoxylin and eosin, and viewed by light microscopy. **A:** Control A strain mouse (original magnification, ×150). **B:** Control B6 strain mouse (×150). Each photomicrograph shows normal lung architecture of a large-diameter airway, vascular tissue, and surrounding alveoli. **C:** Exposed A strain mouse (×125). **D:** Exposed B6 strain mouse (×200). Each strain developed enlargement (fluid-filled cuffing) of the perivascular and peribronchial space. **E:** Exposed A strain mouse (×700). **F:** Exposed B6 strain mouse (×700). Each strain developed alveolar epithelial disruption, alveolar wall thickening, interstitial leukocytes, and luminal erythrocytes.

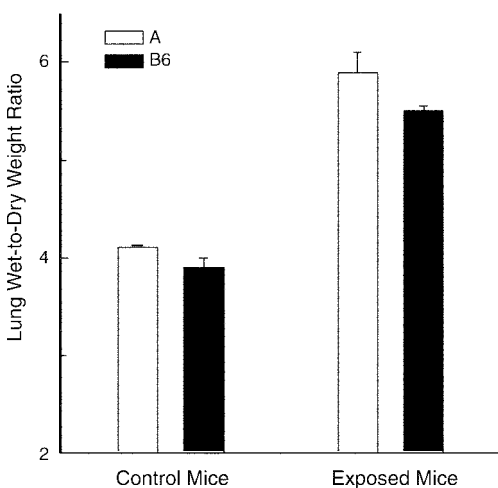


Figure 4. Lung wet-to-dry weight ratios of A and B6 inbred mice after continuous exposure to NiSO₄ aerosol. The white bars show the mean responses of the A strain mice; the black bars show the mean responses of the B6 strain mice. The bars on the left show lung wet-to-dry weight ratios from nonexposed control mice. The bars on the right show lung wet-to-dry weight ratios for mice exposed continuously to NiSO₄ at 150 µg/m³ (MMAD, 0.2 µm; $\sigma_g = 1.9$), with tissue obtained at the time of death. Statistical comparisons within a strain of exposed animals with respective nonexposed controls were significantly different. Statistical comparison of control A with control B6 mice or exposed A with exposed B6 mice were not significantly different. Values are presented as means \pm SE ($n = 5$ mice/strain for each exposure group). Statistical analysis was performed using a 2-way ANOVA followed by a Student-Newman-Keuls test of significance. Statistical significance for all comparisons of means was accepted at $P < 0.05$.

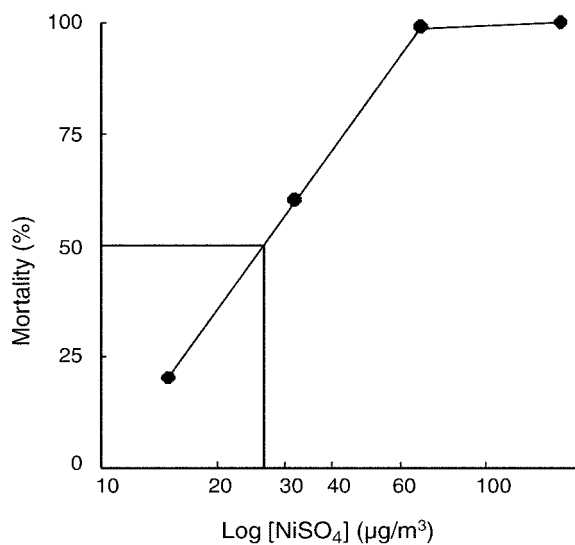


Figure 5. Dose-response relationship for mortality of sensitive A inbred mice during continuous exposure to fine NiSO₄ aerosol. Mice were exposed to the indicated concentrations of NiSO₄ aerosol (MMAD, 0.2 µm; $\sigma_g = 1.9$) for up to 14 days ($n = 10$ mice/dose; 5 males and 5 females). The LD₅₀ of NiSO₄ was estimated to be 27 µg/m³.

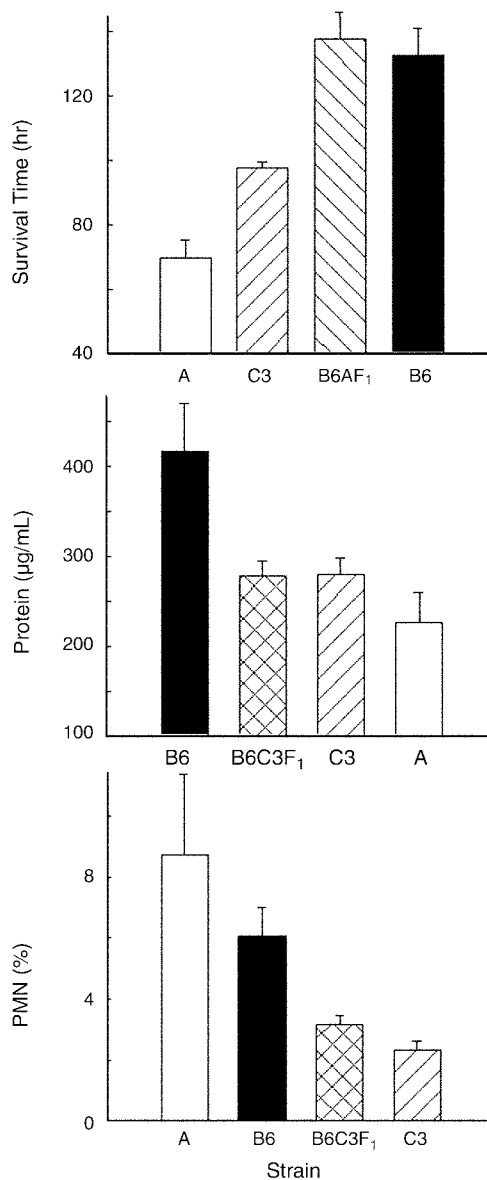


Figure 6. Discordance in the survival time (top panel), lavage protein (middle panel), and lavage PMN (bottom panel) phenotypes in selected mouse strains after continuous exposure to fine NiSO₄ aerosol. Strain responses are arranged from sensitive phenotypes (low survival time, high lavage protein, or high lavage PMNs) to resistant phenotypes. Survival times were measured during continuous exposure to NiSO₄ at 150 µg/m³. Protein concentration and percentage of PMNs were measured in lavage fluid after 48 hours of continuous exposure to NiSO₄ at 150 µg/m³. The strains tested were the parental strains A, C3, and B6, and the corresponding offspring of a cross of B6 with A (B6AF₁) and a cross of B6 with C3 (B6C3F₁). In each case, the response of the F₁ hybrid cross resembled that of the corresponding resistant parental strain. None of the 3 phenotypes shared the same strain pattern. Values are means \pm SE ($n = 5$ to 6 mice/strain for PMNs and protein; $n = 12$ to 27 mice/strain for survival time). Control values for PMNs were $\leq 1.1\% \pm 0.2\%$ in each strain; for protein, A = 80 ± 7 , C3 = 70 ± 8 , B6 = 119 ± 13 , and B6C3F₁ = 88 ± 5.4 µg/mL of lavage fluid.

Table 1. Macrophages and PMNs Recovered in Bronchoalveolar Lavage Fluid from Control Mice or from Mice Exposed to Nickel Sulfate^a

Strain	Control		Exposed ^b	
	Macrophage	PMNs	Macrophage	PMNs
A	16.3 ± 2.4	0.1 ± 0.02	20.0 ± 2.4	1.9 ± 0.7 ^{c,d}
B6	18.1 ± 1.1	0.1 ± 0.01	24.3 ± 4.5	1.4 ± 0.2 ^{c,d}
C3	17.8 ± 0.8	0.1 ± 0.01	19.3 ± 2.4	0.5 ± 0.2 ^{c,e}
B6C3F ₁	8.6 ± 0.9 ^e	0.1 ± 0.02	20.0 ± 1.2 ^c	0.7 ± 0.1 ^{c,e}

^a Values are cell number ($\times 10^4$) and presented as means \pm SE ($n = 5$ to 6 mice/strain/exposure). Statistical analysis was performed using a two-way ANOVA followed by a Student-Newman-Keuls test of significance. The factors for each analysis were strain (A vs C3 vs B6C3F₁ vs B6) and exposure (exposed vs control). Statistical significance for all comparisons of means was accepted at $P < 0.05$.

^b Exposure was to NiSO₄ at 150 $\mu\text{g}/\text{m}^3$ (MMAD, 0.2 μm) for 48 hours.

^c Significantly different from within-strain control.

^d Significantly different from C3 or B6C3F₁.

^e Significantly different from A or B6. Lymphocytes and epithelial cells were less than $0.1 \pm 0.01 \times 10^4$ cells and did not change significantly with exposure.

Table 2. Effect of Particle Size on Pulmonary Inflammation in B6 Mice Intratracheally Instilled with Saline (Control) or Nickel Oxide (300 $\mu\text{g}/\text{kg}$ body weight)

Particle Size (nm)	Cell Count ($\times 10^5$)	Cell Viability (%)	Protein (mg BSA/mL)	Neutrophils (%)
Control	2.2 ± 0.5	96 ± 0.7	0.08 ± 0.01	0.8 ± 0.4
40	1.6 ± 0.1	98 ± 0.1	0.09 ± 0.01	12.0 ± 6.0
130	2.7 ± 0.2	97 ± 0.4	0.07 ± 0.01	0.9 ± 0.3
300	1.8 ± 0.1	98 ± 0.3	0.08 ± 0.01	0.5 ± 0.1
1000	1.6 ± 0.5	97 ± 1.0	0.07 ± 0.01	0.8 ± 0.5

than that of the B6 parental strain, but not significantly different from that of the C3 parental strain). In this series of tests, protein and PMN counts were obtained from the same mouse; therefore, the association between these variables could be examined. The correlation coefficients (r^2) for the B6, C3, and B6C3F₁ mice were 0.11, 0.10, and 0.04, respectively. These results indicated that within a strain, protein in lavage fluid poorly correlated with PMNs in lavage fluid (ie, these traits were discordant) (Figure 6).

To examine the role of particle size, 4 size fractions of NiO powder in saline suspension were intratracheally instilled in mice. To study the role of speciation, mice were exposed by inhalation to 50-nm NiO, 60-nm NiSO₄, and 250-nm NiSO₄ aerosols. Responses in the form of PMNs or protein in lavage fluid from animals exposed to submicrometer NiO particles by intratracheal instillation were not statistically different from those of control animals (Tables 2 and 3). In addition, these responses in mice breathing 50-nm NiO particles (340 $\mu\text{g}/\text{m}^3$) for 6 to 72 hours

were not statistically different from those of controls. These results are in close agreement with those of other investigators using similar doses, but larger ($> 2 \mu\text{m}$) particles (Benson et al 1986, 1988, 1995; Dunnick et al 1988). In contrast, mice inhaling NiSO₄ particles had increases in PMNs and protein in lavage fluid that increased significantly with length of exposure (Table 4). In these tests, significant increases were noted after 48 hours and after 72 hours.

GENE EXPRESSION IN LUNGS OF B6 MICE

To determine the extent to which genes were differentially expressed during the initiation and progression of acute lung injury, we first assessed gene expression by cDNA microarray analysis in B6 mice. Of the 8,734 cDNAs analyzed at each exposure time, few genes initially changed in their level of expression relative to control. As lung injury progressed, however, the changes increased in number and magnitude (Figure 7). At 3 hours, 17 genes were differentially expressed (3 had increased and 14 had

Table 3. Effect of Particle Concentration on Pulmonary Inflammation in B6 Mice Intratracheally Instilled with Saline (Control) or Nickel Oxide (40 nm)^a

Mass Instilled (µg/kg)	Cell Count (± 10 ⁵)	Cell Viability (%)	Protein (mg BSA/ml)	Neutrophils (%)
Control	2.2 ± 0.5	96 ± 0.7	0.08 ± 0.01	0.8 ± 0.4
3	2.0 ± 0.2	98 ± 0.3	0.10 ± 0.01	0.4 ± 0.3
30	1.6 ± 0.1	99 ± 0.4	0.09 ± 0.01	0.2 ± 0.1
300	1.6 ± 0.1	98 ± 0.1	0.09 ± 0.01	12.0 ± 6.0
3000	1.9 ± 0.1	98 ± 0.5	0.04 ± 0.01	0.3 ± 0.1

^a Bronchoalveolar lavage was performed 18 hours after instillation. Values are means ± SE. Comparison of two means of multiple groups were evaluated by ANOVA in conjunction with Dunnett's test (treated groups compared to a control group). No value was statistically significant when compared to control ($P > 0.05$).

Table 4. Pulmonary Inflammation in B6 Mice After Inhalation of Nickel Oxide or Nickel Sulfate^a

Variable ^b	Control	Duration of Exposure			
		6 hours	24 hours	48 hours	72 hours
Cell Count (× 10⁵)	1.5 ± 0.1				
NiO 50 nm: 340 µg/m ³		1.1 ± 0.1	1.5 ± 0.7	1.9	1.9 ± 0.3
NiSO ₄ 60 nm: 420 µg/m ³			1.2 ± 0.1	2.3 ± 0.6	2.9 ± 0.2 ^c
NiSO ₄ 250 nm: 480 µg/m ³			1.7 ± 0.1	2.0 ± 0.6	1.2 ± 0.2 ^c
Cell Viability (%)	97 ± 0.6				
NiO 50 nm: 340 µg/m ³		96 ± 0.4	99 ± 0.6	99	99 ± 0.4
NiSO ₄ 60 nm: 420 µg/m ³			94 ± 0.4	94 ± 0.8	93 ± 0.8 ^c
NiSO ₄ 250 nm: 480 µg/m ³			89 ± 1.4 ^c	92 ± 0.9 ^c	93 ± 0.4 ^c
Protein (mg BSA/mL)	0.10 ± 0.01				
NiO 50 nm: 340 µg/m ³		0.05 ± 0.01	0.05 ± 0.01	0.05	0.05 ± 0.01
NiSO ₄ 60 nm: 420 µg/m ³			0.11 ± 0.01	0.26 ± 0.01 ^c	0.41 ± 0.05 ^c
NiSO ₄ 250 nm: 480 µg/m ³			0.14 ± 0.01	0.21 ± 0.03	1.09 ± 0.08 ^c
Neutrophils (%)	0.4 ± 0.3				
NiO 50 nm: 340 µg/m ³		0.9 ± 0.4	5.0 ± 0.7	0.2	0.1 ± 0.9
NiSO ₄ 60 nm: 420 µg/m ³			0.6 ± 0.2	22.1 ± 7.2 ^c	14.6 ± 6.6 ^c
NiSO ₄ 250 nm: 480 µg/m ³			2.6 ± 0.7	6.8 ± 4.1	33.5 ± 4.5 ^c

^a Bronchoalveolar lavage was performed 15 hours after a 6-hour exposure. Values are means ± SE ($n = 3$ to 4 mice/treatment) except values without SE, which are means alone ($n = 2$).

^b The particle geometric standard deviation for 50 nm NiO = 1.6, for 60 nm NiSO₄ = 1.7, and for 250 nm NiSO₄ = 1.9.

^c Significantly different from control. Statistical analysis was performed using a 2-way ANOVA followed by Dunnett's test (treated groups compared with control group). Statistical significance for all comparisons of means was accepted at $P < 0.05$.

decreased). The largest increase was 3 times the control, and the largest decrease was 4-fold lower than the control. In contrast, at 96 hours, 255 genes were differentially expressed (125 had increased and 130 had decreased). At 96 hours, the maximal increase was 13 times the control and the maximal decrease was 33-fold lower than the control.

To assess the coregulation of gene expression, results were grouped according to similarities in expression with time. Genes differentially expressed relative to control at 2 or more times (≥ 1.8 -fold, 100 genes) were clustered into 4 major temporal groups (Figure 8). Group I contained genes that increased steadily throughout nickel exposure and

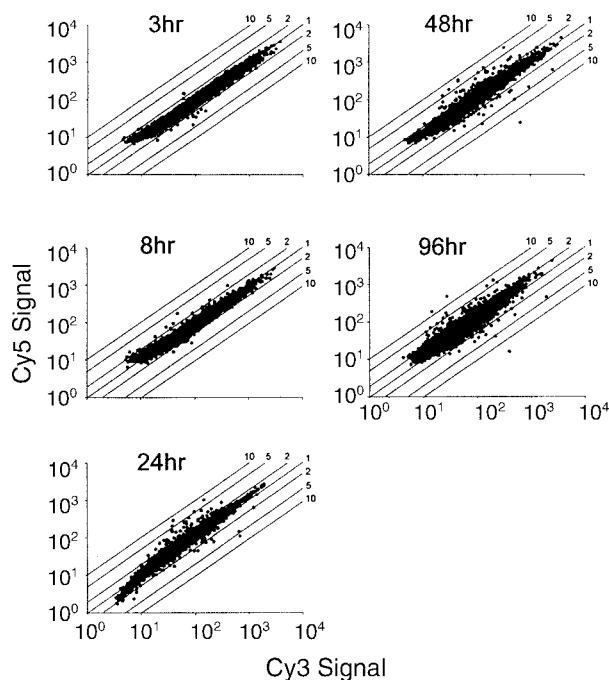


Figure 7. Differential gene expression in lungs from B6 mice exposed to NiSO₄. Polyadenylated mRNA from the B6 mouse lung was isolated after exposure to NiSO₄ (110 µg/m³; MMAD, 0.2 µm), for 3, 8, 24, 48, or 96 hours, and labeled during reverse transcription with the fluorescent dye Cy5. These samples were competitively hybridized with Cy3-labeled cDNA from the lungs of unexposed B6 control mice to microarrays of 8,734 murine cDNAs. After hybridization of Cy3 and Cy5 samples, scans were acquired for each fluorophore at each target cDNA element. Each point represents the Cy3-versus-Cy5 signal value for each cDNA element, and slanted lines delineate fold changes.

included the metallothionein-1, glyceraldehyde-3-phosphate dehydrogenase (GAPDH), thioredoxin reductase-1, lactotransferrin, small proline-rich protein 1a, and galectin-3 genes. Group II contained genes that had a delayed increase and included secretory leukoprotease inhibitor and lysyl oxidase. Group III contained genes that steadily decreased in response to nickel and contained mainly nonannotated ESTs (with no homology to known genes) and a few known genes, including ubiquitin hydrolyzing enzyme-1 and L-selectin. Group IV contained genes that had a delayed decrease and included SP-C and Clara cell secretory protein (CCSP). Of the 100 genes that were clustered, 53 were known genes, 15 were ESTs highly homologous to known genes, and 32 were ESTs with nominal homology to known genes. Groups I and II contained genes that increased and were enriched in annotations when compared with Groups III and IV, possibly reflecting the bias of experimenters to find increases that occur with exposures. In addition, the number of known genes and ESTs that increased approximated the number of genes that decreased, suggesting that gene expression achieved a new equilibrium (genomic balance) in response to nickel.

To assess the pathophysiology of changes in gene expression, genes within these 4 temporal groups were further organized into functional categories (Table 5). Genes sharing common temporal patterns often shared common functions. Temporal Group I included several genes categorized in functional groups of metabolism (eg, aldolase, enolase, and GAPDH) and immunity (eg, galectin-3 and signal transducer and activator of transcription-3 [STAT-3]). Group II was enriched in genes of the oxidoreductase category including heme oxygenase-1 and lysyl oxidase. Combining temporal Groups I and II (genes that either increased steadily or were delayed) revealed several genes in the category of protein modification and maintenance and included 2 antiproteases, secretory leukoprotease inhibitor and serine proteinase inhibitor-2 (*spi2*). Group IV genes often fell into a group defined as cell-specific genes, including SP-C, CCSP, and cytochrome P450 2f2. Members of this category were found to be genes expressed constitutively in the lung, including 2 nonannotated ESTs that were further sequenced and found to have homology with SP-B (obtained by BLAST search after sequencing of selected clones).

Expression levels of 2 genes that increased using microarray analysis, metallothionein-1 and heme oxygenase-1, were also examined by Northern blot analysis. The extent of expression changes and temporal patterns for both genes determined by the two methods were similar (Figure 9). Metallothionein-1 expression increased by 3 hours (microarray, 2.5-fold; Northern blot, 2.3 ± 0.4 -fold) and continued to increase through 8 hours (microarray, 4.2-fold; Northern blot, 5.3 ± 0.8 -fold), 24 hours (microarray, 6.2-fold; Northern blot, 11.4 ± 3.4 -fold), and 48 hours (microarray, 6.5-fold; Northern blot, 9.8 ± 2.3 -fold). Metallothionein-1 expression reached its highest level by 96 hours (microarray, 13.1-fold; Northern blot, 11.6 ± 0.7 -fold). Heme oxygenase-1 increased in expression at 8 hours (microarray, 2.6-fold; Northern blot, 3.8 ± 0.6 -fold) and again at 96 hours (microarray, 4.8-fold; Northern blot, 3.0 ± 1.3 -fold). (This cDNA on the 96-hour microarray covered 37% of its grid, failing to meet the criterion of 40% coverage; however, the balanced differential value is included because of verification by Northern blot analysis.)

Decreases in gene expression for SP-B and SP-C obtained by the microarray analysis were compared with those assessed by S1 nuclease protection assays for SP-A, SP-B, and SP-C (Figure 10). (Note that the microarray lacked a cDNA encoding SP-A.) The microarray and the S1 analyses displayed the same trend: expression of SPs decreased with progression of lung injury. As observed with the microarray analysis, SP-B and SP-C expression decreased by 24 hours relative to control (microarray, SP-B, 3-fold; SP-C, 6-fold; and S1 analysis, SP-B, 7-fold; SP-C, 6-fold). Gene expression

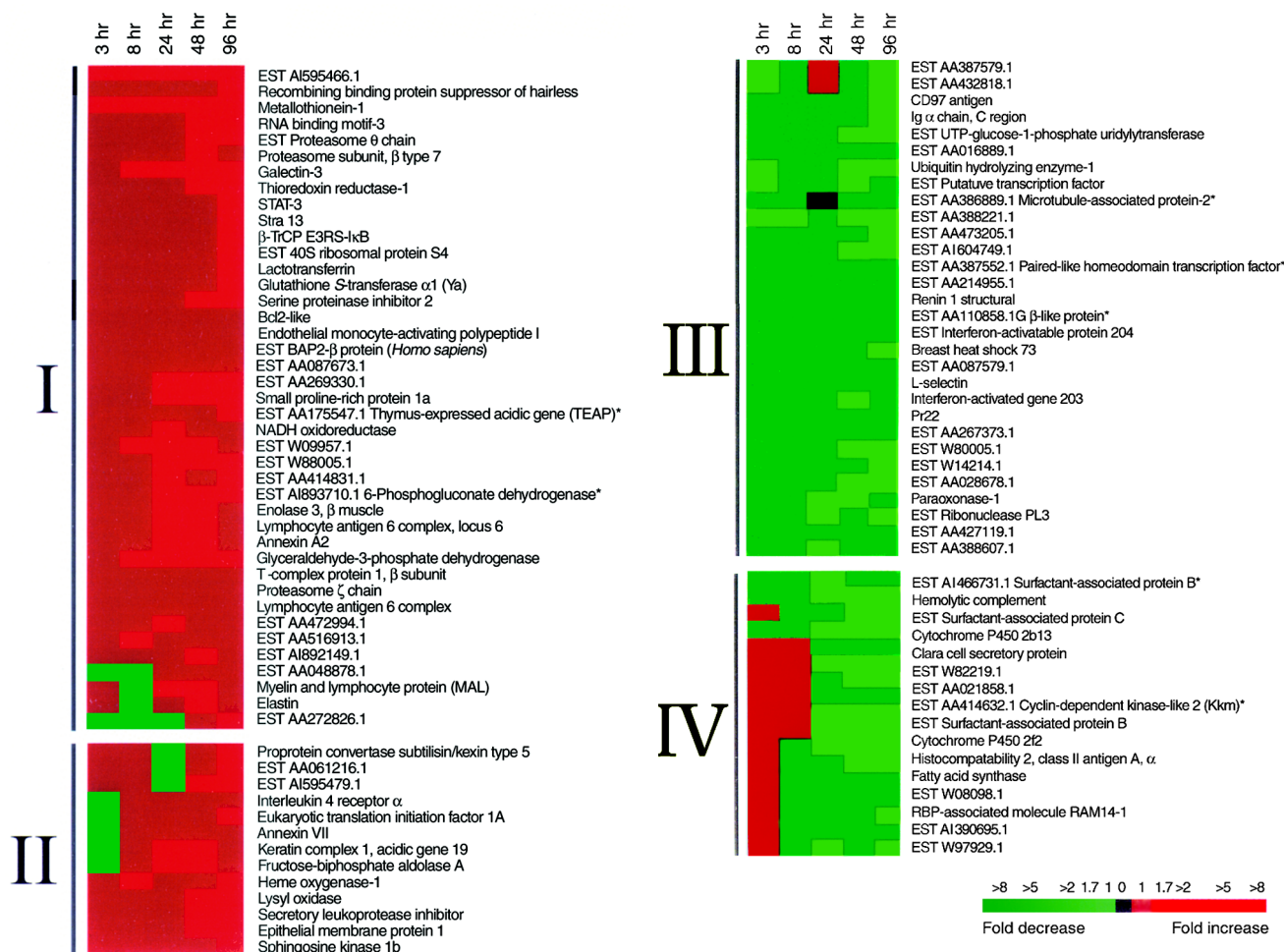


Figure 8. Temporal clustering of mRNA levels coregulated in B6 mouse lung after exposure to NiSO₄ (110 μ g/m³; MMAD 0.2 μ m). Lung cDNA was analyzed by microarrays containing 8,734 murine cDNA elements. Genes with 2 or more changes relative to control (balanced differential > 1.7-fold) were clustered using the gene similarity metric developed by Eisen and colleagues (1998). Cells representing increased gene expression relative to control are colored red, and those representing decreased expression relative to control are colored green. Black is assigned to missing values. The scale displays relative levels of expression. Large groups displaying similar expression patterns (coregulation) are designated I, II, III, and IV. Only ESTs designated as highly similar to known genes are annotated. *Nonannotated EST found by BLAST search (nonredundant GenBank, EMBL, DDBJ, and PDB sequences) to be highly homologous to known gene.

continued to decrease through 48 hours (microarray, SP-B, 5-fold; SP-C, 30-fold; and S1 analysis, SP-B, 14-fold; SP-C, 50-fold) and through 96 hours (microarray, SP-B, 4-fold; SP-C, 33-fold; and S1 analysis, SP-B, 13-fold; SP-C, 100-fold). SP-A also decreased after 24 hours of exposure. Although the quantified results were not identical, differential expression patterns were similar between assays.

QUANTITATIVE TRAIT LOCUS ANALYSIS

To begin the identification of genetic determinants for nickel-induced acute lung injury, offspring generated from F₁ mice (A \times B6 or B6 \times A) backcrossed with A strain mice (F₁ \times A or A \times F₁) were phenotyped by exposure to NiSO₄

(Figure 11). As noted in Figure 2, the A strain was sensitive, and the B6 and the F₁ mice were resistant, suggesting that a major dominant gene could impart resistance to the offspring (a Mendelian single gene effect). The distribution of backcross (F₁ \times A and A \times F₁) phenotypes displayed decreased kurtosis (increased dispersion due to variance), which is inconsistent with a single gene effect. Quantitative trait locus analysis of any data set assumes that the population is normally distributed. Because the phenotype distribution exhibited skewness, survival times were log-transformed to generate a normal distribution (Figure 12).

To initially identify possible QTLs influencing survival of nickel-induced lung injury, the 55 most sensitive backcross mice (survival time \leq 66 hours) and the 54 most resistant

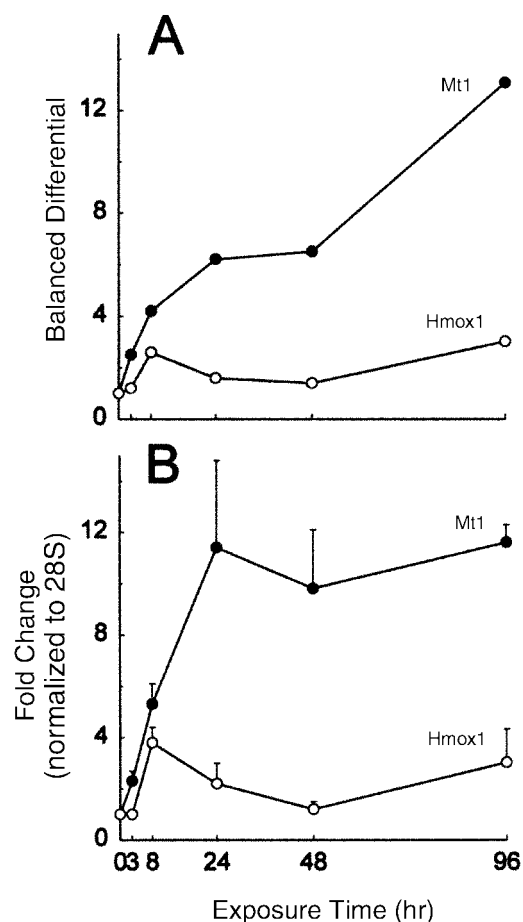


Figure 9. Comparison by microarray and Northern blot analyses of 2 genes that increased in B6 mice exposed to NiSO₄ (110 µg/m³; MMAD, 0.2 µm). **A:** Lung mRNA (pooled from *n* = 3 mice/treatment) was analyzed by cDNA microarrays, and balanced differential expression values were calculated. **B:** Lung mRNA (*n* = 3 mice/treatment) was analyzed by Northern blots. Mt1 and rat Hmox1 cDNAs were used as the templates for [³²P]-labeled riboprobes (hybridization at 65°C, 16 hours). Each blot was subsequently probed using a [³²P]-labeled oligonucleotide to 28S rRNA (hybridization at 42°C, 3 hours). Levels of Mt1 and rat Hmox1 were quantified by phosphorimaging and normalized to 28S rRNA and are presented as fold of control (± SE of 3 samples).

backcross mice (survival time ≥ 112 hours), representing the polar extremes in survival time, were typed for 77 microsatellite markers throughout the genome, and results from this cohort of mice were analyzed by MAP-MAKER/QTL. The theoretical levels for significant and suggestive linkage proposed by Lander and Kruglyak (1995) were used to identify potential QTLs in the polar responders. Regions reaching suggestive linkage (ie, lod scores ≥ 1.9) were identified on chromosomes 1, 6, 8, 9, 12, and 16, with lod scores for these 6 putative QTLs ranging from 2.1 to 2.8. Together, these 6 QTLs explained more than 62% of the genetic variation in the 109 extreme-responding

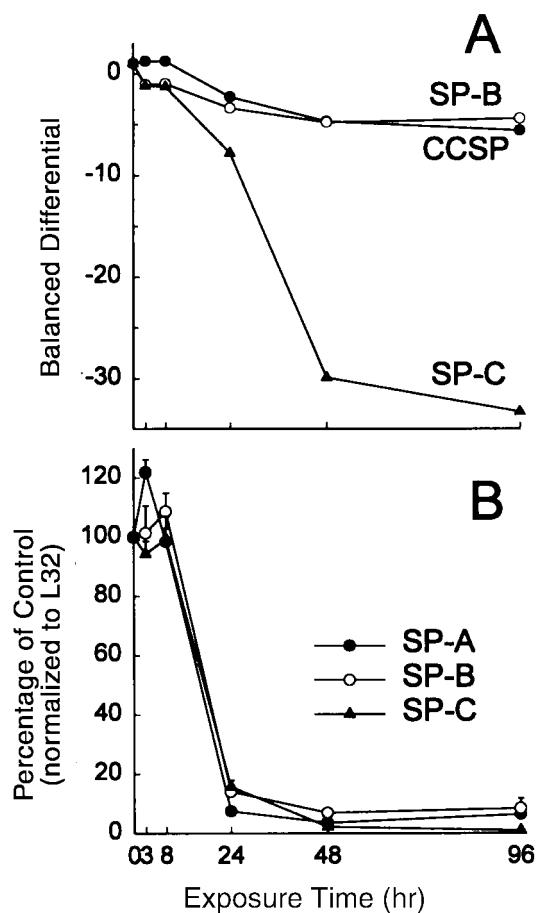


Figure 10. Comparison of cDNA microarray and S1 nuclease protection assays of mRNA levels of genes constitutively expressed in lungs from B6 mice exposed to NiSO₄ (110 µg/m³; MMAD, 0.2 µm). **A:** Lung mRNA (pooled from *n* = 3 mice/treatment) was analyzed by cDNA microarrays, and balanced differential expression values were calculated. **B:** Lung mRNA (*n* = 3 mice/treatment) was analyzed by S1 nuclease protection assays. DNA probes specific for murine SP-A, SP-B, SP-C, and L32 were linearized, end-labeled with ³²P-ATP, combined, and hybridized (3 µg, 55°C, 16 hours) with total lung RNA used for microarray analysis. Single-stranded regions were digested away from protected double-stranded fragments by S1 nuclease. The protected fragments were then denatured, electrophoresed, and quantified by phosphorimaging. Levels of SP-A, SP-B, and SP-C were normalized to L32 quantified by phosphorimaging and are presented as percentage of control (± SEM of 3 separate assays).

backcross mice (Table 6). Using a modified formula of Wright (Silver 1995), which incorporates the MSTs and variances of the parental, backcross, and F₁ populations, 5 genes were estimated to be independently segregating with survival of nickel-induced acute lung injury.

To determine the significance of these QTLs and to better ensure detection of minor contributing QTLs in the total backcrosses (*n* = 307), all backcross mice were typed for the original 77 microsatellite markers and another 32 microsatellite markers in the suggestive QTL intervals.

Table 5. Functional Categories of Differentially Expressed Genes in B6 Mice

Total	Gene Increased in Expression	Total	Gene Decreased in Expression
Signal transduction / regulation (category total 788; changes 7)			
4	<ul style="list-style-type: none"> β-TrCP E3RS-IκB Endothelial monocyte-activating polypeptide 1 Interleukin 4 receptor α STAT-3 	3	<ul style="list-style-type: none"> EST CD97 L-Selectin Pr22
Oxidoreductases (category total 148; changes 7)			
4	<ul style="list-style-type: none"> Glyceraldehyde-3-phosphate dehydrogenase Lysyl oxidase Metallothionein-1 NADH oxidoreductase 	3	<ul style="list-style-type: none"> Cytochrome P450 2b13 Cytochrome P450 2f2 Fatty acid synthase
Metabolism (category total 1230; changes 29)			
21	<ul style="list-style-type: none"> Aldolase 1, A isoform Annexin A2 β-TrCP E3RS-IκB eIF-1A Enolase 3, β muscle EST 40S ribosomal protein S4 EST Proteasome θ chain EST Proteasome θ chain Glutathione S-transferase α1 (Ya) Glyceraldehyde-3-phosphate dehydrogenase Lactotransferrin Metallothionein-1 NADH oxidoreductase Proprotein convertase subtilisin/kexin type 5 Proteasome subunit, β type 7 Proteasome ζ chain Recombining binding protein suppressor of hairless Secretory leukoprotease inhibitor Serine proteinase inhibitor 2 (spi2/eb1) Sphingosine kinase 1b (SPHK1b) STAT-3 T-complex protein 1, β subunit 	8	<ul style="list-style-type: none"> Clara cell secretory protein Cytochrome P450 2f2 EST Ribonuclease PL3 EST UTP-glucose-1-P uridylyltransferase Fatty acid synthase Hemolytic complement Renin 1, structural Ubiquitin hydrolyzing enzyme-1
Immunity (category total 205; changes 9)			
5	<ul style="list-style-type: none"> Endothelial monocyte-activating polypeptide I Galectin-3 Interleukin 4 receptor α NADH oxidoreductase STAT-3 	4	<ul style="list-style-type: none"> Hemolytic complement Histocompatibility 2, class II antigen A, α chain Ig α chain, C region L-Selectin

(Table continues on next page)

Table 5 (continued). Functional Categories of Differentially Expressed Genes in B6 Mice

Total	Gene Increased in Expression	Total	Gene Decreased in Expression
Protein modification/maintenance (category total 172; changes 9)			
7	EST Proteasome θ chain Proprotein convertase subtilisin/kexin type 5 Proteasome subunit, beta type 7 Proteasome ζ chain Secretory leukoprotease inhibitor Serine proteinase inhibitor (spi2/eb1) T-complex protein 1, β subunit	2	Hemolytic complement Renin 1, structural
Structure and cell-specific genes (category total 1435; changes 26)			
15	Annexin A2 β -TrCP E3RS-I κ B Elastin Endothelial monocyte-activating polypeptide 1 Epithelial membrane protein 1 EST 40S ribosomal protein S4 Galectin-3 Interleukin 4 receptor α Keratin complex 1, acidic, gene 19 Lactotransferrin Lymphocyte antigen 6 complex NADH oxidoreductase Recombining binding protein suppressor of hairless Secretory leukoprotease inhibitor Serine proteinase inhibitor 2 (spi2/eb1)	10	Adenylate cyclase 7 Clara cell secretory protein (CCSP) Cytochrome P450 2f2 EST CD97 EST ribonuclease PL3 Hemolytic complement Histocompatibility 2, class II antigen A, α chain Paraoxonase-1 Renin 1, structural Surfactant-associated protein C
Adhesion and molecular recognition (category total 97; changes 5)			
2	Galectin-3 NADH oxidoreductase	3	Histocompatibility 2, class II antigen A, α chain Ig α chain, C region L-Selectin
Hydrolases (category total 267; changes 9)			
4	EST proteasome θ chain Proprotein convertase subtilisin/kexin type 5 Proteasome subunit, β type 7 Proteasome ζ chain	5	EST ribonuclease PL3 Fatty acid synthase Renin 1, structural Hemolytic complement Paraoxonase-1
Transferases (category total 280; changes 3)			
1	Glutathione S-transferase α 1 (Ya)	2	EST UTP-glucose-1-P uridylyltransferase Fatty acid synthase
Environmental response (category total 94; changes 2)			
1	Metallothionein-1	1	EST ribonuclease PL3
Membrane transport (category total 93; changes 1)			
1	Lactotransferrin	0	
Nucleic acid synthesis (category total 84; changes 2)			
1	Recombining binding protein suppressor of hairless	1	EST ribonuclease PL3

(Table continues on next page)

Table 5 (continued). Functional Categories of Differentially Expressed Genes in B6 Mice

Total	Gene Increased in Expression	Total	Gene Decreased in Expression
Growth and development (category total 544; changes 5)			
5	<ul style="list-style-type: none"> β-TrCP E3RS-IκB Bcl2-like Interleukin 4 receptor α NADH oxidoreductase Recombining binding protein suppressor of hairless Rom I 	0	
Kinesis (category total 171; changes 1)			
1	Annexin A2	0	
Lyases (category total 45; changes 3)			
2	<ul style="list-style-type: none"> Aldolase 1, A isoform Enolase 3, β muscle 	1	Fatty acid synthase
Ligases (category total 60; changes 0)			
Isomerases (category total 33; changes 0)			

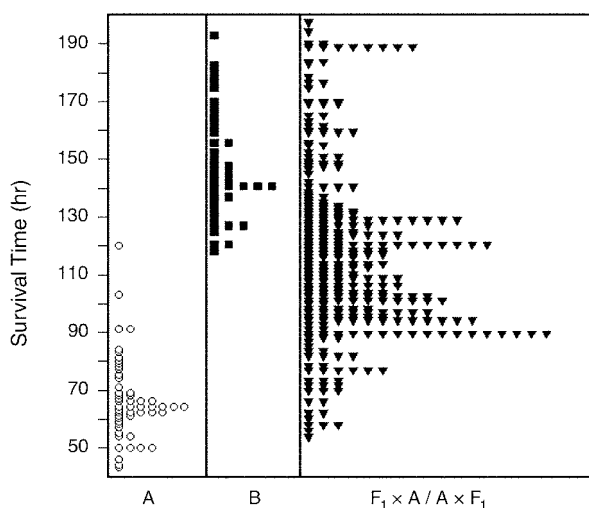


Figure 11. Phenotype distribution pattern of A and B6 strain mice and their F₁ hybrid offspring after exposure to fine NiSO₄. Parental strains A and B6, their first-generation progeny (F₁), and backcrosses (F₁ × A/A × F₁) were exposed continuously to NiSO₄ at 150 μg/m³ (MMAD, 0.2 μm; σ_g = 1.85), and the time of death was recorded. Each symbol indicates the survival time of a single mouse.

Linkages determined to be significant ($\alpha = 0.05$) or suggestive ($\alpha = 0.1$) were set at empirical levels determined by 10,000 permutations of the total backcross data set using QTL Cartographer (Basten et al 1997). Accordingly, experimentwise levels were determined at a lod score ≥ 2.6 for significant linkages and a lod score ≥ 2.3 for suggestive linkages. Three of the 6 QTLs (chromosomes 1, 6, and 12) were linked to survival of nickel-induced acute lung injury by MAPMAKER/QTL analysis of the total backcross population (Figure 13). The QTL on chromosome 6 was significantly linked, reaching a peak lod score of 3.0 at *D6Mit183*. In keeping with the previous nomenclature, we have designated this QTL on chromosome 6 as *Aliq4*, for acute lung injury QTL4. The other putative QTLs had lod scores suggestive of linkage. The QTL on chromosome 1 reached suggestive linkage, with a peak 4 cM distal to *D1Mit213* and a lod score of 2.5. In addition, proximal chromosome 12 had 2 intervals reaching suggestive linkage (both had lod scores of 2.3), with peaks at *D12Mit185* and *D12Mit112*. Reanalysis and verification of the genotypes for markers in this region of chromosome 12 did not eliminate the dual peaks. Assuming independence of loci, the 3 QTLs had a combined lod score of 7.9 and explained about 12% of the genetic variance (Table 6). The QTLs on chromosome 8 (peak 6 cM distal to *D8Mit65*; lod score, 2.2), chromosome 9 (*D9Mit227*; lod score, 1.6), and chromosome 16 (*D16Mit152*;

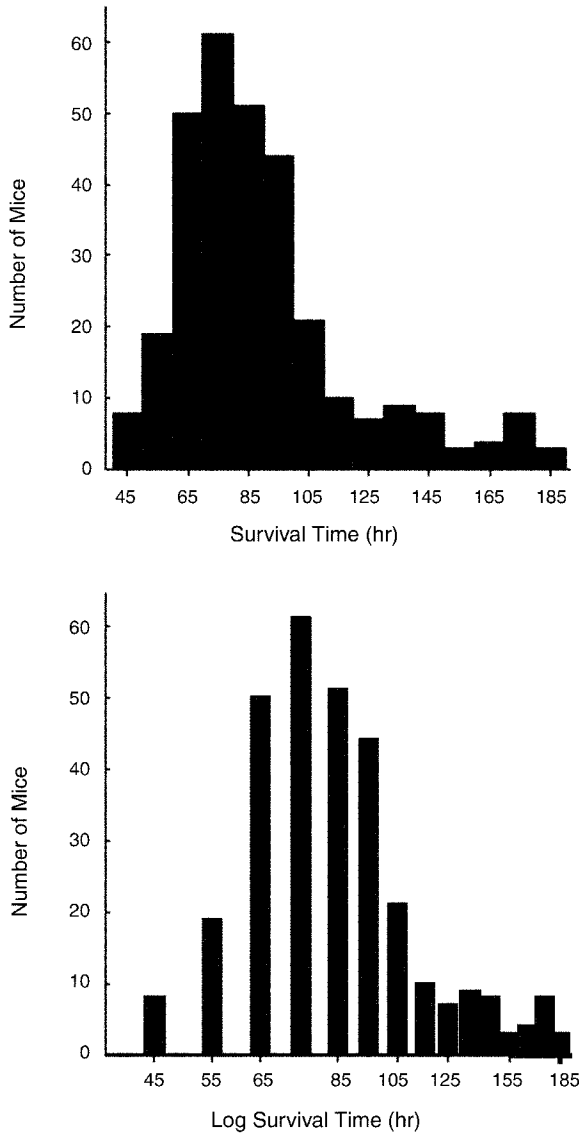


Figure 12. Survival time distributions of backcross mice before and after log transformation. The survival times of 307 $F_1 \times A/A \times F_1$ backcross mice were grouped into 10-hour intervals (top panel). Log transformation eliminated the left skewness of the original data set to meet the assumption of a normal distribution for MAPMAKER/QTL analysis (bottom panel).

lod score, 1.6), initially identified as suggestive loci in the phenotypic extreme backcrosses, did not reach experimentwise suggestive linkage (ie, lod score ≥ 2.3) in the total backcross population. To test for possible interactions among the putative QTLs, the total backcross data set was analyzed with Epistat (Chase et al 1997) and the *cumulative search* function of MAPMAKER/QTL (Lincoln et al 1992b). No significant interactions between the putative QTLs were found.

Table 6. MAPMAKER/QTL Analysis of Nickel-Induced Acute Lung Injury in Total and Extreme-Responding Backcross Populations^a

Backcross Population ^b	QTL Analysis			QTL Analysis with Cumulative Search			
	QTL Position	Lod Score	% Variance Explained	QTL Scan [Fixed Loci/QTL]	Position of Largest Lod Score Change	Lod Score (Change)	% Variance Explained
Extreme Responders (<i>n</i> = 109) (66 hr \leq MST \leq 112 hr)	<i>D1Mit213</i> + 2 cM	2.8	11.9	No fixed loci	<i>D6Mit183</i> (<i>Aliq4</i>)	2.8	11.3
	<i>D6Mit183</i>	2.8	11.3	[<i>Aliq4</i>]	<i>D1Mit213</i> + 4 cM	5.8 (+3.0)	22.5
	<i>D8Mit65</i> + 2 cM	2.5	10.5	[<i>Aliq4</i>] [1]	<i>D9Mit229</i>	8.4 (+2.6)	31.2
	<i>D12Mit12</i>	2.5	9.9	[<i>Aliq4</i>][1] [9]	<i>D8Mit65</i> + 6 cM	10.6 (+2.2)	37.1
	<i>D9Mit227</i> + 4 cM	2.4	9.9	[<i>Aliq4</i>][1] [9] [8]	<i>D16Mit152</i>	12.1 (+1.5)	40.4
	<i>D16Mit152</i>	2.1	8.9	[<i>Aliq4</i>][1] [9] [8] [16]	<i>D12Mit185</i>	12.5 (+0.4)	41.6
Total Backcrosses (<i>n</i> = 307)	<i>D6Mit183</i> (<i>Aliq4</i>)	3.0	4.4	No fixed loci	<i>Aliq4</i>	3.0	4.4
	<i>D1Mit213</i> + 4 cM	2.5	4.1	[<i>Aliq4</i>]	<i>D1Mit213</i> + 4 cM	6.0 (+3.0)	9.1
	<i>D12Mit112</i>	2.3	3.4	[<i>Aliq4</i>][1]	<i>D12Mit112</i>	8.3 (+2.3)	12.2

^aMAPMAKER/QTL was used to scan the genome of backcross mice for putative QTLs linked to the nickel susceptibility phenotype. For cumulative search analyses, loci on chromosomes in brackets were fixed to remove the variance explained by the more prominent QTLs and the genome was rescanned to identify QTLs that could explain more of the overall genetic variance. *Aliq4* on chromosome 6 was the major QTL identified (at *D6Mit183*) and modifier loci were suggested on chromosomes 1 and 12. Loci on chromosomes 8, 9 and 16 suggested linkage only in the extreme-responding cohort.

^b Backcross mice were the offspring of F_1 hybrids of $A \times B6$ or $B6 \times A$ crossed with A strain mice ($F_1 \times A$ or $A \times F_1$).

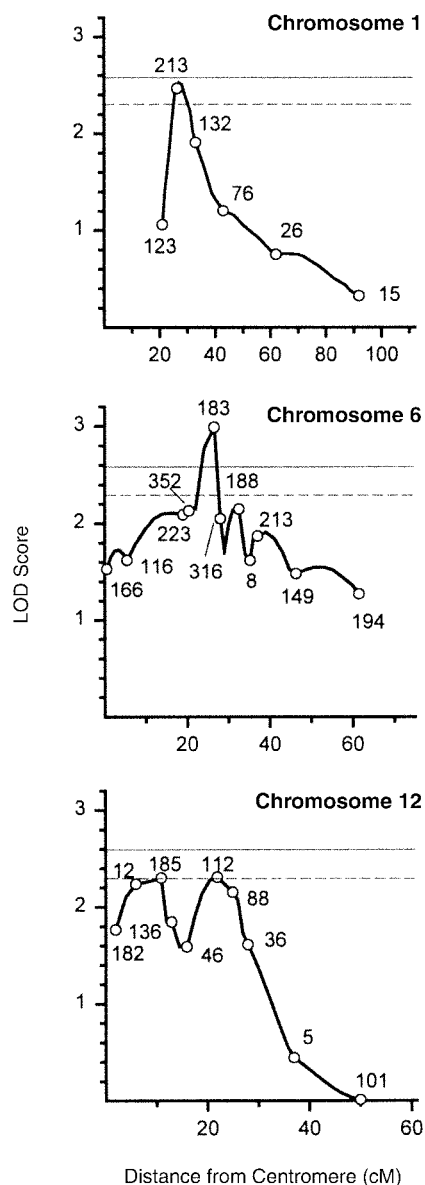


Figure 13. QTL analysis for acute lung injury induced by NiSO₄. Backcross mice ($F_1 \times A$, $n = 162$; and $A \times F_1$, $n = 145$ mice) were exposed continuously to NiSO₄ at 150 $\mu\text{g Ni/m}^3$ (MMAD, 0.2 μm ; $\sigma_g = 1.85$), the time of death was recorded, and an initial genome scan was performed with 77 microsatellite markers (location identified by number near line) distributed at intervals of 20 to 30 cM. Regions on chromosomes 1, 6, 8, 9, 12, and 16 had lod scores above 1.5 and were subsequently genotyped for another 27 microsatellite markers. The results were analyzed by the MAP-MAKER/QTL software program. White circles on curves represent positions of the designated microsatellite markers. Solid horizontal lines (at lod score 2.6) and dashed horizontal lines (at lod score 2.3) denote significant or suggestive linkage, respectively, as determined empirically by 10,000 permutations of the original data set using QTL Cartographer (Basten et al 1997). *Aliq4* peaked at *D6Mit183* on chromosome 6, and regions with suggestive linkage were determined on chromosomes 1 and 12.

HAPLOTYPE ANALYSIS

To determine the contribution of each QTL and QTL combination to the overall phenotype, MSTs of backcross mice with the same haplotype (ie, sensitive vs resistant alleles) were calculated and then compared with the MSTs of mice with the opposing haplotype (Figure 14). For each backcross, only a homozygous A (AA) or heterozygous (H) genotype could be obtained in the typing of microsatellite markers. When the MSTs were determined for the groups of mice containing either the AA or H genotype at each of the markers representing the QTLs, the largest difference in MST was found for *D6Mit183*. Mice heterozygous at that locus survived an average of 12 hours longer than those mice homozygous for the A allele. Different haplotype combinations at 2 QTLs showed the greatest MST difference for mice heterozygous for QTLs on chromosomes 1 and 6, with H-H mice surviving an average of 25 hours longer than mice AA at both loci (Figure 14).

Continuing this analysis, examination of different combinations of 3 QTLs revealed that the MST of backcross mice heterozygous for markers on chromosomes 6, 12, and 16 was 40 hours longer than that of backcross mice AA at these markers. The best agreement between phenotype and genotype for 4 QTLs was noted with haplotypes H-H-H-AA for markers on chromosomes 6, 12, 16, and 9—results that directly correlated with QTL results. Mice with this haplotype survived an average of 52 hours longer than mice that were AA-AA-AA-H for the 4 QTLs, respectively. Analysis of the different haplotypes for 5 QTLs showed an MST difference of 75 hours between mice that were H-H-H-H-AA at chromosomes 1, 6, 12, 16, and 9, respectively, and mice that were AA-AA-AA-AA-H for these markers. Adding in the genotype at the QTL on chromosome 8 decreased the MST difference between the haplotypes (AA-AA-AA-AA-AA-H vs H-H-H-H-H-AA) from 75 hours to 70 hours for QTLs on chromosomes 1, 6, 8, 12, 16, and 9, respectively, although the number of mice in each group was low (ie, 5 mice had a sensitive haplotype for these QTLs and 4 had a resistant haplotype).

COMPARISON OF MICROARRAY AND GENOMEWIDE SCAN

To examine expression of candidate genes identified by the QTL analysis, microarray analysis was performed with lung mRNA from A strain mice, and the results were compared with those previously determined in B6 mice. This comparative analysis was limited to the first 48 hours of exposure because A strain mice succumbed before 96 hours.

The numbers of gene expression changes in A and B6 mice for the different exposure times are summarized in Table 7. As was noted for the B6 mice, relatively few of the

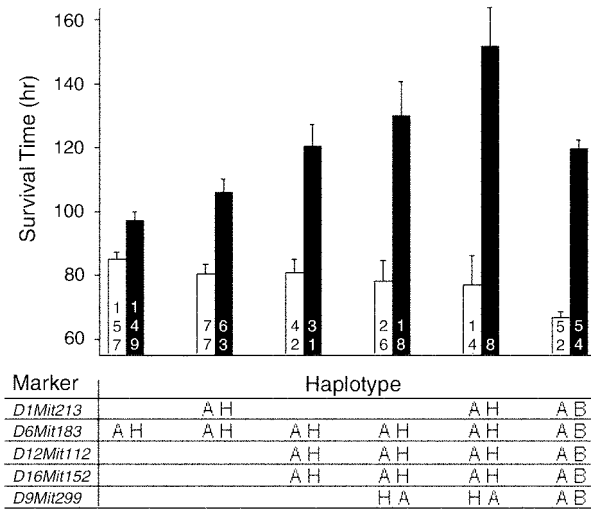


Figure 14. Haplotype analysis. Displayed are the survival time differences of backcross mice with resistance haplotypes versus those with sensitivity haplotypes at microsatellite markers representing the putative QTLs. The two bars on the far right represent survival times of A and B6 control strains. White bars represent backcross mice with AA genotype (represented as A); black bars represent backcross mice with AB or BA genotype (represented as H), or BB genotype (represented as B) for B6 control mice. The number within each bar is the number of backcross mice with the designated genotype or haplotype. Values are means \pm SEs. All comparisons of sensitivity haplotypes (white bars) versus resistance haplotypes (black bars) were significant as assessed using a 2-way ANOVA followed by a Student-Newman-Keuls test of significance. Statistical significance for all comparisons of means was accepted at $P < 0.05$.

8,734 sequence-verified murine cDNAs were altered at any of 4 times during nickel exposure and the number of genes that changed increased with exposure time. In the A strain, 146 different genes were changed at one or more times (76 increased and 70 decreased), compared with 200 different genes in B6 mice (111 increased and 89 decreased). The number of genes that changed in A or B6 mice was 280 (3.2% of the total 8,734 cDNAs on the microarray), of which 183 (65%) were known genes and annotated ESTs, and 97 (35%) were nonannotated ESTs. Among these 280 changed genes, 151 (54%) increased and 129 (46%) decreased in expression. Fewer genes (66 total with 36 increases and 30 decreases) were changed in both strains (Table 7).

The different known genes and annotated ESTs displaying balanced differential expression changes greater than $|2.0|$ in A or B6 mice are listed in Table 8 (after 3, 8, or 24 hours of exposure) and Table 9 (after 48 hours of exposure). Genes of potential interest, and therefore candidates for acute lung injury, include those whose expressions reached significance in only one strain (genes identified by a + or - symbol in Tables 8 and 9), and those genes significantly expressed in both strains, but having a balanced differential greater than

Table 7. Number of Significant Gene Expression Changes in A and B6 Mice After Exposure to Nickel Sulfate^a

Exposure Time (hr)	A Mice		B6 Mice		A or B6 Mice		A and B6 Mice	
	Increased	Decreased	Increased	Decreased	Increased	Decreased	Increased	Decreased
3	13	8	2	8	14	6	1	0
8	15	1	20	5	28	12	7	0
24	22	10	38	18	44	8	16	4
48	30	24	65	33	75	15	20	1
No. Different ^d	57	35	91	50	116	35	32	4
No. \uparrow or \downarrow	76 \uparrow	70 \downarrow	111 \uparrow	89 \downarrow	151 \uparrow	129 \downarrow	36 \uparrow	30 \downarrow
Total changes	146 in A		200 in B6		280 in either		66 in both	

^a \uparrow Increase; \downarrow decrease.

^b Genes are known genes plus annotated ESTs (ie, those with known homologues).

^c Nonannotated ESTs (ie, no homology to known genes).

^d Number of different known genes and annotated ESTs (genes) or nonannotated ESTs (ESTs) that reached a balanced differential expression ratio $\geq |1.8|$ for any exposure time. Note that individual genes may be included in multiple time points.

Table 8. Differential Expression Changes After 3, 8, or 24 Hours of Nickel Sulfate Exposure^a

Increased Expression Changes	A	B6	Decreased Expression Changes	A	B6
	Mice	Mice		Mice	Mice
3 Hours of Exposure					
Elastin	+		cAMP-regulated phosphoprotein ARPP-19		-
Growth differentiation factor 1	+		EST Putative transcription factor	x	x
Lysyl oxidase	+		EST Survival motor neuron protein 1	-	
Metallothionein-1	x	x	EST UTP-glucose-1-P uridylyltransferase	x	x
MAP kinase phosphatase-1	++		PAF acetylhydrolase 1B, α		-
Nuclear receptor subfamily 4A, member 1	++		Renin 1, structural	-	
8 Hours of Exposure					
Cysteine-rich protein 61	x	x	EST Interferon-activatable protein 204		-
Eph receptor A2	+		KIAA0729 protein	x	
EST 6-phosphogluconate dehydrogenase	+		Renin 1, structural		-
Galectin-3		+	Ubiquitin hydrolyzing enzyme-1	x	x
Glyceraldehyde-3-phosphate dehydrogenase	x	x			
Growth differentiation factor 1	x	x			
Heme oxygenase-1	x	x			
Keratin complex 1, acidic gene 19	x	x			
Metallothionein-1	x	x			
MAP kinase phosphatase-1	+				
Secretory proteinase inhibitor-2		+			
Thioredoxin reductase-1	x	x			
24 Hours of Exposure					
Aldolase 1, A isoform	x	x	Anti-HIV-1RT single-chain variable fragment		-
Annexin 2A		+	cAMP-regulated phosphoprotein ARPP-19		-
Calgranulin A	+		Cathepsin B	x	
Enolase 1	x	x	Clara cell secretory protein (CCSP)	x	x
E1B 19K/Bc1-2 binding protein (Nip3)	x	x	Cytochrome P450 2b9	-	

(Table continues on next page)

^a The plus (+) symbol identifies genes that reached a significant expression change only for the indicated strain at that exposure time. The double plus (++) symbol indicates genes that displayed higher expression in the specified strain (by a differential expression ratio at least ≥ 12.0) than in the other strain at the indicated timepoint. The symbol x indicates genes with a balanced differential expression ratio ≥ 1.8 and a ratio ≥ 12.0 compared with the other strain.

Table 8 (continued). Differential Expression Changes After 3, 8, or 24 Hours of Nickel Sulfate Exposure^a

Increased Expression Changes	24 Hours of Exposure (continued)		Decreased Expression Changes	A Mice		B6 Mice	
	A Mice	B6 Mice		A Mice	B6 Mice		
Elastin			Cytochrome P450 2b13	x		x	x
Enolase 3, β muscle	x	x	Cytochrome P450 2f2	x		x	x
EST 51.6-kd protein F59B2.5 (<i>Caenorhabditis elegans</i>)			EST Cyclin-dependent kinase-like 2 (Kkm)	x		x	x
EST 6-Phosphogluconate dehydrogenase	x	x	EST Ribonuclease PL3 precursor	x		x	x
EST Glutathione S-transferase 3			EST Surfactant-associated protein B	x		x	x
EST HSPC010 (<i>Homo sapiens</i>)			EST Surfactant-associated protein C	x		x	--
EST Keratin, complex 2, basic gene 7	x	x	EST WDNM1 protein precursor				--
EST Lymphocyte antigen LY-6A.2/LY-6E.1			Esterase-1	x		x	x
EST Proteasome θ chain	x	x	Histocompatibility 2, class II A, α chain				-
EST Thymus-expressed acidic protein (TEAP)			Interferon-activated gene 203	-		-	
Galectin-3	x	x	Interferon-inducible protein	-		-	
Glyceraldhyde-3-phosphate dehydrogenase	x	x	Palate, lung, nasal epithelium expressed transcript				
Hemoglobin- α , adult chain 1	x	x	Paraoxonase-1	x		x	x
Interleukin 4 receptor α			RBP-associated molecule RAM14-1				-
Keratin complex 1, acidic gene 13	+						
Keratin complex 1, acidic gene 19	x	x					
Lipocalin 2	x	x					
Lymphocyte antigen 6 complex							
Lymphocyte antigen 6 complex, locus C							
Metallothionein-1	x	++					
Myosin and lymphocyte (MAL) protein							
NADH oxidoreductase							
N-myc downstream regulator-1							
Proteasome ζ chain							
Secreted phosphoprotein 1							
Secretory proteinase inhibitor-2	x	x					
Small proline-rich protein 1a	x	x					
Thioredoxin reductase-1	x	x					
Tubulin $\alpha 4$ chain							
Y-box protein 3	x	x					

^a The plus (+) symbol identifies genes that reached a significant expression change only for the indicated strain at that exposure time.

The double plus (++) symbol indicates genes that displayed higher expression in the specified strain (by a differential expression ratio at least $\geq |2.0|$) than in the other strain at the indicated timepoint. The symbol x indicates genes with a balanced differential expression ratio $\geq |1.8|$ and a ratio $\geq |2.0|$ compared with the other strain.

Table 9. Differential Expression Changes After 48 Hours of Nickel Sulfate Exposure^a

	Increased Expression Changes	A Mice	B6 Mice	Decreased Expression Changes	A Mice	B6 Mice
	Aldolase 1, A isoform		+	Anti-HIV-1 RT single-chain variable fragment		-
	Annexin 2A	x	x	Cathepsin B	-	-
	Asparagine synthetase		+	Clara cell secretory protein (CCSP)	xx	x
	β-TuCP protein E3RS-IκB		+	Cytochrome P450 2f2	xx	x
	Calgranulin A	+	+	Cytochrome P450 2b13	-	-
	Cold-induced RNA binding protein		+	EST Cyclin-dependent kinase-like 2 (Kkm)	x	x
	Elastin	x	x	EST Interferon-activatable protein 204		-
	Enolase 3, β muscle		+	EST Mitochondrial import translocase, TIM17	-	-
	Enolase α	x	x	EST Putative transcription factor		-
	Eph receptor A2	x	x	EST PV-1 (formerly gp68)	-	-
	Epithelial membrane protein 1		+	EST Surfactant-associated protein B	x	xx
	EST 6-phosphogluconate dehydrogenase	x	x	EST Surfactant-associated protein C	x	xx
	EST BAP2-β protein (<i>Homo sapiens</i>)		+	EST UTP-glucose-1-P uridylyltransferase		-
	EST Cofilin/Sid23p	x	x	Esterase-1	x	x
	EST Glutathione S-transferase 3, microsomal		+	Fatty acid synthase		-
	EST HSPC010 (<i>Homo sapiens</i>)	x	x	Hemoglobin-α, adult chain 1	-	-
	EST Keratin complex 2, basic gene 7	x	xx	Hemolytic complement	x	xx
	EST Lymphocyte antigen LY-6A.2/LY-6E.1		+	Histocompatibility 2, class II A, α chain	x	x
	EST Proteasome θ chain	x	x	Interferon-activated gene 203		-
	EST Thymus-expressed acidic protein (TEAP)		x	L-selectin		-
	EST WDNM1 protein	+	xx	PAF acetylhydrolase 1B, α		-
	Galectin-3	x	xx	Palate, lung, nasal epithelium expressed transcript	x	x
	Glyceraldehyde-3-phosphate dehydrogenase	x	x	Paraoxonase-1	x	x
	Glycoprotein 49A	+	+	Pr22		-
	Keratin complex 1, acidic, gene 19	x	x	RBP-associated molecule RAM14-1	-	-
	Lactotransferrin		+	Steroid receptor coactivator-1		-
	Laminin-γ2		+	Ubiquitin hydrolyzing enzyme-1	x	x
	Lymphocyte antigen 6 complex		+			
	Lymphocyte antigen 6 complex, locus C	x	x			
	Lysyl oxidase	x	x			
	MAP kinase phosphatase-1	+	+			
	Metal response element transcription factor-2		+			

(Table continues on next page)

^a The plus (+) symbol identifies genes that reached a significant expression change only for the indicated strain at that exposure time. The double plus (++) symbol indicates genes that displayed higher expression in the specified strain (by a differential expression ratio at least ≥ 1.20) than in the other strain at the indicated timepoint. The symbol x indicates genes with a balanced differential expression ratio ≥ 1.81 and a ratio ≥ 1.20 compared with the other strain.

Table 9 (continued). Differential Expression Changes Following 48 Hours of Nickel Sulfate Exposure^a

	A Mice	B6 Mice	Decreased Expression Changes	A Mice	B6 Mice
	Increased Expression Changes				
Metallothionein-1	x	xx			
Myosin and lymphocyte (MAL) protein		+			
NADH oxidoreductase		+			
Proteasome 26S, ATPase subunit 4		+			
Proteasome 26S, non-ATPase subunit 13		+			
Proteasome subunit, β type 7		+			
Proteasome ζ chain		+			
RNA binding motif-3		+			
Secretory leukoprotease inhibitor		+			
Secretory proteinase inhibitor-2		+			
Small proline-rich protein 1a	x				
Sphingosine kinase-1		+			
Thioredoxin reductase-1	x	xx			
Tumor-associated Ca-signal transducer 2 (Trop2)					
Y-box protein 3	x				

^a The plus (+) symbol identifies genes that reached a significant expression change only for the indicated strain at that exposure time.

The double plus (++) symbol indicates genes that displayed higher expression in the specified strain (by a differential expression ratio at least ≥ 2.0) than in the other strain at the indicated timepoint. The symbol x indicates genes with a balanced differential expression ratio ≥ 1.8 and a ratio ≥ 12.0 compared with the other strain.

|2| between strains (gene names identified by ++ or -- symbols in Tables 8 and 9).

A sorting of the 8,734 cDNAs on the microarray was grouped to display those cDNAs with higher expression in the A strain, those with higher expression in the B6 strain, and those increased or decreased similarly in both strains. Fourteen cDNAs for known genes and annotated ESTs and 6 cDNAs for nonannotated ESTs displayed higher expression in A mice compared to the B6 strain. These 20 cDNAs were further separated into 3 subgroups: (1) increased in A, but decreased in B6 mice; (2) increased in both strains, but more in A mice; and (3) decreased in both strains, but more in B6 mice (Figure 15). Similarly, 20 cDNAs (18 known and annotated ESTs and 2 nonannotated ESTs) displayed higher expression in B6 mice than in A mice, and these 20 cDNAs were further subdivided into 3 groups: (1) those increased in B6 mice, but decreased in A mice; (2) those increased in both strains, but more in B6 mice; and (3) those decreased in both strains, but more in A mice (Figure 16). Examples of cDNAs with similar expression changes in both strains are displayed in Figure 17.

To assess the possible pathophysiologic consequences of the similarities and differences in the gene expressions in A and B6 mice after exposure, the known sequences and annotated ESTs were categorized into major groups according to function. Although most of the genes could be placed into any one of several categories, the majority shared functions with genes in 1 of 5 groups: cell energy and metabolism; cell growth and development; inflammation; oxidative stress; or signal transduction and cell regulation (Table 10). Only 6 of the cDNAs were not categorized owing to a lack of information on known, predicted, or suspected functions.

Table 11 shows the candidate genes identified in QTL and microarray analyses of nickel-induced lung injury that we think are the most promising for further study.

TRANSGENIC MICE

Finding that the gene encoding TGF- α is located in *Aliq4* led us to test transgenic lines of mice that express different levels of hTGF- α in their lung (Korfagen et al 1994). Survival varied among the transgenic mouse lines and increased with increasing levels of hTGF- α expression (Figure 18). The survival times of nontransgenic mice (FVB/N, strain-matched controls) (73 ± 3 hours) and line 6108 mice (75 ± 2 hours) were not significantly different. In contrast, the survival time of line 4 mice (87 ± 2 hours) was longer than that of nontransgenic and

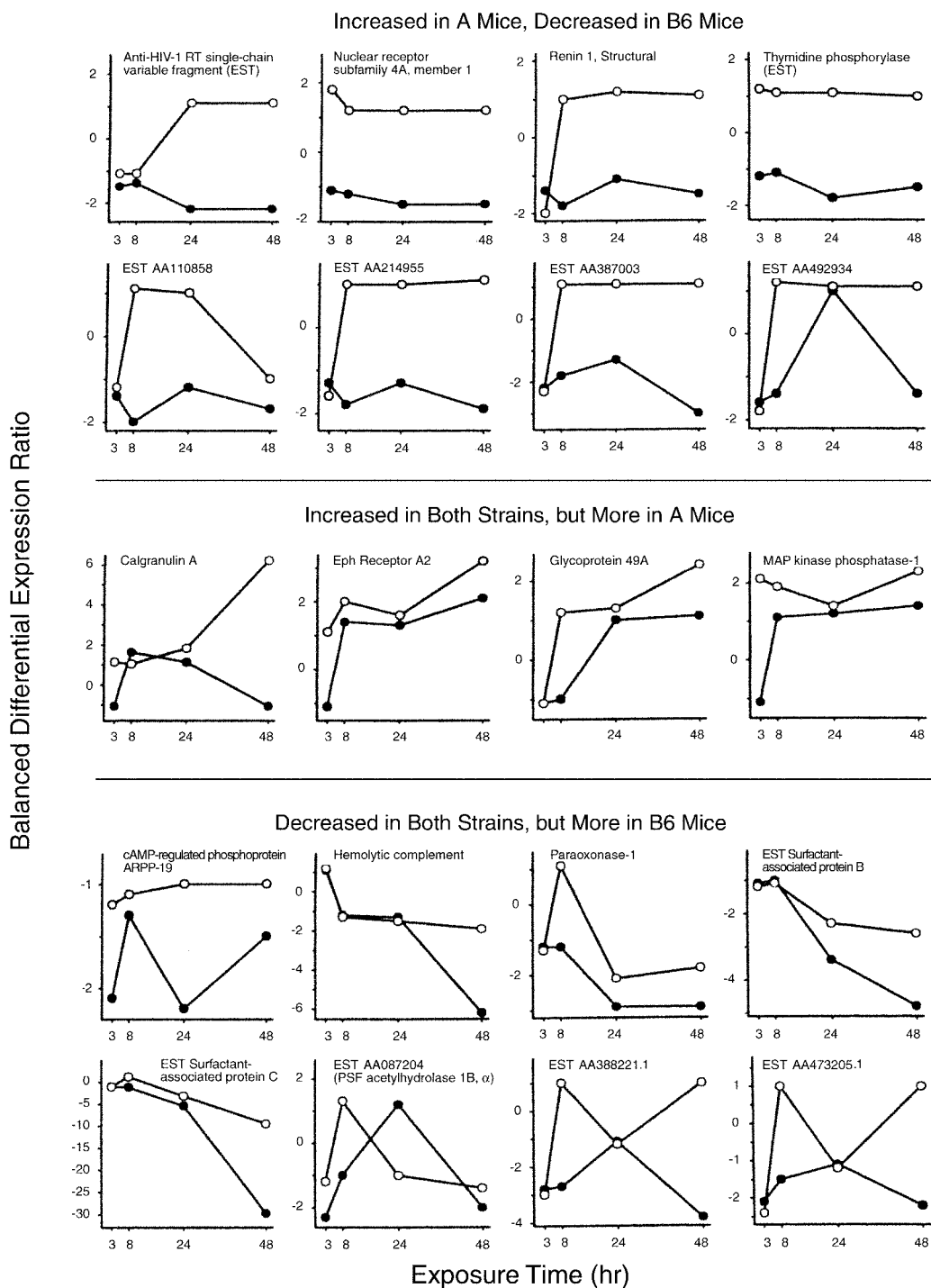


Figure 15. Genes with higher expression in A than in B6 strain mice during nickel-induced acute lung injury. Polyadenylated mRNA from the A and B6 mouse lungs were isolated after exposure to NiSO₄ (110 µg/m³; MMAD, 0.2 µm), for 3, 8, 24, or 48 hours, and labeled during reverse transcription with the fluorescent dye Cy5. Samples (pooled from n = 3 mice/strain/treatment) were competitively hybridized with Cy3-labeled cDNA from the lungs of unexposed A or B6 control mice to microarrays of 8,734 murine cDNAs. After hybridization of Cy3 and Cy5 samples, scanned images were acquired for each fluorophore at each target cDNA element. Lines represent the temporal patterns of expression (balanced differential expression ratio) for genes that displayed an increased expression in the A strain (white circles) relative to the B6 strain (black circles).

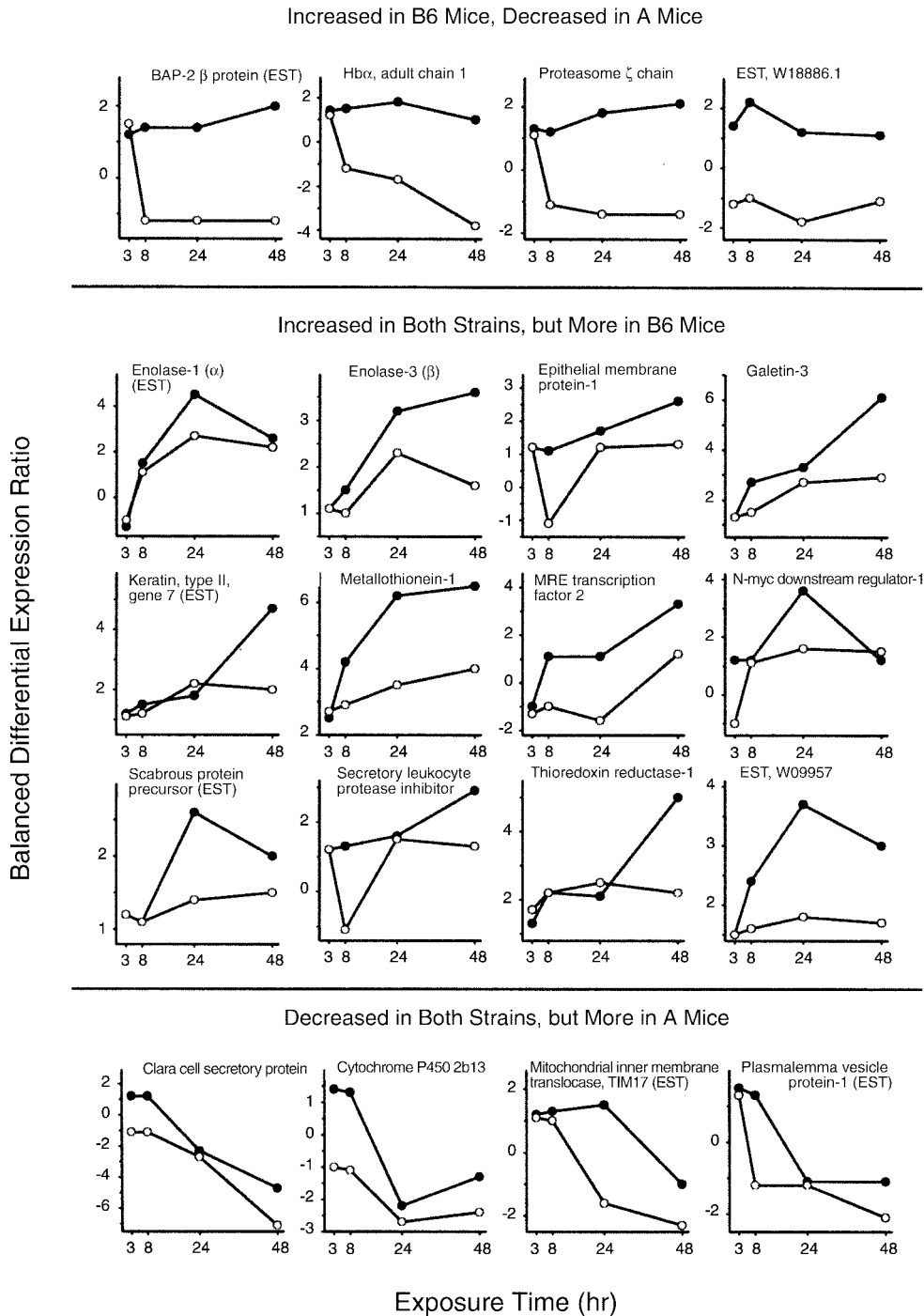


Figure 16. Genes with higher expression in B6 than in A strain mice during nickel-induced acute lung injury. Polyadenylated mRNAs from the A and B6 mouse lungs were isolated after exposure to NiSO₄ (110 µg/m³; MMAD, 0.2 µm), for 3, 8, 24, or 48 hours, and labeled during reverse transcription with the fluorescent dye Cy5. Samples (pooled from n = 3 mice/strain/treatment) were competitively hybridized with Cy3-labeled cDNA from the lungs of unexposed A and B6 control mice to microarrays of 8,734 murine cDNAs. After hybridization of Cy3 and Cy5 samples, scanned images were acquired for each fluorophore at each target cDNA element. Lines represent the temporal patterns of expression (balanced differential expression ratio) for genes that displayed an increased expression in the B6 strain (black circles) relative to the A strain (white circles).

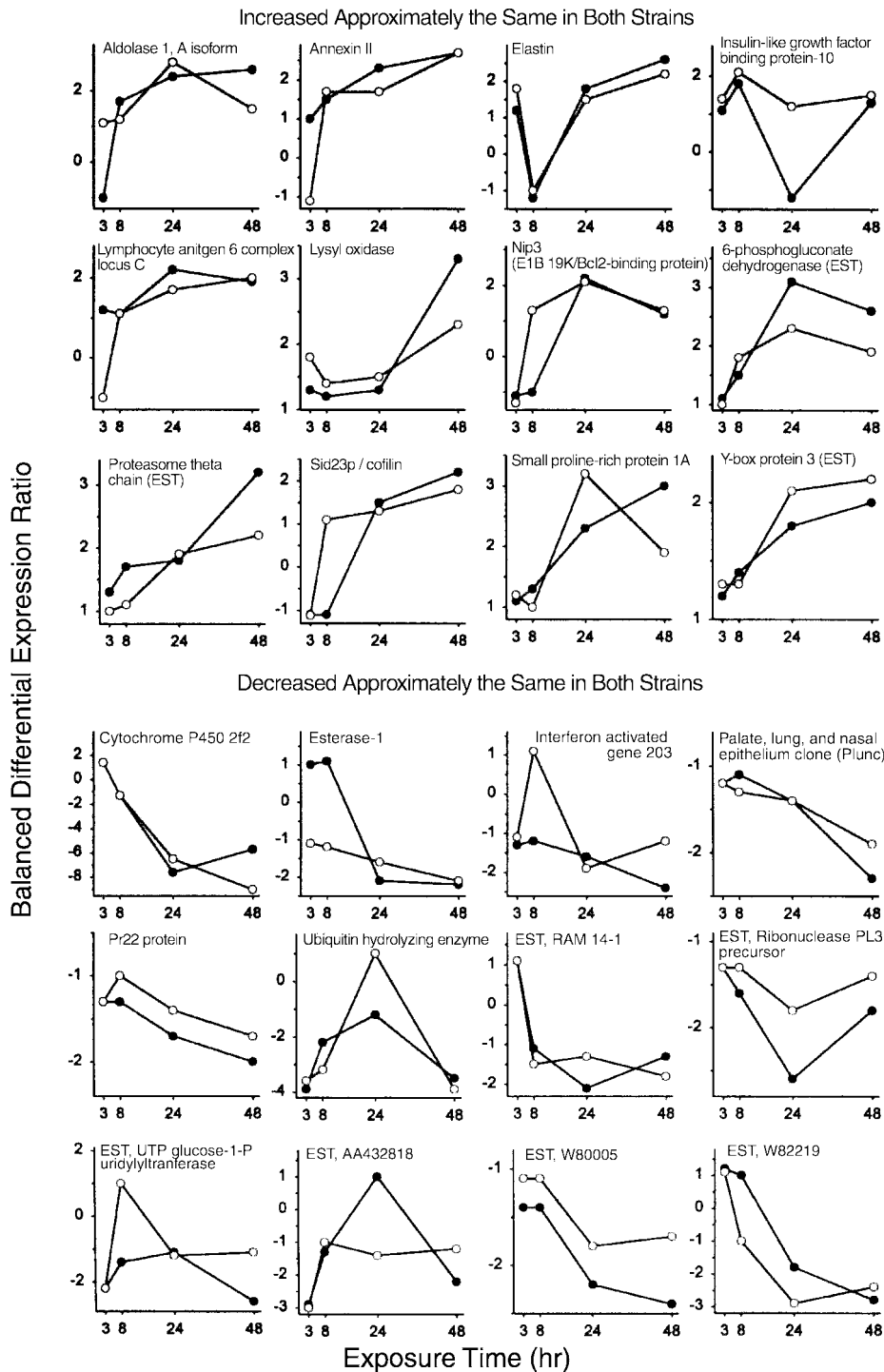


Figure 17. Gene expression changes similar in A and B6 strain mice during nickel-induced acute lung injury. Polyadenylated mRNAs from the A and B6 mouse lungs were isolated after exposure to NiSO_4 ($110 \mu\text{g}/\text{m}^3$; MMAD, $0.2 \mu\text{m}$), for 3, 8, 24, or 48 hours, and labeled during reverse transcription with the fluorescent dye Cy5. Samples (pooled $n = 3$ mice/strain for each treatment) were competitively hybridized with Cy3-labeled cDNA from the lungs of unexposed A and B6 control mice to microarrays of 8,734 murine cDNAs. After hybridization of Cy3 and Cy5 samples, scanned images were acquired for each fluorophore at each target cDNA element. Lines represent the temporal patterns of expression (balanced differential expression ratio) for genes that displayed approximately the same expression change in the A (white circles) and B6 strains (black circles).

Table 10. Functional Clustering of Known Genes and Annotated ESTs Altered After Nickel-Induced Acute Lung Injury in Strains A and B6

Cell Energy and Metabolism	Cell Growth and Differentiation	Inflammation	Oxidative Stress	Signal Transduction and Cell Regulation
Aldolase 1, A isoform	BAP-2β protein (<i>Homo sapiens</i>)	Annexin 2A	Glutathione S-transferase 3	β-TrCP E3RS-IκB
Asparagine synthetase	Cofilin/Sid23p	Calgranulin A	Heme oxygenase-1	cAMP-regulated phosphoprotein
Cold-induced RNA-binding protein	Cysteine-rich protein 61	Cathepsin B	Lactotransferrin	ARPP-19
Cytochrome P450 2b9	E1B 19K/B1c-2 binding protein (NIP3)	Clara cell secretory protein	Metallothionein-1	Cyclin-dependent kinase-like 2 (Kkm)
Cytochrome P450 2b13	Elastin	Hemolytic complement	Thioredoxin	Eph receptor A2
Cytochrome P450 2f2	Epithelial membrane protein 1	Histocompatibility 2, class II A, α chain	reductase-1	Glycoprotein 49A
Enolase 1	Galectin-3	Interferon-activatable protein 204		MAP kinase phosphatase-1
Enolase 3, β muscle	Growth differentiation factor 1	Interferon-activated gene 203		Metal response element transcription factor-2
Esterase 1	Hemoglobin-α, adult chain 1	Interferon-inducible protein		N-myc downstream regulator-1
Fatty acid synthase	Keratin complex 1, acidic gene 13	Interleukin 4 receptor α		Nuclear receptor subfamily 4A, member 1
Glyceraldehyde-3-phosphate dehydrogenase	Keratin complex 2, basic gene 7	L-selectin		RBP-associated molecule RAM14-1
Lipocalin 2	Laminin-γ2	Lymphocyte antigen 6		Pr22
NADH oxidoreductase	Lysyl oxidase	Lymphocyte antigen 6, complex C		Steroid receptor coactivator-1
Paraoxonase-1	Myelin and lymphocyte protein	Lymphocyte antigen LY-6A.2 / LY-6E.1		Tumor-associated Ca-signal transducer (Trop2)
6-Phosphogluconate dehydrogenase	Palate, lung, nasal epithelium expressed transcript	PAF acetylhydrolase 1B, α		Y-box protein 3
Proteasome 26S, ATPase, subunit 4	Ribonuclease PL3 precursor			
Proteasome 26S, non-ATPase, subunit 13	Secreted phosphoprotein 1			
Proteasome θ chain, β type 3	Secretory leukoprotease inhibitor			
Proteasome ζ chain, α type 5	Serine proteinase inhibitor-2			
Proteasome subunit, β type 7	Small proline-rich protein 1a			
Renin 1, structural	Sphingosine kinase-1			
RNA binding motif-3	Surfactant-associated protein B			
Mitochondrial import translocase, TIM17	Surfactant-associated protein C			
Ubiquitin hydrolyzing enzyme-1	Survival motor neuron protein 1			
UTP-glucose-1-phosphate uridylyltransferase	Tubulin α4 chain			
	WDNM1 protein			
	WDNM1 protein precursor			

Unknown Function
Anti-HIV-1 RT single-chain variable fragment
HSPC010 (*Homo sapiens*)
Hypothetical 51.6-kd protein F59B2.5 (*Caenorhabditis elegans*)
KIAA0729 protein
Plasmalemmal vesicle protein-1
Thymus-expressed acidic protein (TEAP)

Table 11. Candidate Genes Identified from QTL and Microarray Analyses of Nickel-Induced Acute Lung Injury in Mice

Chromosome	QTL Interval (cM)	Candidate Location (cM)	Human Homology	QTL Analysis		Microarray Analysis
				QTL Analysis	Microarray Analysis	
Candidate genes located within (or near) QTL intervals						
1	23–36	21 31	2 (q31–q32.3) 2 (q32–q34)	<i>Creb1</i> , cAMP response element binding protein-1	<i>Col3a1</i> , procollagen type III, $\alpha 1$	
6	12–38	27 28 31 38	7 (p14) 7 (p21–p15) 2 (p12–p11.2) 2 (p13)	<i>Aqp1</i> , aquaporin-1 <i>Crhr2</i> , corticotropin releasing hormone receptor-2 <i>Sftpb</i> , surfactant-associated protein B <i>Tgfa</i> , transforming growth factor- α	<i>Sftpb</i> , surfactant-associated protein B	
8	18–38	18 26 43 45 C1	8 (p21.1) 4 (q34–q35) Unknown 16 (q13) 22 (q12)	<i>Gr1</i> , glutathione reductase-1 <i>Klk3</i> , kallikrein-3, plasma <i>Hmox1</i> , heme oxygenase-1	<i>Gr1</i> , glutathione reductase-1 <i>Es1</i> , esterase-1 <i>Mt1</i> , metallothionein-1 <i>Hmox1</i> , heme oxygenase-1	
12	1–31	4 15 31 34 C1–C3	2 (p24.3) 2 (p25) 14 (q21–q24) 14 (q22) 14 (q13)	<i>Nmyc1</i> , neuroblastoma, myc-related oncogene-1 <i>Tpo</i> , thyroid peroxidase <i>Hif1a</i> , hypoxia inducible factor-1, α subunit <i>Hsp70-2</i> , heat-shock protein, 70-kDa 2 <i>Ttff1</i> , thyroid transcription factor-1		
16	47–67	61 61	21 (q22.1–q22.2) 21 (q22.1)	<i>Il10rb</i> , interleukin 10 receptor β <i>Sod1</i> , superoxide dismutase-1		
Candidate genes not located within (or near) QTL intervals (identified by microarray)						
2		23.5	9 (q33)		<i>Hc</i> , hemolytic complement (C5)	
3		43.6	1 (q21)		<i>S100a8</i> , calgranulin A (S100 calcium-binding protein A8)	
7		6.5	Unknown		<i>Cyp2b9</i> , cytochrome P450 2b9	
11		16	16 (p13.3)		<i>Hba-a1</i> , hemoglobin α , adult chain 1	
14		32.5	8 (p21)		<i>Sftpc</i> , surfactant-associated protein C	
17	<i>Alh3</i>	50.8	Unknown		<i>Pipn16</i> , MAP kinase phosphatase-1	
Unknown		Unknown	Unknown		<i>Lgals3</i> , galectin-3 (lectin, galactose binding, soluble 3)	
Unknown		Unknown	8		<i>Ndr1</i> , N-myc downstream regulator-1 (Cap43)	

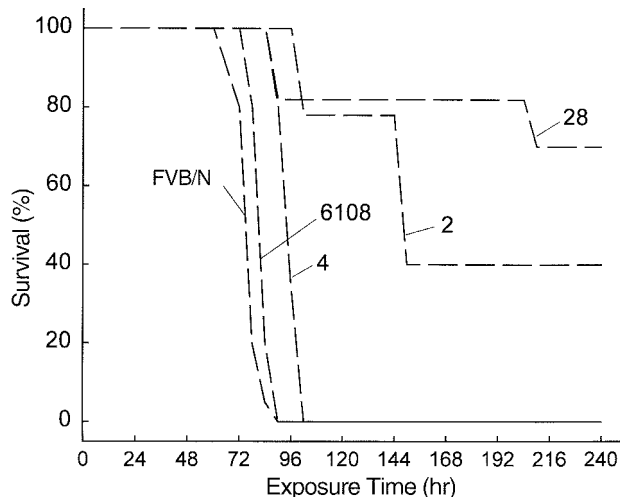


Figure 18. Attenuation of acute lung injury in transgenic mice lines expressing varying levels of hTGF- α . Mouse lines with increasing amounts of hTGF- α expressed in the lung had increasing survival times with continuous exposure to fine NiSO₄ (70 μ g Ni/m³; MMAD, 0.2 μ m). The nontransgenic mice were FVB/NJ strain (the strain of the embryonic stem cells used to produce the transgenic mouse lines). The MSTs of nontransgenic mice (72 hours) and line 6108 mice (75 hours) were not significantly different. However, the transgenic mouse line 4 survived longer (87 hours) than nontransgenic and line 6108 mice. Line 2 and line 28 mice survived the longest. Two of the 5 mice from line 2 survived the entire exposure period, as did 4 of the 6 line 28 mice. Statistical significance ($P < 0.01$) was determined for survival curves using a Kaplan-Meier product limit survival curve method with differences in survival between groups determined by log rank test. The analysis was performed with SAS 6.12 statistical software's life-test procedure (SAS, Cary NC) ($n = 5$ to 10 mice). The hTGF- α protein levels expressed in lung homogenates for each strain were as follows: FVB/N = 0, line 6108 = 120, line 4 = 230, line 2 = 540, and line 28 = 570 pg/mL.

line 6108 mice. Line 2 and line 28 mice survived longer than the other strains, with 2 of 5 line 2 mice and 4 of 6 line 28 mice surviving the entire exposure (240 hours).

Within 24 hours of exposure, mild perivascular edema began to develop in the lungs of nontransgenic mice, while the lungs of line 28 mice had minimal changes. By 48 hours, perivascular edema became more pronounced in nontransgenic mice with evidence of inflammatory cell infiltration. In contrast, line 28 mice did not demonstrate evidence of edema or inflammation. By 72 hours, extensive edema was detected in nontransgenic mice. This edema extended beyond the perivascular area and into the adjacent alveoli with increased inflammatory cell infiltration in the perivascular and alveolar areas. Again, line 28 mice remained unaffected at 72 hours, with little or no evidence of pulmonary edema or inflammation. Lung wet-to-dry weight ratios of nontransgenic mice did not differ from those of line 28 mice before exposure. After 72 hours

of nickel exposure, wet-to-dry weight ratios of lungs from nontransgenic mice increased above control values. This effect was significantly attenuated in transgenic line 28 mice compared with nontransgenic FVB/N mice (Figure 19). The amount of nickel present in the lungs before exposure was below the limit of detection (0.4 μ g/g tissue) for both nontransgenic and line 28 mice; however, the amount of nickel retained at 72 hours increased to 0.7 ± 0.2 and 2.1 ± 0.3 μ g/g lung wet weight, respectively. Paradoxically, this strain difference in nickel lung burden after exposure was significant ($P \leq 0.01$).

Neutrophil levels in the BAL fluid obtained from nontransgenic or line 28 mice before exposure were low ($< 1\%$). At 72 hours, the percentage of neutrophils increased significantly ($26\% \pm 2\%$) in BAL fluid obtained from nontransgenic mice, but not in that from line 28 mice ($7\% \pm 3\%$). Differences in the percentage of neutrophils between line 28 and nontransgenic mice were statistically significant at 72 hours ($P \leq 0.01$). Before exposure, BAL fluid protein levels were significantly elevated in nontransgenic mice (3.9 ± 0.2 mg/mL) compared with those of line 28 mice (2.4 ± 0.5 mg/mL). At 72 hours, BAL fluid protein increased in nontransgenic mice (37 ± 10 mg/mL) and line 28 mice (8.1 ± 2.0 mg/mL); again this increase was significantly attenuated in line 28 mice compared with nontransgenic mice.

Before exposure, levels of interleukin 1 β , interleukin 6, and macrophage inflammatory protein-2 in lung homogenates from nontransgenic mice were similar to those in samples from line 28 mice (Figure 20). After 24 and 48 hours, cytokine levels for both nontransgenic and line 28 mice were not significantly different. However, by 72 hours, all 3 cytokine levels increased markedly in nontransgenic mice, but remained at or near the levels seen before exposure in line 28 mice.

The levels of SP-B in lung homogenates of line 28 mice were lower than those in nontransgenic mice, but SP-D levels were nearly equivalent (Figure 21). Before exposure, SP-B levels in line 28 mice were less than half (44%) of the normal amount found in the nontransgenic strain. After 72 hours of nickel exposure, SP-B and SP-D levels decreased significantly from control levels for the nontransgenic mice. In these mice, exposure resulted in a decrease of SP-B levels to 28% of the preexposure control value, whereas SP-D levels only decreased to 73% of control values. In contrast, in the line 28 mice, SP-B levels were unchanged after 72 hours of exposure, remaining at 49% of the nonexposed levels of the nontransgenic controls, and at 112% of (slightly above) the line 28 preexposure control level. In line 28 mice, 72 hours of exposure resulted in a decrease in SP-D to 57% of the unexposed control level.

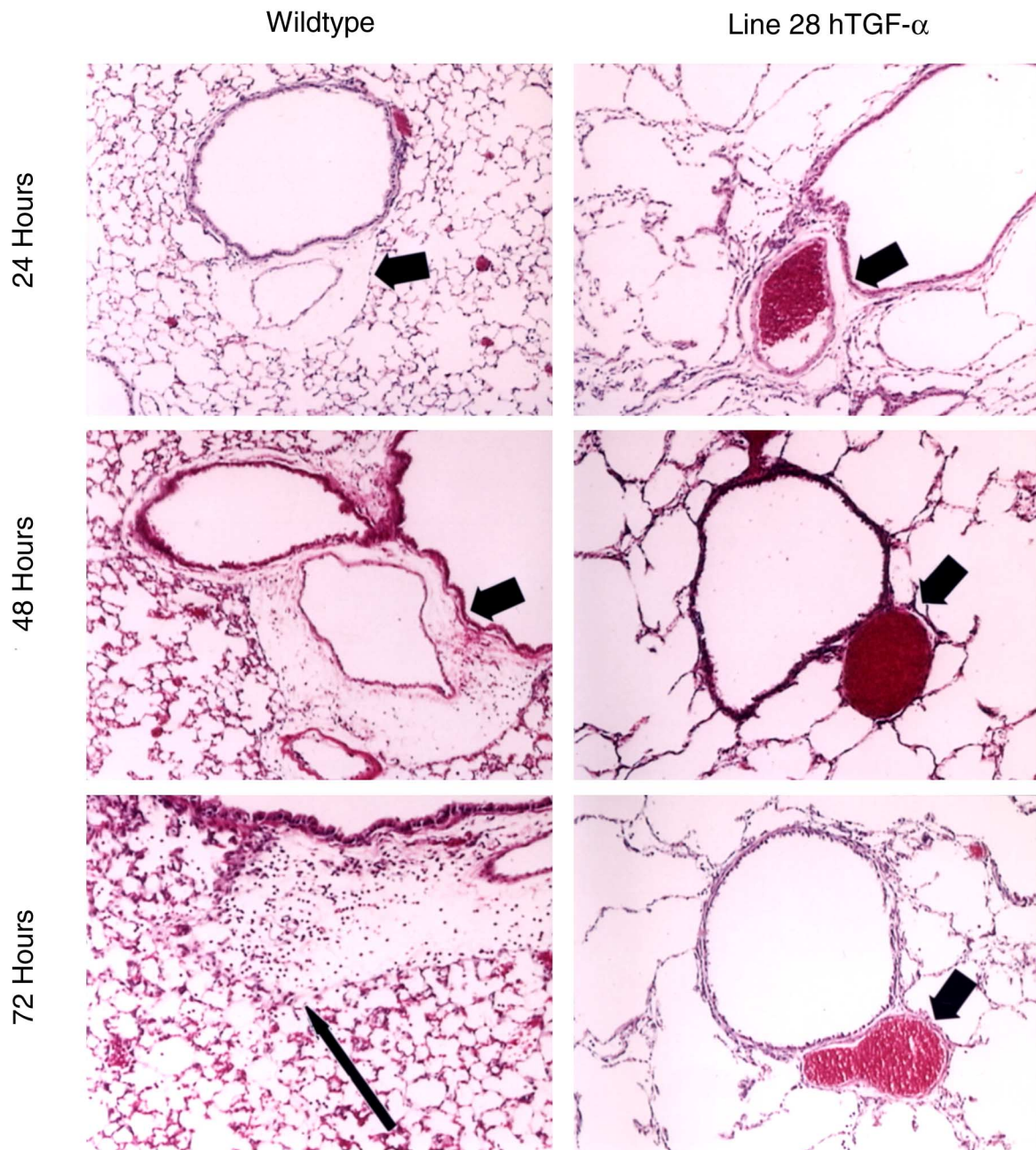


Figure 19. Lung histology of wildtype FVB/N strain-matched control mice (left) and hTGF- α transgenic line 28 mice (right) after exposure to fine NiSO₄ aerosol. Tissues from mice exposed to NiSO₄ (70 μ g Ni/m³; MMAD, 0.2 μ m) were fixed with phosphate-buffered formaldehyde solution, embedded in paraffin, stained with hematoxylin and eosin, and viewed by light microscopy. Wildtype control mice (FVB/N strain) developed alveolar epithelial disruption, alveolar wall thickening, interstitial leukocytes, and luminal erythrocytes. The short thick arrows indicate perivascular space that is enlarged markedly at 48 hours in wildtype FVB/N mice as compared with little change at 48 or 72 hours in line 28 mice. The long thin arrow indicates a focal area of sporadic leukocyte infiltrations noted mainly in the wildtype FVB/N mice as compared with line 28 mice.

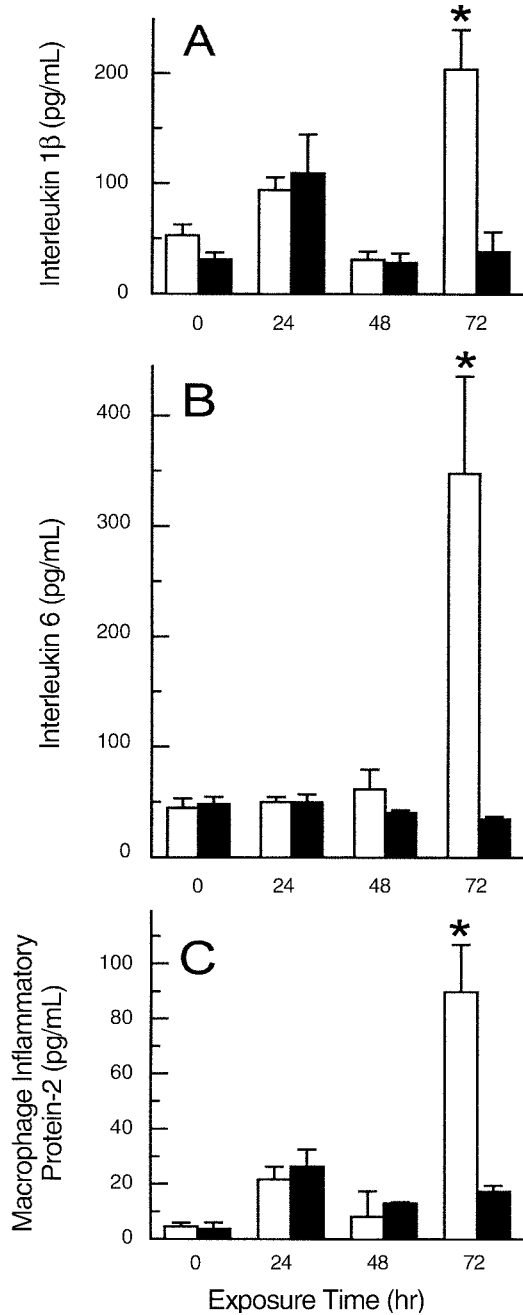


Figure 20. Cytokine protein levels in lungs of nontransgenic FVB/N control mice (white bars) and hTGF- α transgenic line 28 mice (black bars) after exposure to filtered air or continuous exposure to fine NiSO₄ aerosol. At 72 hours, nontransgenic FVB/N mice had a marked increase in interleukin 1 β (A), interleukin 6 (B), and macrophage inflammatory protein-2 (C), whereas levels in lungs from hTGF- α transgenic line 28 mice exposed to NiSO₄ were not different from preexposure control values. Statistical analysis was performed using a 2-way ANOVA followed by a Student-Newman-Keuls test of significance. The factors for each analysis were strain (nontransgenic vs line 28) and exposure (exposed vs control). Statistical significance for all comparisons of means was accepted at $P < 0.05$. Values are mean \pm SE.

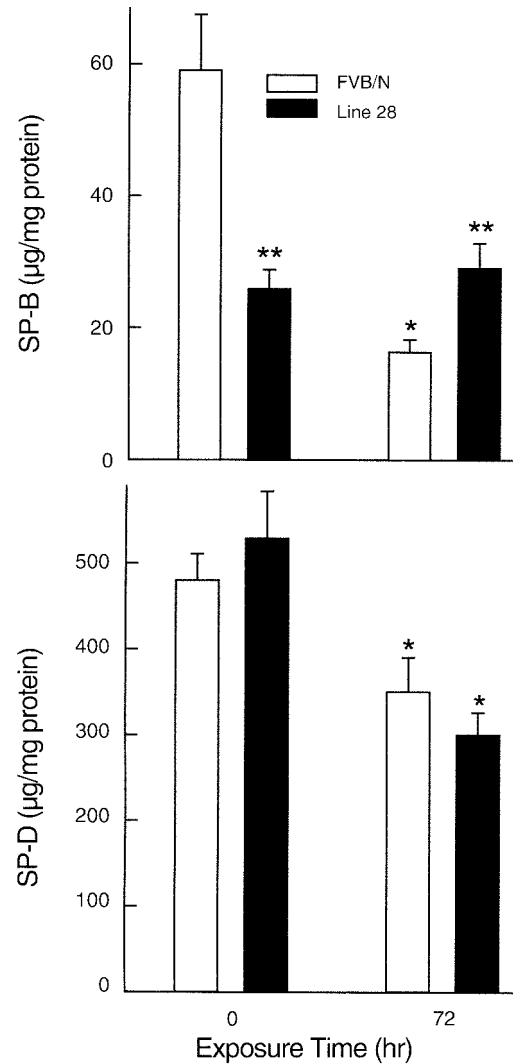


Figure 21. Surfactant-associated protein levels in lungs of nontransgenic FVB/N control mice (white bars) and hTGF- α transgenic mice (black bars) after exposure to filtered air or continuous exposure to fine NiSO₄ aerosol. At 72 hours, nontransgenic FVB/N mice had a marked decrease in SP-B, whereas levels in lungs from hTGF- α transgenic line 28 mice exposed to NiSO₄ were not different from preexposure control values. Changes in SP-D levels were smaller and did not differ between strains.

DISCUSSION

STRAIN PHENOTYPE PATTERNS

We found that submicrometer NiSO₄, a transition metal contained in particulate matter, induced acute lung injury in mice. Susceptibility varied more between than within inbred mouse strains. The A strain was found to be sensitive and the B6 strain was found to be resistant. The cross of these strains produced offspring with a resistant phenotype, indicating that sensitivity is inherited as a recessive trait. The strain phenotype patterns for fine NiSO₄, ultrafine PTFE, and O₃ exposure were similar, suggesting that the trait of sensitivity to acute lung injury could be independent of the agent producing injury. Histopathologic findings indicated comparable injuries in the two strains at the time of death. Acute lung injury was observed in the A strain at the lowest dose of nickel tested (15 µg/m³). In contrast, the strain phenotype patterns of protein in lavage fluid, PMNs in lavage fluid, and acute lung injury survival time differed, suggesting each trait is inherited independently.

One possibility to explain the consistent strain phenotype patterns for response to fine NiSO₄, ultrafine PTFE, and O₃ exposure is that these agents activate common response pathways. All 3 irritants can penetrate to the distal regions of the lung (Stokinger 1957; Benson et al 1988; Bassett et al 1989; Oberdörster et al 1990; Pryor et al 1990; Oberdörster 1995). Of the 3 agonists, O₃ is the best studied and can readily oxidize surface proteins (eg, surfactant) and phospholipids (eg, unsaturated fatty acids) (Leikauf and Shertzer 1999). Ultrafine PTFE also has been found to deplete sulfhydryls and to activate compensatory antioxidant pathways (increasing transcript levels of several antioxidant enzymes in the lung) (Pryor et al 1990; Oberdörster et al 1998; Johnston et al 1998).

In this study, we selected a fine nickel aerosol as a surrogate for particulate matter because it is a transition metal capable of initiating lung injury. The mechanisms by which transition metals can lead to cellular injury and oxidative stress are complex. Transition metals can stimulate oxidant-generating pathways directly (through redox cycling, when electrochemical potential is favored in a biological medium) (Stohs and Bagchi 1995), or indirectly (through activation of leukocytes or oxidant-generating cells, through cytokine priming of leukocytes, through interactions with amino acids, or through the replacement of other metals that can undergo redox cycling) (Salnikow et al 1994, 2000; Stringer and Kobzik 1998; Bal et al 2000; Salnikow and Costa 2000). Instillation of soluble metals, including nickel, has produced effects similar to those of

residual oil fly ash, another surrogate for particulate matter (Costa and Dreher 1997; Kodavanti et al 1998a,b).

The histopathology after O₃, PTFE, or nickel exposure was comparable in the A and B6 strains at the time of death, suggesting that resistance is an ability to forestall injury. Such a response would be consistent with a gradual loss in the lung metabolic capability to handle each of the chemicals or their resulting intermediates, such as oxidized macromolecules or degraded macromolecules (ubiquitinated peptides) (Gonder et al 1985; Mansour et al 1987; Johnston et al 1998; Leikauf and Shertzer 1999). Other mediating pathways could include cell proliferation programs regulated by oxygen-sensing molecules and cell death programs regulated by hypoxia-sensing molecules (Zhu and Bunn 1999, D'Angio and Finkelstein 2000). Thus, our finding that the strain phenotype patterns are similar with the 3 agonists tested implies that shared common genomic programs are activated during acute lung injury.

EVALUATION OF DOSE-RESPONSE RELATIONS

Acute lung injury was observed after continuous low-level nickel exposure at concentrations of 150 µg/m³ or lower, which extends findings in the current literature. In A strain mice, 20% mortality occurred with continuous exposure to nickel at a concentration of 15 µg/m³ (2 of 10 mice had died at 148 hours and at 173 hours, respectively). This concentration is below the current recommended occupational threshold limit value for human exposure to soluble nickel (100 µg/m³), but above the levels typically found in ambient particulate matter (see Introduction).

In past studies with F344/N rats and B6C3F₁ mice, 100% mortality occurred (10 of 10 mice died within 288 hours) with intermittent exposure to a higher nickel concentration of 1600 µg/m³ (Benson et al 1988; IARC 1990; NTP 1996). Our findings that B6 mice impart to their offspring resistance to acute lung injury, and C3 mice impart to their offspring resistance to protein or PMNs in lavage fluid, suggest that B6C3F₁ mice represent a resistant model for these responses to inhaled irritants. This finding may be important considering that B6C3F₁ mice are typically the only mice used in inhalation tests conducted by the NTP of the National Institute of Environmental Health Sciences. In addition, the previous studies with B6C3F₁ mice differed in other ways from the exposure protocol used in this study. In the previous studies, exposures were intermittent (6 hours/day, for 5 days/week; ie, 6-hour exposures separated by 18-hour recovery periods) and to an aerosol of larger diameter (MMAD, > 2.0 µm), whereas in this study exposures were continuous and to an aerosol with a smaller particle diameter (MMAD, 0.2 µm). The size

may influence lung dosimetry because regional deposition in the mouse respiratory tract can vary owing to the high collection efficiency of murine nasal passages for particles larger than 1.0 μm .

RELATION BETWEEN INFLAMMATION AND ACUTE LUNG INJURY

Previously, Prows and colleagues (1997 and 1999) reported that O_3 -induced acute lung injury is an oligogenetic trait with linkage to at least 2 significant QTLs. The major locus, *Aliq1*, was isolated to a region on mouse chromosome 11 that has marked synteny with human chromosome 17. Interesting candidate genes in this region include inducible nitric oxide synthetase, a cluster of the small inducible soluble cytokines, and myeloperoxidase; each has properties that could mediate oxidant injury and inflammation. Thus, at least for O_3 , several of the positional candidate genes are mediators of inflammation.

Independently, Kleeberger and colleagues (1997b) identified a locus for O_3 -induced lung inflammation on mouse chromosome 17 (syntenic to human chromosome 6). The findings with NiSO_4 presented here are consistent with the strain phenotype pattern and mode of inheritance observed with O_3 . The strain patterns with O_3 or NiSO_4 differed with the phenotype, acute lung injury or inflammation; but with either irritant, the same strains were sensitive and resistant, and sensitivity was inherited as a recessive trait. In addition, increases in NiSO_4 -induced PMNs in lavage fluid did not correlate with protein in lavage fluid. This conclusion is limited in that these variables were measured at only one time (48 hours), a choice based on the findings of Kleeberger et al (1997b) with O_3 . Nonetheless, the consistency of inter-strain differences in response to NiSO_4 and O_3 across these studies (and sustaining evidence with another oxidant, ultrafine PTFE) supports our underlying hypothesis that individual susceptibility to acute lung injury induced by fine nickel particles is a heritable trait. The discordance of the strain patterns for the 3 NiSO_4 -induced phenotypes (acute lung injury, lavage protein, or lavage PMNs) suggests that different genetic programs, which can be inherited in different arrays, control these 3 traits. As mentioned above, recent studies with O_3 support independent genetic determinants for susceptibility to acute lung injury or PMN inflammation. This leads to an important possibility: increases in proteins or PMNs in lavage fluid are not related causally to acute lung injury. This possibility implies that measurements of proteins or PMNs obtained by BAL may have little value in predicting the survival time of patients with acute lung injury, a finding consistent with previous animal studies (Eiermann et al 1983; Evans et al 1988; Kleeberger and Hudak 1992) and clinical observations (Tate and

Repine 1983; Goldman et al 1992; Pittet et al 1997).

In contrast, other clinical reports related the level of PMN influx to the severity of acute lung injury (Lee et al 1981; Weiland et al 1986). Nonetheless, this association does not prove that PMNs are responsible for acute lung injury. For example, neutropenic patients who have been exposed to radiation or cytotoxic drugs develop acute lung injury (Maunder et al 1986; Ognibene et al 1986). Although PMNs may play a direct or indirect role in acute lung injury under certain circumstances (Wiener-Kronish et al 1990), PMNs or their products may not be required for lung injury to occur. Therefore, auxiliary pathways that are not PMN dependent (including those involving activation of constitutive epithelial cells and macrophages) must exist and be capable of initiating and propagating acute lung injury. Although neutrophils mediate acute lung injury in several experimental models (eg, hydrochloric acid exposure), we have found discordance between survival and neutrophil infiltrates after NiSO_4 exposure, a finding that also agrees with O_3 exposure.

INITIAL EVALUATION OF PARTICLE SIZE AND CHEMICAL SPECIATION

Responses (PMNs or protein in lavage fluid) of animals exposed to submicrometer NiO particles by intratracheal instillation or inhalation were not statistically different from those of control animals (Tables 2 and 3). These results are in close agreement with those of other investigators using similar doses, but larger ($> 2 \mu\text{m}$) particles (Benson et al 1986, 1988; Dunnick et al 1988). In those studies, B6C3F₁ mice exposed to NiO at concentrations as high as 23,600 $\mu\text{g}/\text{m}^3$ survived a 12-day intermittent exposure with few acute effects (Benson et al 1986; Dunnick et al 1988). Nonetheless, while NiO is less acutely toxic than other nickel species, the nickel lung burden associated with it is greater because clearance of the insoluble nickel particles is greatly reduced (Benson et al 1988; Dunnick et al 1988; Tanaka et al 1988). For insoluble NiO particles larger than 2 μm , this increased lung burden contributes to biological consequences typically seen with chronic exposures.

Nevertheless, because particle solubility is inversely proportional to particle diameter, we expected to see, after exposure to 40-nm NiO, lung injury more characteristic of soluble nickel species. Numerous studies have demonstrated the increased reactivity of ultrafine particles. One such study using 20-nm metallic nickel particles at a dose (400 $\mu\text{g}/\text{kg}$ of body weight) similar to those used in this study showed substantial lung injury in rats 3 days after instillation (Zhang et al 1998). Oxidative damage appears to account for the greater acute toxicity of metallic nickel in these size ranges. In our experiments, however, we were

not able to duplicate this phenomenon, either because the particles were not small enough (40 nm rather than 20 nm), or because the dose was not large enough to adequately compare results with those of other investigators.

In previous studies with NiSO₄ particles larger than 2.0 μm, mice exposed to nickel concentrations of 1600 μg/m³ or higher died of severe lung injury after a 12-day intermittent NiSO₄ exposure (Benson et al 1988; Dunnick et al 1988). In our experiments, animals exposed to either 60-nm or 250-nm NiSO₄ particles developed inflammation. The 60-nm particle resulted in an earlier inflammatory response, whereas the 250-nm particle led to a greater response. In addition, in A strain mice the minimal lethal dose of nickel (<15 μg/m³) was lower among those continuously exposed to 0.2-μm particles than among those intermittently exposed to 2.5-μm particles. Deposition of particles at or below this size range is not well characterized in mice; therefore, interpretation of these results is difficult. One possibility is that the depositional efficiency in the alveolar region of the lung is not equal for 60-nm and 250-nm particles. Another possibility is that deposition of 250-nm NiSO₄ particles may produce the greatest effect in the mouse alveolus because they are small enough to penetrate the upper respiratory tract (ie, deeper than the > 2.0-μm aerosol penetrates) and yet large enough to impart a higher dose per cell apical surface area. Each 250-nm particle contains 72 times more nickel than a 60-nm particle.

ALTERED REGULATION OF GENE EXPRESSION IN B6 MICE

After selected times of NiSO₄ exposure, differential gene expression in mouse lung progressed with lung injury. The number of significant changes demonstrates the complex pathophysiology of acute lung injury induced by nickel. Groups of genes sharing common temporal patterns of expression often shared common functions. Overall, the number of genes that increased after each exposure period approximated the number of genes that decreased, suggesting a reequilibration of the lung's genomic balance after nickel exposure.

A portion of the genes displaying differential expression in this study previously had been found to increase in the lung after nickel exposure, including the metallothionein-1, lactotransferrin, and GAPDH genes. Metallothionein-1, which increased more than any other gene measured (> 13-fold at 96 hours) (Figures 8 and 9), encodes a thiol-rich protein that increases in lung injury induced by nickel (Bauman et al 1993), cigarette smoke (Gilks et al 1998), and O₃ (Mango et al 1998), and can protect against metal-induced oxidative damage to critical macromolecules (Pitt et al 1997). Like metallothionein-1, lactotransferrin also

increases in response to nickel and, as a metal-binding protein, may provide antioxidant protection as well (Ghio et al 1998). Another gene previously found to increase in expression with nickel exposure is GAPDH (Graven et al 1998). As a component of anaerobic glycolysis, increased GAPDH expression may provide an adaptive response to changes in oxygen tension.

In addition to these increased genes, several other genes have been associated with acute lung injury, including the heme oxygenase-1 and secretory leukoprotease inhibitor genes. Heme oxygenase-1 levels increased modestly after exposure (Figure 9), but heme oxygenase-1 can protect against hyperoxia-induced acute lung injury (Otterbein et al 1999). Secretory leukoprotease inhibitor is a local source of antiprotease protection in the lung, inhibits protease destruction of the extracellular matrix (Thompson and Ohlsson 1986), and accumulates slowly after treatment with elastase (Abbinante-Nissen et al 1993). In addition, patients with acute lung injury have been shown to have elevated concentrations of secretory leukoprotease inhibitor (Sallenave et al 1999).

Genes that decreased in response to nickel and that have been associated previously with acute lung injury included CCSP and SP-A, SP-B, and SP-C (Figure 10). Mice deficient in CCSP have an elevated response to oxidants (Mango et al 1998), indicating this protein may be critical to antioxidant defenses in the airways. Interestingly, secreted CCSP protein concentrations are elevated in patients who recover from acute lung injury but diminished in those who do not survive (Jorens et al 1995). Surfactant-associated proteins modulate alveolar surface tension, prevent atelectasis, inactivate reactive oxygen species, and augment host antimicrobial defenses (Weaver and Whitsett 1991). Diminished SP concentrations have been observed in patients with acute lung injury (Gregory et al 1991; Lewis and Jobe 1993), and gene transcription decreases with administration of tumor necrosis factor-α (TNF-α), a cytokine often elevated in acute lung injury (Bachurski et al 1995).

By assessing the temporal and functional relationships of differentially expressed genes in B6 mice, our analyses revealed the progression of the pulmonary response to injury. Group I genes of particular interest included galectin-3, STAT-3, and small proline-rich protein 1a (Figure 8). In pulmonary injury, it is common for type II cells to proliferate and squamous cells to differentiate in order to replace damaged type I cells and cover the unprotected alveolar basement membrane (Vracko 1972; Adamson and Bowden 1974; Lewis and Jobe 1993; Jobe and Ikegami 1998). Galectin-3 expression increases with injury in both cell types (Kasper and Hughes 1996) and is a

galactose-binding and IgE-binding lectin that stimulates macrophage migration, cell survival (by suppressing apoptosis), cytokine release, and proliferation (Warfel and Zucker-Franklin 1992; Inohara et al 1998). The signals initiating type II cell differentiation remain largely unknown, but may include STAT-3 (Tesfaigzi et al 1996a; Fernandes et al 1999; Stephanou et al 2000), which is activated during hemorrhagic lung injury (Meng et al 2000). Signal transducer and activator of transcription (STAT) proteins also mediate activation of several cytokine genes, including TNF- α (Chappell et al 2000). Similarly, small proline-rich protein 1a (Tesfaigzi et al 1996b) is induced in epithelial cell differentiation in response to injury. Thus, nickel-induced acute lung injury results in increased expression of genes possibly involved in epithelial replacement.

Several of the genes that increased during nickel exposure are known to be induced during hypoxia. In response to reduced oxygen concentrations, the transactivating factor hypoxia-inducible factor-1 binds to a consensus sequence within regulatory regions of aldolase (Semenza et al 1994, 1996), enolase (Aaronson et al 1995; Semenza et al 1996), GAPDH (Graven et al 1998), and heme oxygenase-1 (Murphy et al 1991; Otterbein et al 1999). Another neighboring gene in this cluster, 6-phosphogluconate dehydrogenase, acts in consort with GAPDH, and together these enzymes may help to restore metabolic homeostasis via a pentose phosphate pathway by supporting fatty acid synthesis, NADPH generation used to reduce glutathione, and ribose 5-phosphate generation for nucleic acid biosynthesis. Although it is unknown whether it is induced by hypoxia-inducible factor-1 activation, 6-phosphogluconate dehydrogenase has been implicated in acute lung injury (Kozar et al 2000).

Some of the induced genes that displayed delayed increases (Group II) may be involved in the progression of acute lung injury. Two of these—secretory leukoprotease inhibitor, an antiprotease, and lysyl oxidase, an enzyme critical to elastin stabilization (McGowan 1992)—may indicate maintenance of the extracellular matrix. Epithelial membrane protein-1 functions in cell growth, squamous differentiation, and apoptosis (Jetten and Suter 2000). Other members of this group may signify alteration of components of the inflammatory response; for example, T-lymphocyte maturation-associated protein, a surface antigen, indicates T-cell differentiation. One limitation of our analysis was the paucity of other microarray elements involved in the pulmonary inflammatory response, limiting the ability to assess their changes in relationship to other genes in this large-scale assessment. For example, concentrations of interleukin 1 β , interleukin 6, and macrophage inflammatory protein-2 were elevated in FVB/N mice after nickel exposure (Figure 20) but were not contained in the library of clones on the microarray.

Another cluster, Group IV, contained several genes that are expressed constitutively in the lung and have been associated with acute lung injury. This cluster is characterized by genes that were maintained initially, then decreased (typically at 24 hours), and remained diminished throughout the rest of the exposure. The leading members were SP-C (Figures 8 and 10), which is predominately expressed by type II cells, and CCSP and cytochrome P450 2f2, which are predominately expressed in Clara cells (Plopper et al 1997). In addition to known genes, ESTs with nominal homology to known genes clustered into each of the 4 temporal groups. Using a BLAST analysis, we found that 2 ESTs in this group had high homology with SP-B. Interestingly, Groups III and IV, which contain genes that decreased with exposure, had the highest percentage of ESTs. Because other ESTs displayed expression patterns similar to those of known genes, they may similarly play significant roles in normal pulmonary function and thus are excellent candidates for further study. In addition, because less is currently known about genes that are down-regulated during injury, characterization of these sequences may provide insight into their possible roles, and open new areas of research on the disruption of lung function during acute lung injury and possible mechanisms of repair.

Overall, genes involved in oxidant injury, extracellular matrix repair, cell proliferation, and hypoxia increased, while those involved in constitutive lung function (SPs and CCSP) decreased. Perhaps the clearest difference noted in this study was the decreased expression of SPs. Alteration of surfactant homeostasis is a critical event in the pathophysiology of acute lung injury, and although they constitute only a small portion of the surfactant complex, SPs are critical for life. For example, mice deficient in SP-B succumbed to respiratory failure within 20 minutes after birth (Clark et al 1995). Our findings are consistent with the ongoing attempts to treat acute lung injury with exogenous surfactant-containing SPs (Jobe and Ikegami 1998), possibly in combination with antioxidant therapy. The delayed temporal pattern of surfactant decreases also implies that administration of exogenous surfactant may have to be early (before focal atelectasis develops) and sustained to achieve effective therapy.

NICKEL-INDUCED ACUTE LUNG INJURY—A COMPLEX QUANTITATIVE TRAIT

To further explore a genetic basis for the difference in the ability of A and B6 mice to survive nickel-induced lung injury, QTL analysis was performed in 307 backcross mice generated from these strains using MAPMAKER/QTL and QTL Cartographer. A significant QTL was identified on chromosome 6, with a peak lod score at the microsatellite

marker *D6Mit183* (located 26.5 cM distal to the centromere). Two other QTLs, on chromosomes 1 and 12, were suggestive of linkage.

Possible positional candidate genes for the major QTL on chromosome 6 (*Aliq4*) were identified in the region spanning ± 1 lod unit change around the *D6Mit183* marker. Three genes within this interval are of immediate interest as candidates for involvement in acute lung injury. The first positional candidate gene for *Aliq4* is *Aqp1*, a member of the membrane transport family of genes that are the primary water channels of the pulmonary epithelium and endothelium (Matthay et al 1998). Pulmonary edema is one of the distinguishing characteristics of acute lung injury, and diminished levels of *Aqp1* may alter hydrostatically driven fluid accumulation (Bai et al 1999). Second, the expression of SP genes was identified in the microarray analysis and the S1 nuclease protection assays to be markedly decreased after nickel exposure. Indeed, decreases in 2 ESTs with homology to SP-B (*Sftpb*) were among the largest changes noted in the microarray analysis. Third, growth factors can stimulate alveolar epithelial cell proliferation and alveolar fluid clearance, and may protect against acute lung injury. Accordingly, the TGF- α gene (*Tgfa*) is also a positional candidate for *Aliq4*.

COMPARATIVE MICROARRAY OF A AND B6 MICE DURING NICKEL EXPOSURE

To complement the QTL analysis and further assess the importance of candidate genes, microarray analysis was performed and gene expression changes were directly compared with those we previously determined in B6 mice. Because A strain mice succumbed before 96 hours of nickel exposure, this comparative analysis was limited to the first 48 hours. In general, more expression changes were noted in the B6 mice than in the A mice. At the earliest exposure time more significant expression changes were noted in the A mice, but as the exposure continued more expression changes occurred in the B6 mice. Known genes and annotated ESTs showed increased expression more often than decreased expression. When nonannotated ESTs were included in the analysis, however, the percentage of genes that increased in expression (54%) approximated the percentage that decreased (46%). This discrepancy might be explained by a bias of researchers to report genes that are increased in expression. However, it is plausible that genes decreased in expression are equally important in disease pathogenesis, though less attention may have been given to these genes.

To identify the genes with the greatest difference between the strains, the acceptance stringency was increased to a

2-fold change in expression in one or both strains. In total, 133 different cDNAs met these criteria in either the A or B6 exposed mice, including 93 differences that were known genes and annotated ESTs (Table 9) and 40 nonannotated ESTs. Among these changes, about one third (45/133) occurred in both strains (A and B6). The remaining changes were divided between those cDNAs that were expressed more in A mice (Figure 15) and those that were expressed more in B6 mice (Figure 16). Theoretically, any of these expression differences could represent a potential candidate gene for controlling at least part of the difference in phenotypic response. Equally important, genes with lesser differences between the strains, which were not highlighted by the stringent criteria used in this study, are also likely to be candidates.

Among the potential candidate genes identified in the comparison of A and B6 expression profiles, complement and SPs have long been suggested as important factors in acute lung injury (Luce 1998). In fact, therapeutic strategies for acute lung injury have been directly aimed at complement inhibition (Yeatman et al 1999; Heller et al 2000) or surfactant replacement (Evans et al 1996, MacIntyre 2000). In contrast, other genes, including those for calgranulin A (*S100a8*), cytochrome P450 2b9 (*Cyp2b9*), galectin-3 (*Lgals3*), hemoglobin- α adult chain-1 (*Hba-a1*), mitogen-activated protein (MAP) kinase phosphatase-1 (*Ptpn16*), and N-myc downstream regulator-1 (*Ndr1*), have not heretofore been implicated in acute lung injury (Table 11).

Among these candidates, 3 produce proteins with functional relevance to lung injury. First, a member of the S100 protein family, calgranulin A (*S100a8*), also called macrophage-related protein-8 (MRP8), increased 6.2-fold in A mice but decreased in B6 mice (Figure 15), suggesting that it may be related to the increased susceptibility of the A strain to acute lung injury. Although the biological function of calgranulin A still is under investigation, it is a Ca²⁺-binding protein expressed in activated macrophages and a potent chemoattractant for monocytes and neutrophils (Lackmann et al 1992). Complexing with S100A9, calgranulin A forms a cell-surface and cytoskeleton-associated heterodimer upon calcium mobilization and may serve as a metal-sensitive and oxidant-sensitive arachidonate transport protein (Harrison et al 1999; Kerkhoff et al 1999; Eue et al 2000). Associated with acute and chronic lung diseases including bleomycin-induced fibrosis (Kumar et al 1998), bronchitis (Roth et al 1992), and cystic fibrosis (Wilkinson et al 1988), this protein may reflect the presence of rapidly migrating monocytes and possibly a difference in the activation state of macrophages (or other inflammatory cells) that is not reflected in lavage cell differential analysis.

Second, hemoglobin- α , adult chain-1 (*Hba-a1*) expression was increased in B6 mice and decreased in A mice during the first 24 to 48 hours of exposure, with the A mice reaching levels that were 4-fold less than those in B6 mice at 48 hours. If one assumes that an increase in message led to an increase in active protein, then B6 mice may have an increased ability to deliver molecular oxygen to tissues during the initial and following hours, thereby fending off hypoxia and extending survival. Alternatively, the increase in gene activity could reflect a difference in the amount or maturity of red blood cells in the lung.

A third gene not previously associated with acute lung injury, but whose expression was differentially altered in the 2 strains by nickel exposure, is MAP kinase phosphatase-1 (*Ptpn16*). Induced by growth factors, cytokines, and stress (Garrington and Johnson 1999), as well as hypoxia (Laderoute et al 1999), *Ptpn16* is an immediate early gene able to dephosphorylate and inactivate extracellular signal-regulated protein kinases and stress-activated protein kinases (Shapiro and Ahn 1998). Interestingly, residual oil fly ash containing soluble transition metals can activate rat MAP kinase cell signaling pathways (Silbajoris et al 2000) that may be opposed by nonreceptor cytoplasmic protein tyrosine phosphatase. In addition, *Ptpn16* maps 50.8 cM distal to the centromere on mouse chromosome 17. This location places *Ptpn16* within the *Ali3* interval, a QTL linked to survival time for O₃-induced acute lung injury using A and B6 recombinant inbred strains (Prows et al 1997). Thus, because of its key position in MAP kinase signal transduction pathways and its genetic linkage to acute lung injury susceptibility, *Ptpn16* may modulate the fate of cells stimulated by environmental and stress-related insults.

COMBINING RESULTS OF cDNA MICROARRAYS AND QUANTITATIVE TRAIT LOCUS ANALYSES

Ideally, combining the microarray results with those of the QTL analysis (genomewide scan) would identify genes within one of the putative QTL intervals that differ in gene expression between the A and B6 mice. However, many of the microarray's cDNAs encoded genes that are yet to be mapped or annotated, so this initial analysis must be viewed cautiously (Table 11). In addition, candidate genes identified in QTLs are not all on the existing microarray. Finally, a measure of gene expression (cDNA microarray) may not reflect functional polymorphism in a protein, even when expression is identical between strains. Nonetheless, of the 3 leading candidate genes that reside in *Aliq4*, the QTL interval on chromosome 6, *Sftpb* was decreased more in the B6 mice than in the A mice (which is paradoxical given the resistant phenotype of the B6

strain), *Aqp1* did not change with exposure, and *Tgfa* is not included on the microarray. Independently, we have determined that nickel exposure increased TGF- α mRNA levels about 2-fold in a mouse line with a mixed Swiss Black-CD1-129 background (unpublished findings 2000), but we have yet to determine whether mRNA levels differ in A and B6 strains. Another candidate that varied between the A and B6 strains and mapped near a QTL was procollagen type III, $\alpha 1$ (*Col3a1*), on chromosome 1. Several genes residing in the QTL interval on chromosome 8, including esterase-1 (*Es1*), metallothionein-1 (*Mt1*), glutathione reductase-1 (*Gr1*), and heme oxygenase-1 (*Hmox1*), were altered by exposure. Candidates on chromosomes 12 or 16 either did not change or were not on the microarray (Table 11).

FUNCTIONAL GENOMIC EVALUATION OF POSITIONAL CANDIDATE GENES

Each of the positional candidate genes in the QTL regions identified is worthy of further investigation. The present study explored one candidate gene, *Tgfa*, using transgenic mice. These tests demonstrated differences between hTGF- α transgenic and nontransgenic mice in the development of acute lung injury with NiSO₄ exposure. All mice from the 3 highest-expressing hTGF- α transgenic mouse lines survived significantly longer than the nontransgenic strain-matched mice. Characterization of the lung injury demonstrated reduced inflammatory cytokine production, cellular infiltration, and lung wet-to-dry weight ratio, and preservation of SP-B at 72 hours of exposure in the highest-expressing transgenic line (line 28) compared with nontransgenic mice.

The survival time among transgenic mice continuously exposed to submicrometer NiSO₄ increased with increasing levels of hTGF- α transgene and resembled a dose-response curve. The lowest-expressing line 6108, which contained hTGF- α at 96 pg/mL in lung homogenates, did not survive significantly longer than nontransgenic mice. However, line 4 mice (with hTGF- α at 390 pg/mL in lung homogenates) had modest, yet significant protection, with all line 4 mice surviving longer than the longest-surviving nontransgenic or line 6108 mouse. The next-highest-expressing transgenic mice (line 2) demonstrated a significantly greater survival curve than lower-expressing transgenic lines, and the highest-expressing line 28 had the best survival outcome. Several line 2 and line 28 mice survived the entire exposure period. Thus, levels of hTGF- α between 600 and 900 pg/mL in lung homogenates, as produced by line 2 and line 28 mice, provided significant protection against NiSO₄-induced injury.

The characterization of nontransgenic and line 28 mice demonstrated markedly reduced exudative pulmonary edema as assessed by histology, BAL protein levels, and lung wet-to-dry weight ratios. This attenuation of pulmonary edema after submicrometer NiSO₄ exposure in TGF- α transgenic mice is similar to our finding in TGF- α transgenic mice exposed to ultrafine PTFE (Hardie et al 1999). The mechanism by which TGF- α prevents or reduces pulmonary edema is uncertain; however, the beneficial effects of hTGF- α in this model of acute lung injury may occur through several mechanisms, including acting directly on alveolar type II cells to increase alveolar fluid clearance. Previously, Folkesson and colleagues (1996) demonstrated that instillation of TGF- α increased alveolar fluid clearance (within 1 to 4 hours), and they suggested that TGF- α binds to its receptor or receptors expressed by type II cells and stimulates a tyrosine protein kinase pathway that directly leads to sodium channel activation. We have not measured alveolar fluid clearance in our transgenic mice; however, clearance of pulmonary edema mediated by TGF- α may be one mechanism whereby TGF- α provides protection against lung injury induced by NiSO₄ or PTFE.

Another possible mechanism of increased survival may involve the diminished macrophage activation, cytokine production, and inflammatory cell infiltration observed in TGF- α transgenic mice. The reduced BAL neutrophils and lung homogenate cytokines 72 hours into NiSO₄ exposure in line 28 mice compared with nontransgenic mice indicated attenuated lung leukocyte activation. Currently, it is uncertain whether TGF- α can directly alter chemokine and cytokine production by lung cells *in vitro*. Before exposure, the lung homogenate levels of interleukin 1 β , interleukin 6, and macrophage inflammatory protein-2 were nearly identical between line 28 mice and nontransgenic control mice, suggesting that high levels of hTGF- α did not augment cytokine production. Following NiSO₄ exposure, nontransgenic mice had higher neutrophil and cytokine levels than transgenic mice, suggesting that hTGF- α inhibited the induction of these responses. In human colonic epithelial cells *in vitro*, preconditioning with TGF- α inhibited bradykinin-induced prostaglandin production, suggesting that TGF- α has a role in limiting the acute inflammatory responses (Beltinger et al 1999). Whether TGF- α can modify selective components of the inflammatory cascade and act to modify lung inflammation after NiSO₄ exposure is unknown.

Although we propose that survival of nickel-induced acute lung injury is likely to be independent of the presence of PMN (primarily neutrophil) infiltrates, these infiltrates have been the focus of many animal models and were markedly inhibited in transgenic mice compared

with nontransgenic mice. In humans, neutrophil influx into the airspaces occurs before the development of acute lung injury (Fowler et al 1983, 1987). Normally less than 2% of the cells in BAL fluid are neutrophils, but they may constitute as much as 90% of the cells in BAL fluid recovered from patients with acute respiratory distress syndrome. Several reports have linked the level of neutrophil influx with severity of acute lung injury (Lee et al 1981; Weiland et al 1986). Nonetheless, for the reasons stated above, the association of neutrophils with acute lung injury does support causality in this study.

Other potential mechanisms whereby TGF- α improves survival may involve protection from injury through maintenance of normal epithelial integrity, stimulation of cell proliferation, and wound repair processes. Currently, it is not known whether TGF- α transgenic mice have augmented cell turnover *in vivo*, and the precise role of growth factors in the lung is not completely understood. Nonetheless, growth is clearly important in maintaining normal epithelial integrity and stimulating repair processes. Previously, Aggarwal et al (1994) demonstrated that transfection or exogenous addition of TGF- α to colon carcinoma cell lines decreased the antiproliferative effects of TNF- α . In addition, Reinartz and colleagues (1996) reported that TNF- α -induced apoptosis was significantly reduced in cell lines of human keratinocytes preincubated with TGF- α . Accelerated wound healing associated with TGF- α -induced cell proliferation, as demonstrated *in vitro* in rabbit gastric mucosa and *in vivo* in rodents, attenuates injury to the gastric mucosa induced by ethanol and aspirin. In these injury models, TGF- α antibodies decrease cell proliferation, exogenous TGF- α protects against forms of epithelial injury, and TGF- α reduces gut injury exaggerated in TGF- α knockout mice (Konturek et al 1992, 1998a,b; Tarnawski et al 1992; Romano et al 1996; Egger et al 1997, 1998). The expression of hTGF- α by type II epithelial cells may increase epithelial cell regeneration and migration after NiSO₄-induced injury, thus accelerating restoration of the epithelial integrity and attenuating the degree of lung injury.

RELATION BETWEEN LUNG REMODELING AND INCREASED SUSCEPTIBILITY

Previously, we noted that TGF- α transgenic mice have varying levels of lung remodeling (Korfhagen et al 1994, Hardie et al 1997), and we questioned whether this could account for the differences in survival and in attenuation of pulmonary edema and inflammation observed in our studies. Initially, we hypothesized that mice with the emphysematous and fibrotic changes of the line 28 mice would be sensitive to irritant-induced acute lung injury,

and we were surprised by the increase in their survival. Although we cannot rule out the possibility of some benefit from lung remodeling in transgenic mice, 3 lines of evidence support our hypothesis that TGF- α attenuates lung injury independent of lung remodeling.

First, we did not detect less NiSO₄ retention in the lungs of line 28 transgenic mice compared with nontransgenic control mice (actually, retention was slightly higher). Although NiSO₄ deposition and clearance were not directly measured, lung retention data for nontransgenic and line 28 mice suggest that the two groups received similar doses of NiSO₄ in the lung, or that line 28 mice may have received slightly more NiSO₄. Thus, differences in retention probably do not explain the observed difference in susceptibility.

Second, the higher-expressing line 4 mice survived significantly longer than the lower-expressing line 6108 mice, despite a lack of detectable histologic, morphologic, or physiologic differences between these 2 lines (Hardie et al 1997). The increased survival of line 4 mice would thus suggest that TGF- α provides a significant survival benefit independent of any lung remodeling.

Third, previous studies of emphysema in animal models have demonstrated that emphysematous lungs often are no more or less susceptible to injury by irritants than normal lungs (March et al 2000). For example, Harkema and colleagues (1982) found no differences in survival, inflammation, or pulmonary function between emphysematous and normal rats after hyperoxia. Similarly, Busch and associates (1984) found that elastase-induced emphysematous rats and guinea pigs developed little difference in their pulmonary and inflammatory response to ammonium sulfate relative to control animals. Likewise, Raub and colleagues (1983) exposed hamsters to olefin-O₃-sulfur dioxide reaction products (23 hours/day, for 4 weeks) and were unable to discern differences in the inflammatory response or pulmonary function between emphysematous and nonemphysematous animals. Thus, lung remodeling alone is unlikely to account for the protection against NiSO₄ injury in TGF- α transgenic mice. Further, emphysema alone may not explain the increased susceptibility to particulate matter we observed in mice, which may also reflect on whether persons with chronic obstructive pulmonary disease are always more responsive to acute challenges from particulate matter.

RELATION BETWEEN TGF- α AND SURFACTANT-ASSOCIATED PROTEINS

Directed expression of TGF- α in the lung may protect against NiSO₄-induced injury through maintenance of SP levels. We examined lung homogenate protein levels of

SP-B and SP-D at time 0 and after 72 hours of NiSO₄ exposure. At baseline, SP-D levels of nontransgenic and line 28 mice were similar; however, line 28 mice had less than half the SP-B levels of nontransgenic mice. After 72 hours of NiSO₄ exposure, SP-D levels in nontransgenic mice fell approximately 27% and SP-B levels were reduced almost 75% compared with unexposed nontransgenic mice. The decrease in SP-D and SP-B in nontransgenic mice is consistent with the cDNA microarray findings demonstrating reduced SP-A, SP-B, and SP-C mRNA levels in mice after NiSO₄ exposure.

A small hydrophobic peptide produced only in the lung, SP-B enhances surfactant absorption and spreading and is necessary for the surface-tension-reducing properties of pulmonary surfactant. For line 28 mice, SP-D decreased approximately 40% from time 0, while SP-B levels remained unaffected (remaining at 49% of the nonexposed levels of the nontransgenic controls and at 112% of the line 28 preexposure control). The preservation of SP-B levels after 72 hours of NiSO₄ exposure in line 28 mice may have contributed to the increased survival and lack of pulmonary edema and inflammation in this TGF- α transgenic line. Mice that are homozygotic SP-B gene-targeted succumb to respiratory failure shortly after birth, whereas heterozygotic SP-B gene-targeted mice containing 50% of wildtype SP-B levels survive, suggesting that a 50% loss of SP-B can be tolerated. However, heterozygotic mice develop increased lung permeability and BAL protein leakage as well as histologic evidence of pulmonary edema, hemorrhage, and inflammation, compared with wildtype mice after 72 hours of hyperoxia (Tokieda et al 1999a). Administration of surfactant with the active SP-B peptide to heterozygous SP-B mice can prevent alveolar capillary leak and histologic abnormalities caused by oxygen-induced injury (Tokieda et al 1999b). While unexposed line 28 mice have lower SP-B levels than nontransgenic mice matched by age and strain, the preservation of SP-B levels after NiSO₄ exposure may contribute to the increased survival and reduced lung injury.

In addition, SP-D and SP-A are members of a family of host defense lectins, called collectins, and are important components of the innate immune response in the lung (Crouch et al 2000). A wide variety of respiratory pathogens, as well as nonmicrobial particles including dust mite allergen, are bound by SP-D. It enhances uptake of microbes by macrophages and neutrophils and regulates interleukin 2 production by T-lymphocytes. Both SP-D and SP-B are produced in Clara cells and type II cells. The basis for the decreased levels of SP-B in nontransgenic mice, but not line 28 mice, and the decreased levels of SP-D in both strains is not clear. We do not detect histologic

evidence of epithelial, bronchiolar, or alveolar cell necrosis or death in line 28 mice, making it unlikely that selective cell loss contributed to decreased SP-D levels. Differences in TGF- α -induced transcription, mRNA stability, or protein activity may account for the selective preservation of SP-B levels, but further studies are required to support such a conclusion.

SUMMARY

In this study, strains of mice varied in their susceptibility to acute lung injury, protein content of lavage fluid, and inflammation in response to a soluble component of particulate matter, NiSO₄. Each phenotype was inherited as an independent recessive trait. The NiSO₄ concentrations used to produce acute lung injury were as low as 15 $\mu\text{g}/\text{m}^3$. The strain phenotype patterns were shared by 3 irritants, fine NiSO₄, ultrafine PTFE, and O₃, suggesting that this is a conserved response mechanism, possibly related to oxidant injury. Findings with microarrays and a genomewide scan suggest that NiSO₄-induced acute lung injury is a complex trait (ie, under the control of at least 5 genes, possibly involved in epithelial cell growth, surfactant function, and fluid movement). A major QTL was identified on mouse chromosome 6 that contains several positional candidate genes with relevance to acute lung injury. These include TGF- α , *Sftpb*, and *Aqp1*. Transgenic mice expressing increased levels of TGF- α were protected from acute lung injury, and this protection may have involved preservation of SP-B levels in the lung. The QTLs identified provide chromosomal regions linked with lung injury induced by particulate matter and contain excellent positional candidates for further investigation. Future research identifying susceptibility genes in model species combined with an assessment of human synteny and function could provide valuable insights into why certain individuals are at greater risk for the adverse effects of particulate matter.

ACKNOWLEDGMENTS

The authors thank Alvaro Puga PhD for helpful advice and technical assistance. Susan McDowell, Scott Weselkamper, and Clay Miller received University of Cincinnati graduate assistantships, and this work is in partial fulfillment of their degree requirements at the University of Cincinnati. For a complete list of cDNA expression changes contained in the manuscript, address correspondence to George D Leikauf PhD, Department of Environmental Health, University of Cincinnati, PO Box 670056, Cincinnati OH 45267-0056.

REFERENCES

- Aaronson RM, Graven KK, Tucci M, McDonald RJ, Farber HW. 1995. Non-neuronal enolase is an endothelial hypoxic stress protein. *J Biol Chem* 270:27752–27757.
- Abbinante-Nissen JM, Simpson LG, Leikauf GD. 1993. Neutrophil elastase increases secretory leukocyte protease inhibitor transcript levels in airway epithelial cells. *Am J Physiol* 265:L286–L292.
- Adamson IY, Bowden DH. 1974. The type 2 cell as progenitor of alveolar epithelial regeneration. A cytodynamic study in mice after exposure to oxygen. *Lab Invest* 30:35–42.
- Aggarwal BB, Pocsik E, Ali-Osman F, Totpal K. 1994. Transfection of cells with transforming growth factor- α leads to cellular resistance to the antiproliferative effects of tumor necrosis factor. *FEBS Lett* 354:12–16.
- Bachurski CJ, Pryhuber GS, Glasser SW, Kelly SE, Whitsett JA. 1995. Tumor necrosis factor- α inhibits surfactant protein C gene transcription. *J Biol Chem* 270:19402–19407.
- Bai C, Fukuda N, Song Y, Ma T, Matthay M, Verkman A. 1999. Lung fluid transport in aquaporin-1 and aquaporin-4 knockout mice. *J Clin Invest* 103:555–561.
- Bal W, Liang R, Lukszo J, Lee SH, Dizdaroglu M, Kasprzak KS. 2000. Ni(II) specifically cleaves the C-terminal tail of the major variant of histone H2A and forms an oxidative damage-mediating complex with the cleaved-off octapeptide. *Chem Res Toxicol* 13:616–624.
- Barbu V, Dautry F. 1989. Northern blot normalization with a 28S rRNA oligonucleotide probe. *Nucleic Acids Res* 17:7115.
- Barceloux DG. 1999. Nickel. *J Toxicol Clin Toxicol* 37:239–258.
- Bassett DJP, Elbon CL, Reichenbaugh SS, Boswell GA, Stevens TM, McGowan MC, Kerr JS. 1989. Pretreatment with EDU decreases rat lung cellular responses to ozone. *Toxicol Appl Pharmacol* 100:32–40.
- Basten CJ, Weir BS, Zeng ZB. 1994. Zmap: A QTL cartographer. In: *Proceedings of the 5th World Congress on Genetics Applied to Livestock Production: Computing Strategies and Software*. Ontario, Canada.
- Basten CJ, Weir BS, Zeng ZB. 1997. *QTL Cartographer: A Reference Manual and Tutorial for QTL Mapping*. Department of Statistics, North Carolina State University, Raleigh NC.

- Bauman JW, Liu J, Klaassen CD. 1993. Production of metallothionein and heat-shock proteins in response to metals. *Fundam Appl Toxicol* 21:15–22.
- Beltinger J, Hawkey CJ, Stack WA. 1999. TGF- α reduces bradykinin-stimulated ion transport and prostaglandin release in human colonic epithelial cells. *Am J Physiol* 276:C848–C855.
- Benson JM, Burt DG, Carpenter RL, Eidson AF, Hahn FF, Haley PJ, Hanson RL, Hobbs CH, Pickrell JA, Dunnick JK. 1988. Comparative inhalation toxicity of nickel sulfate to F344/N rats and B6C3F₁ mice exposed for twelve days. *Fundam Appl Toxicol* 10:164–178.
- Benson JM, Chang IY, Cheng YS, Hahn FF, Kennedy CH, Barr EB, Maples KR, Snipes MB. 1995. Particle clearance and histopathology in lungs of F344/N rats and B6C3F₁ mice inhaling nickel oxide or nickel sulfate. *Fundam Appl Toxicol* 28:232–244.
- Benson JM, Henderson RF, McClellan RO, Hanson RL, Rebar AH. 1986. Comparative acute toxicity of four nickel compounds to F344 rat lung. *Fundam Appl Toxicol* 7:340–347.
- Bingham E, Barkley W, Zerwas M, Stemmer K, Taylor P. 1972. Responses of alveolar macrophages to metals. I. Inhalation of lead and nickel. *Arch Environ Health* 25:406–414.
- Biswas P, Wu CY. 1998. Control of toxic metal emissions from combustors using sorbents: A review. *J Air Waste Manag Assoc* 48:113–127.
- Bradford MM. 1976. A rapid and sensitive method for the quantification of microgram quantities of protein using the principle of protein-dye binding. *Anal Biochem* 72:248–254.
- Braxton S, Bedilion T. 1998. The integration of microarray information in the drug development process. *Curr Opin Biotechnol* 9:643–649.
- Brecher RW, Austen M, Light HE, Stepien E. 1989. *Eco Logic* (Contract Report). Environmental Substances Division, Environmental Health Center, Health and Welfare Canada, Ottawa, Ontario.
- Bright P, Burge PS, O'Hickey SP, Gannon PF, Robertson AS, Boran A. 1997. Occupational asthma due to chrome and nickel electroplating. *Thorax* 52:28–32.
- Busch RH, Buschbom RL, Cannon WC, Lauhala KE, Miller FJ, Graham JA, Smith LG. 1984. Effects of ammonium sulfate aerosol exposure on lung structure of normal and elastase-impaired rats and guinea pigs. *Environ Res* 33:454–472.
- Camner P, Johansson A. 1992. Reaction of alveolar macrophages to inhaled metal aerosols. *Environ Health Perspect* 97:185–188.
- Chan WH, Lusia MA. 1986. Smelting operations and trace metals in air and precipitation in the Sudbury Basin. *Adv Environ Sci Technol* 17:113–143.
- Chappell VL, Le LX, LaGrone L, Mileski WJ. 2000. Stat proteins play a role in tumor necrosis factor alpha gene expression. *Shock* 14:400–402.
- Chase K, Adler FR, Lark KG. 1997. Epistat: A computer program for identifying and testing interactions between pairs of quantitative trait loci. *Theor Appl Genet* 94:724–730.
- Clark JC, Wert SE, Bachurski CJ, Stahlman MT, Stripp BR, Weaver TE, Whitsett JA. 1995. Targeted disruption of the surfactant protein B gene disrupts surfactant homeostasis, causing respiratory failure in newborn mice. *Proc Natl Acad Sci USA* 92:7794–7798.
- Cornell RG, Landis JR. 1984. Mortality patterns among nickel/chromium alloy foundry workers. *IARC Sci Publ* 53:87–93.
- Costa DL, Dreher KL. 1997. Bioavailable transition metals in particulate matter mediate cardiopulmonary injury in healthy and compromised animal models. *Environ Health Perspect* 105(Suppl 5):1053–1060.
- Crouch E, Hartshorn K, Ofek I. 2000. Collectins and pulmonary innate immunity. *Immunol Rev* 173:52–65.
- Dalton T, Palmiter RD, Andrews GK. 1994. Transcriptional induction of the mouse metallothionein-I gene in hydrogen peroxide-treated Hepa cells involves a composite major late transcription factor/antioxidant response element and metal response promoter elements. *Nucleic Acids Res* 22:5016–5023.
- D'Angio CT, Finkelstein JN. 2000. Oxygen regulation of gene expression: A study in opposites. *Mol Genet Metab* 71:371–380.
- Dobrin DJ, Potvin R. 1992. *Air Quality Monitoring Studies in the Sudbury Area: 1978 to 1988*. PIBS 1870. Ontario Ministry of the Environment, Technical Assessment Section, Northeastern Region, Toronto, Ontario.
- Dockery DW, Pope CA III, Xu X, Spengler JD, Ware JH, Fay ME, Ferris BG Jr, Speizer FE. 1993. An association between

- air pollution and mortality in six US cities. *N Engl J Med* 329:1753–1759.
- Dreher KL, Jaskot RH, Lehmann JR, Richards JH, McGee JK. 1997. Soluble transition metals mediate residual oil fly ash induced acute lung injury. *J Toxicol Environ Health* 50:285–305.
- Dunnick JK, Benson JM, Hobbs CH, Hahn FF, Cheng YS, Eidson AF. 1988. Comparative toxicity of nickel oxide, nickel sulfate hexahydrate, and nickel subsulfide after 12 days of inhalation exposure to F344/N rats and B6C3F₁ mice. *Toxicology* 50:145–156.
- Dunnick JK, Elwell MR, Radovsky AE, Benson JM, Hahn FF, Nikula KJ, Barr EB, Hobbs CH. 1995. Comparative carcinogenic effects of nickel subsulfide, nickel oxide, or nickel sulfate hexahydrate chronic exposures in the lung. *Cancer Res* 55:5251–5256.
- Dye JA, Adler KB, Richards JH, Dreher KL. 1997. Epithelial injury induced by exposure to residual oil fly-ash particles: Role of reactive oxygen species? *Am J Respir Cell Mol Biol* 17:625–633.
- Egger B, Carey HV, Procaccino F, Chai NN, Sandgren EP, Lakshmanan J, Buslon VS, French SW, Buchler MW, Eysselein VE. 1998. Reduced susceptibility of mice overexpressing transforming growth factor alpha to dextran sodium sulphate induced colitis. *Gut* 43:64–70.
- Egger B, Procaccino F, Lakshmanan J, Reinshagen M, Hoffmann P, Patel A, Reuben W, Gnanakkan S, Liu L, Barajas L, Eysselein VE. 1997. Mice lacking transforming growth factor alpha have an increased susceptibility to dextran sulfate-induced colitis. *Gastroenterology* 113:825–832.
- Eiermann GJ, Dickey BF, Thrall RS. 1983. Polymorphonuclear leukocyte participation in acute oleic-acid-induced lung injury. *Am Rev Respir Dis* 128:845–850.
- Eisen MB, Spellman PT, Brown PO, Botstein D. 1998. Cluster analysis and display of genome-wide expression patterns. *Proc Natl Acad Sci USA* 95:14863–14868.
- Eue I, Pietz B, Storck J, Klempt M, Sorg C. 2000. Transendothelial migration of 27E10(+) human monocytes. *Int Immunol* 12:1593–1604.
- Evans DA, Wilmott RW, Whitsett JA. 1996. Surfactant replacement therapy for adult respiratory distress syndrome in children. *Pediatr Pulmonol* 21:328–336.
- Evans TW, Brokaw JJ, Chung KF, Nadel JA, McDonald DM. 1988. Ozone-induced bronchial hyperresponsiveness in the rat is not accompanied by neutrophil influx or increased vascular permeability in the trachea. *Am Rev Respir Dis* 138:140–144.
- Fairley D. 1990. The relationship of daily mortality to suspended particulates in Santa Clara County, 1980–1986. *Environ Health Perspect* 89:159–168.
- Ferguson RC, Banks CV. 1951. Spectrophotometric determination of nickel using 1,2-cycloheptanedione dioxime (heptoxime). *Anal Chem* 23:448–454.
- Fernandes A, Hamburger AW, Gerwin BI. 1999. ErbB-2 kinase is required for constitutive stat 3 activation in malignant human lung epithelial cells. *Int J Cancer* 83:564–570.
- Folkesson HG, Pittet JF, Nitenberg G, Matthay MA. 1996. Transforming growth factor-alpha increases alveolar liquid clearance in anesthetized ventilated rats. *Am J Physiol* 271:L236–L244.
- Fowler AA, Hamman RF, Good JT, Benson KN, Baird M, Eberle DJ, Petty TL, Hyers TM. 1983. Adult respiratory distress syndrome: Risk with common predispositions. *Ann Intern Med* 98:593–597.
- Fowler AA, Hyers TM, Fisher BJ, Bechard DE, Centor RM, Webster RO. 1987. The adult respiratory distress syndrome: Cell populations and soluble mediators in the air spaces of patients at high risk. *Am Rev Respir Dis* 136:1225–1231.
- Garrington TP, Johnson GL. 1999. Organization and regulation of mitogen-activated protein kinase signaling pathways. *Curr Opin Cell Biol* 11:211–218.
- Ghio AJ, Richards JH, Dittrich KL, Samet JM. 1998. Metal storage and transport proteins increase after exposure of the rat lung to an air pollution particle. *Toxicol Pathol* 26:388–394.
- Gilks CB, Price K, Wright JL, Churg A. 1998. Antioxidant gene expression in rat lung after exposure to cigarette smoke. *Am J Pathol* 152:269–278.
- Goldman G, Welbourn R, Rothlein R, Wiles M, Kobzik L, Valeri CR, Shepro D, Hechtman HB. 1992. Adherent neutrophils mediate permeability after atelectasis. *Ann Surg* 216:372–380.
- Goldstein BD, Lai LY, Ross SR, Cuzzi-Spada R. 1973. Susceptibility of inbred mouse strains to ozone. *Arch Environ Health* 27:412–413.
- Gonder JC, Proctor RA, Will JA. 1985. Genetic differences in oxygen toxicity are correlated with cytochrome P-450 inducibility. *Proc Natl Acad Sci USA* 82:6315–6319.

- Graven KK, McDonald RJ, Farber HW. 1998. Hypoxic regulation of endothelial glyceraldehyde-3-phosphate dehydrogenase. *Am J Physiol* 274:C347–355.
- Gregory TJ, Longmore WJ, Moxley MA, Whitsett JA, Reed CR, Fowler AAD, Hudson LD, Maunder RJ, Crim C, Hyers TM. 1991. Surfactant chemical composition and biophysical activity in acute respiratory distress syndrome. *J Clin Invest* 88:1976–1981.
- Haber LT, Erdreich L, Diamond GL, Maier AM, Ratney R, Zhao Q, Dourson ML. 2000. Hazard identification and dose response of inhaled nickel-soluble salts. *Regul Toxicol Pharmacol* 31:210–230.
- Hackett RL, Sunderman FW Jr. 1968. Pulmonary alveolar reaction to nickel carbonyl: Ultrastructural and histochemical studies. *Arch Environ Health* 16:349–362.
- Hardie WD, Bruno MD, Huelsman KM, Iwamoto HS, Carrigan PE, Leikauf GD, Whitsett JA, Korfhagen TR. 1997. Postnatal lung function and morphology in transgenic mice expressing transforming growth factor- α . *Am J Pathol* 151:1075–1083.
- Hardie WD, Prows DR, Leikauf GD, Korfhagen TR. 1999. Attenuation of acute lung injury in transgenic mice expressing human transforming growth factor- α . *Am J Physiol* 277:L1045–L1050.
- Harrison CA, Raftery MJ, Walsh J, Alewood P, Iismaa SE, Thliveris S, Geczy CL. 1999. Oxidation regulates the inflammatory properties of the murine S100 protein S100A8. *J Biol Chem* 274:8561–8569.
- Harkema JR, Mauderly JL, Hahn FF. 1982. The effects of emphysema on oxygen toxicity in rats. *Am Rev Respir Dis* 126:1058–1065.
- Heller A, Kunz M, Samakas A, Haase M, Kirschfink M, Koch T. 2000. The complement regulators C1 inhibitor and soluble complement receptor 1 attenuate acute lung injury in rabbits. *Shock* 13:285–290.
- Holroyd KJ, Eleff SM, Zhang LY, Jakab GJ, Kleeberger SR. 1997. Genetic modeling of susceptibility to nitrogen dioxide-induced lung injury in mice. *Am J Physiol* 273:L595–L602.
- Ichinose T, Suzuki AK, Tsubone H, Sagai M. 1982. Biochemical studies on strain differences of mice in the susceptibility to nitrogen dioxide. *Life Sci* 31:1963–1972.
- International Agency for Research on Cancer. 1986. IARC Monographs on the Evaluation of Carcinogenic Risks to Humans: Tobacco Smoking, Vol. 38. IARC, Lyon, France.
- International Agency for Research on Cancer. 1990. IARC Monographs on the Evaluation of Carcinogenic Risks to Humans: Chromium, Nickel, and Welding, Vol. 49. IARC, Lyon, France.
- Inohara H, Akahani S, Raz A. 1998. Galectin-3 stimulates cell proliferation. *Exp Cell Res* 245:294–302.
- Jetten AM, Suter U. 2000. The peripheral myelin protein 22 and epithelial membrane protein family. *Prog Nucleic Acid Res Mol Biol* 64:97–129.
- Jobe AH, Ikegami M. 1998. Surfactant and acute lung injury. *Proc Assoc Am Physicians* 110:489–495.
- Johnston CJ, Finkelstein JN, Gelein R, Oberdörster G. 1998. Pulmonary inflammatory responses and cytokine and antioxidant mRNA levels in the lungs of young and old C57BL/6 mice after exposure to Teflon fumes. *Inhalation Toxicol* 10:931–953.
- Jorens PG, Sibille Y, Goulding NJ, van Overveld FJ, Herman AG, Bossaert L, De Backer WA, Lauwerys R, Flower RJ, Bernard A. 1995. Potential role of Clara cell protein, an endogenous phospholipase A2 inhibitor, in acute lung injury. *Eur Respir J* 8:1647–1653.
- Kaminski N, Allard JD, Pittet JF, Zuo F, Griffiths MJD, Morris D, Huang X, Sheppard D, Heller RA. 2000. Global analysis of gene expression in pulmonary fibrosis reveals distinct programs regulating lung inflammation and fibrosis. *Proc Natl Acad Sci USA* 97:1778–1783.
- Kasper M, Hughes RC. 1996. Immunocytochemical evidence for a modulation of galectin 3 (Mac-2), a carbohydrate binding protein, in pulmonary fibrosis. *J Pathol* 179:309–316.
- Kerkhoff C, Vogl T, Nacken W, Sopalla C, Sorg C. 1999. Zinc binding reverses the calcium-induced arachidonic acid-binding capacity of the S100A8/A9 protein complex. *FEBS Lett* 460:134–138.
- Kleeberger SR, Bassett DJP, Jakab GJ, Levitt RC. 1990. A genetic model for evaluation of susceptibility to ozone-induced inflammation. *Am J Physiol* 258:L313–L320.
- Kleeberger SR, Hudak BB. 1992. Acute ozone-induced change in airway permeability: Role of infiltrating leukocytes. *J Appl Physiol* 72:670–676.
- Kleeberger SR, Levitt RC, Zhang LY. 1993. Susceptibility to ozone-induced inflammation. I. Genetic control of the response to subacute exposure. *Am J Physiol* 264:L15–L20.
- Kleeberger SR, Levitt RC, Zhang LY, Longphre M, Harkema J, Jedlicka A, Eleff SM, DiSilvestre D, Holroyd KJ. 1997a.

- Linkage analysis of susceptibility to ozone-induced lung inflammation in inbred mice. *Nat Genet* 17:475–478.
- Kleeberger SR, Zhang LY, Jakab GJ. 1997b. Differential susceptibility to oxidant exposure in inbred strains of mice: Nitrogen dioxide versus ozone. *Inhalation Toxicol* 9:601–621.
- Kodavanti UP, Jaskot RH, Su WY, Costa DL, Ghio AJ, Dreher KL. 1997. Genetic variability in combustion particle-induced chronic lung injury. *Am J Physiol* 272:L521–L532.
- Kodavanti UP, Meng ZH, Hauser R, Christiani DC, Ledbetter A, McGee J, Richards J, Costa DL. 1998a. Pulmonary responses to oil fly ash particles in the rat differ by virtue of their specific soluble metals. *Toxicol Sci* 43:204–212.
- Kodavanti UP, Meng ZH, Hauser R, Christiani DC, Ledbetter A, McGee J, Richards J, Costa DL. 1998b. In vivo and in vitro correlates of particle-induced lung injury: Specific roles of bioavailable metals. In: *Relationships Between Respiratory Disease and Exposure to Air Pollution* (Mohr U, Dungworth DL, Brain JD, Driscoll KE, Grafström RC, Harris CC, eds). ILSI Monographs. ILSI Press, Washington DC.
- Konturek PC, Bobrzynski A, Konturek SJ, Bielanski W, Faller G, Kirchner T, Hahn EG. 1998a. Epidermal growth factor and transforming growth factor alpha in duodenal ulcer and non-ulcer dyspepsia patients before and after *Helicobacter pylori* eradication. *Scand J Gastroenterol* 33:143–151.
- Konturek SJ, Brzozowski T, Majka J, Dembinski A, Slomiany A, Slomiany BL. 1992. Transforming growth factor alpha and epidermal growth factor in protection and healing of gastric mucosal injury. *Scand J Gastroenterol* 27:649–655.
- Konturek PC, Brzozowski T, Pierzchalski P, Kwiecien S, Pajdo R, Hahn EG, Konturek SJ. 1998b. Activation of genes for spasmolytic peptide, transforming growth factor alpha and for cyclooxygenase (COX)-1 and COX-2 during gastric adaptation to aspirin damage in rats. *Aliment Pharmacol Ther* 12:767–777.
- Korfhagen TR, Swantz RJ, Wert SE, McCarty JM, Kerlakian CB, Glasser SW, Whitsett JA. 1994. Respiratory epithelial cell expression of human transforming growth factor-alpha induces lung fibrosis in transgenic mice. *J Clin Invest* 93:1691–1699.
- Kozar RA, Weibel CJ, Cipolla J, Klein AJ, Haber MM, Abedin MZ, Trooskin SZ. 2000. Antioxidant enzymes are induced during recovery from acute lung injury. *Crit Care Med* 28:2486–2491.
- Kumar RK, Harrison CA, Cornish CJ, Kocher M, Geczy CL. 1998. Immunodetection of the murine chemotactic protein CP-10 in bleomycin-induced pulmonary injury. *Pathology* 30:51–56.
- Lackmann M, Cornish CJ, Simpson RJ, Moritz RL, Geczy CL. 1992. Purification and structural analysis of a murine chemotactic cytokine (CP-10) with sequence homology to S100 proteins. *J Biol Chem* 267:7499–7504.
- Laderoute KR, Mendonca HL, Calaoagan JM, Knapp AM, Giaccia AJ, Stork PJS. 1999. Mitogen-activated protein kinase phosphatase-1 (MKP-1) expression is induced by low oxygen conditions found in solid tumor microenvironments. *J Biol Chem* 274:12890–12897.
- Lander E, Kruglyak L. 1995. Genetic dissection of complex traits: Guidelines for interpreting and reporting results. *Nat Genet* 11:241–247.
- Lander ES, Green P, Abrahamson J, Barlow A, Daly MJ, Lincoln SE, Newburg L. 1987. MAPMAKER: An interactive computer package for constructing primary genetic linkage maps of experimental and natural populations. *Genomics* 1:174–181.
- Lee CT, Fein AM, Lippmann M, Holtzman H, Kimbel P, Weinbaum G. 1981. Elastolytic activity in pulmonary lavage fluid from patients with adult respiratory distress syndrome. *N Engl J Med* 304:192–196.
- Leikauf GD, Kline S, Albert RE, Baxter CS, Bernstein DI, Buncher CR. 1995. Evaluation of a possible association of urban air toxics and asthma. *Environ Health Perspect* 103(Suppl 6):253–271.
- Leikauf GD, McDowell SA, Gammon K, Wesselkamper SC, Bachurski CJ, Puga A, Wiest JS, Leikauf JE, Prows DR. 2000. Functional genomics of particle-induced lung injury. *Inhalation Toxicol* 12(Suppl 3):59–73.
- Leikauf GD, Prows DR, Shertzer HG, Carrigan PE, Zhao Q, Borchers MT, Ormerod E, Simpson LG, Weaver TE, Clark JC, Lee NC, Whitsett JA, Lee JJ, Driscoll KE. 1998. Asthma and acute lung injury: Transgenic models and genetic determinants. In: *Relationships Between Respiratory Disease and Exposure to Air Pollution* (Mohr U, Dungworth DL, Brain JD, Driscoll KE, Grafström RC, Harris CC, eds). ILSI Monographs. ILSI Press, Washington DC, pp 45–58.
- Leikauf GD, Shertzer HG. 1999. Molecular mechanisms and genetic determinants of ozone toxicity in the lung. In:

- Molecular Biology of the Toxic Response (Puga A, Wallace KB, eds), Taylor & Francis, Washington DC, pp 317–335.
- Lewis JF, Jobe AH. 1993. Surfactant and the adult respiratory distress syndrome. *Am Rev Respir Dis* 147:218–233.
- Lincoln SE, Daly MJ, Lander ES. 1992a. Constructing Genetic Maps with MAPMAKER/EXP 3.0. Technical Report, 3rd ed. Whitehead Institute, Cambridge MA.
- Lincoln SE, Daly MJ, Lander ES. 1992b. Mapping Genes Controlling Quantitative Traits with MAPMAKER/QLT 1.1. Technical Report, 2nd ed. Whitehead Institute, Cambridge MA.
- Logan WPD. 1953. Mortality in the London fog incident. *Lancet* 1:336–339.
- Luce JM. 1998. Acute lung injury and the acute respiratory distress syndrome. *Crit Care Med* 26:369–376.
- MacIntyre NR. 2000. Aerosolized medications for altering lung surface-active properties. *Respir Care* 45:676–683.
- Malo JL, Cartier A, Gagnon G, Evans S, Dolovich J. 1985. Isolated late asthmatic reaction due to nickel sulphate without antibodies to nickel. *Clin Allergy* 15:95–99.
- Mango GW, Johnston CJ, Reynolds SD, Finkelstein JN, Plopper CG, Stripp BR. 1998. Clara cell secretory protein deficiency increases oxidant stress response in conducting airways. *Am J Physiol* 275:L348–L356.
- Mansour H, Levacher M, Azoulay-Dupuis E, Moreau J, Marquetty C, Gougerot-Pocidal MA. 1987. Genetic differences in response to pulmonary cytochrome *P*-450 inducers and oxygen toxicity. *J Appl Physiol* 64:1376–1381.
- March TH, Green FHY, Hahn FF, Nikula KJ. 2000. Animal models of emphysema and their relevance to studies of particle-induced disease. *Inhalation Toxicol* 12(Suppl 4):155–187.
- Matthay MA, Flori HR, Conner ER, Ware LB. 1998. Alveolar epithelial fluid transport: Basic mechanisms and clinical relevance. *Proc Assoc Am Physicians* 110:496–505.
- Maunder RJ, Hackman RC, Riff E, Albert RK, Springmeyer SC. 1986. Occurrence of the adult respiratory distress syndrome in neutropenic patients. *Am Rev Respir Dis* 133:313–316.
- McDonnell WF III, Horstman DH, Abdul-Salaam S, House DE. 1985. Reproducibility of individual responses to ozone exposure. *Am Rev Respir Dis* 131:36–40.
- McGowan SE. 1992. Extracellular matrix and the regulation of lung development and repair. *FASEB J* 6:2895–2904.
- Meng ZH, Dyer K, Billiar TR, Tweardy DJ. 2000. Distinct effects of systemic infusion of G-CSF vs. IL-6 on lung and liver inflammation and injury in hemorrhagic shock. *Shock* 14:41–48.
- Milford JB, Davidson CI. 1987. The sizes of particulate sulfate and nitrate in the atmosphere—a review. *J Air Poll Control Assoc* 37:125–134.
- Misra M, Rodriguez RE, North SL, Kasprzak KS. 1991. Nickel-induced renal lipid peroxidation in different strains of mice: Concurrence with nickel effect on antioxidant systems. *Toxicol Lett* 58:121–133.
- Murphy BJ, Laderoute KR, Short SM, Sutherland RM. 1991. The identification of heme oxygenase as a major hypoxic stress protein in Chinese hamster ovary cells. *Br J Cancer* 64:69–73.
- National Institute for Occupational Safety and Health. 1977. Criteria for a Recommended Standard: Occupational Exposure to Inorganic Nickel. DHEW-NIOSH Document 77-164. US Government Printing Office, Washington DC.
- National Toxicology Program. 1996. Toxicology and Carcinogenesis Studies of Nickel Sulfate Hexahydrate (CAS No. 10101-97-0) in F344/N rats and B6C3F₁ Mice (Inhalation Studies). NTP-TRS 454. National Institutes of Health, Research Triangle Park NC.
- National Toxicology Program. Ninth Report on Carcinogens (posted 01/23/01). <http://ehis.niehs.nih.gov/roc/>. Accessed 07/19/01.
- Nriagu JO. 1980. Nickel in the Environment. John Wiley and Sons, New York NY.
- Oberdörster G. 1995. Lung particle overload—implications for occupational exposures to particles. *Regul Toxicol Pharmacol* 21:123–135.
- Oberdörster G, Ferin J, Finkelstein G, Wade P, Corson N. 1990. Increased pulmonary toxicity of ultrafine particles? II. Lung lavage studies. *J Aerosol Sci* 21: 384–387.
- Oberdörster G, Gelein R, Johnston C, Mercer P, Corson N, Finkelstein JN. 1998. Ambient ultrafine particles: Inducers of acute lung injury? In: Relationships Between Respiratory Disease and Exposure to Air Pollution (Mohr U, Dungworth DL, Brain JD, Driscoll KE, Grafström RC, Harris CC, eds). ILSI Monographs. ILSI Press, Washington DC.

- Ognibene FP, Martin SE, Parker MM, Schlesinger T, Reach P, Burch C, Shelhamer JH, Parillo JE. 1986. Adult respiratory distress syndrome in patients with severe neutropenia. *N Engl J Med* 315:547–551.
- Ontario Ministry of the Environment. 1992. Air Quality in Ontario: 1990. PIBS 1804-01/02, A86–A88. Queen's Printer for Ontario, Toronto, Ontario.
- Otterbein LE, Kolls JK, Mantell LL, Cook JL, Alam J, Choi AM. 1999. Exogenous administration of heme oxygenase-1 by gene transfer provides protection against hyperoxia-induced lung injury. *J Clin Invest* 103:1047–1054.
- Paterson AH, Damon S, Hewitt JD, Zamir D, Rabinowitch HD, Lincoln SE, Lander ES, Tanksley SD. 1991. Mendelian factors underlying quantitative traits in tomato: Comparison across species, generations, and environments. *Genetics* 127:181–197.
- Pitt BR, Schwarz M, Woo ES, Yee E, Wasserloos K, Tran S, Weng W, Mannix RJ, Watkins SA, Tyurina YY, Tyurin VA, Kagan VE, Lazo JS. 1997. Overexpression of metallothionein decreases sensitivity of pulmonary endothelial cells to oxidant injury. *Am J Physiol* 273:L856–L865.
- Pittet JF, Mackersie RC, Martin TR, Matthay MA. 1997. Biological markers of acute lung injury: Prognostic and pathogenetic significance. *Am J Respir Crit Care Med* 155:1187–1205.
- Plopper CG, Hyde DM, Buckpitt AR. 1997. Clara cell. In: *The Lung: Scientific Foundations*, 2nd ed (Crystal RG, Barnes PJ, West JB, Weibel ER, eds). Lippincott-Raven, Philadelphia PA, pp 215–228.
- Pope CA III, Kanner RE. 1993. Acute effects of PM₁₀ pollution on pulmonary function of smokers with mild to moderate chronic obstructive pulmonary disease. *Am Rev Respir Dis* 147:1136–1340.
- Pritchard RJ, Ghio AJ, Lehmann JR, Winsett DW, Tepper JS, Park P, Gilmour ML, Dreher KL, Costa DL. 1996. Oxidant generation and lung injury after particulate air pollutant exposure increases with the concentrations of associated metals. *Inhalation Toxicol* 8:457–477.
- Prows DR, Daly MJ, Shertzer HG, Leikauf GD. 1999. Ozone-induced acute lung injury: Genetic analysis of F₂ mice generated from A/J and C57BL/6J strains. *Am J Physiol* 277:L372–L380.
- Prows DR, Shertzer HG, Daly MJ, Sidman CL, Leikauf GD. 1997. Genetic analysis of ozone-induced acute lung injury in sensitive and resistant strains of mice. *Nat Genet* 17:471–474.
- Pryor WA, Nuggehalli SK, Scherer KV Jr, Church DF. 1990. An electron spin resonance study of the particles produced in the pyrolysis of perfluoro polymers. *Chem Res Toxicol* 3:2–7.
- Raub JA, Miller FJ, Graham JA, Gardner DE, O'Neil JJ. 1983. Pulmonary function in normal and elastase-treated hamsters exposed to a complex mixture of olefin-ozone-sulfur dioxide reaction products. *Environ Res* 31:302–310.
- Reinartz J, Bechtel MJ, Kramer MD. 1996. Tumor necrosis factor-alpha-induced apoptosis in a human keratinocyte cell line (HaCaT) is counteracted by transforming growth factor-alpha. *Exp Cell Res* 228:334–340.
- Rodriguez RE, Misra M, North SL, Kasprzak KS. 1991. Nickel-induced lipid peroxidation in the liver of different strains of mice and its relation to nickel effects on antioxidant systems. *Toxicol Lett* 57:269–281.
- Romano M, Lesch CA, Meise KS, Veljaca M, Sanchez B, Kraus ER, Boland CR, Guglietta A, Coffey RJ. 1996. Increased gastroduodenal concentrations of transforming growth factor alpha in adaptation to aspirin in monkeys and rats. *Gastroenterology* 110(5):1448–1455.
- Roth J, Teigelkamp S, Wilke M, Grun L, Tummler B, Sorg C. 1992. Complex pattern of the myelo-monocytic differentiation antigens MRP8 and MRP14 during chronic airway inflammation. *Immunobiology* 186:304–314.
- Sallenave JM, Donnelly SC, Grant IS, Robertson C, Gaudie J, Haslett C. 1999. Secretory leukocyte proteinase inhibitor is preferentially increased in patients with acute respiratory distress syndrome. *Eur Respir J* 13:1029–1036.
- Salnikow K, Costa M. 2000a. Epigenetic mechanisms of nickel carcinogenesis. *J Environ Pathol Toxicol Oncol* 19:307–318.
- Salnikow K, Gao M, Voitkun V, Huang X, Costa M. 1994. Altered oxidative stress responses in nickel-resistant mammalian cells. *Cancer Res* 54:6407–6412.
- Salnikow K, Su W, Blagosklonny MV, Costa M. 2000b. Carcinogenic metals induce hypoxia-inducible factor-stimulated transcription by reactive oxygen species-independent mechanism. *Cancer Res* 60:3375–3378.
- Schroeder WH, Dobson M, Kane DM, Johnson ND. 1987. Toxic trace elements associated with airborne particulate matter: A review. *J Air Pollut Control Assoc* 37:1267–1285.
- Schwartz J. 1992. Particulate air pollution and daily mortality: A synthesis. *Public Health Rev* 19:39–60.

- Schwartz J, Marcus A. 1990. Mortality and air pollution in London: A time series analysis. *Am J Epidemiol* 131:185–194.
- Semenza GL, Jiang BJ, Leung SW, Passantino R, Concordet JP, Maire P, Giallongo A. 1996. Hypoxia response elements in the aldolase A, enolase 1, and lactate dehydrogenase A gene promoters contain essential binding sites for hypoxia-inducible factor 1. *J Biol Chem* 271: 32529–32537.
- Semenza GL, Roth PH, Fang HM, Wang GL. 1994. Transcriptional regulation of genes encoding glycolytic enzymes by hypoxia-inducible factor 1. *J Biol Chem* 269:23757–23763.
- Senior CL, Flagan RC. 1982. Ash vaporization and condensation during combustion of a suspended coal particle. *Aerosol Sci Technol* 1:371–383.
- Shapiro PS, Ahn NG. 1998. Feedback regulation of Raf-1 and mitogen-activated protein (MAP) kinase kinases 1 and 2 by MAP kinase phosphatase-1 (MKP-1). *J Biol Chem* 273:1788–1793.
- Shi ZC. 1986. Acute nickel carbonyl poisoning: A report of 179 cases. *Br J Ind Med* 43:422–424.
- Shirakawa T, Kusaka Y, Fujimura N, Kato M, Heki S, Morimoto K. 1990. Hard metal asthma: Cross immunological and respiratory reactivity between cobalt and nickel? *Thorax* 45:267–271.
- Silbajoris RA, Ghio J, Samet JM, Jaskot R, Dreher KL, Brighton LE. 2000. In vivo and in vitro correlation of pulmonary MAP kinase activation following metallic exposure. *Inhalation Toxicol* 12:453–468.
- Silver LM. 1995. *Mouse Genetics: Concepts and Applications*. Oxford University Press, New York NY.
- Sioutas C, Abt E, Wolfson JM, Koutrakis P. 1999. Evaluation of the measurement performance of the scanning mobility particle sizer and aerodynamic particle sizer. *Aerosol Sci Technol* 30:84–92.
- Stephanou A, Brar BK, Knight RA, Latchman DS. 2000. Opposing actions of STAT-1 and STAT-3 on the Bcl-2 and Bcl-x promoters. *Cell Death Differ* 7:329–330.
- Stohs SJ, Bagchi D. 1995. Oxidative mechanisms in the toxicity of metal ions. *Free Radic Biol Med* 18:321–336.
- Stokinger HE. 1957. Evaluation of the hazards of ozone and oxides of nitrogen: Factors modifying toxicity. *Arch Ind Health* 15:181–190.
- Stringer B, Kobzik L. 1998. Environmental particulate-mediated cytokine production in lung epithelial cells (A549): role of preexisting inflammation and oxidant stress. *J Toxicol Environ Health* 55:31–44.
- Tanaka I, Horie A, Haratake J, Kodama Y, Tsuchiya K. 1988. Lung burden of green nickel oxide aerosol and histopathological findings in rats after continuous inhalation. *Biol Trace Elem Res* 16:19–26.
- Tarnawski A, Lu SY, Stachura J, Sarfeh IJ. 1992. Adaptation of gastric mucosa to chronic alcohol administration is associated with increased mucosal expression of growth factors and their receptor. *Scand J Gastroenterol Suppl* 193:59–63.
- Tate RM, Repine JE. 1983. Neutrophils and the adult respiratory distress syndrome. *Am Rev Respir Dis* 128:552–559.
- Tesfaigzi J, Johnson NF, Lechner JF. 1996a. Induction of EGF receptor and erbB-2 during endotoxin-induced alveolar type II cell proliferation in the rat lung. *Int J Exp Pathol* 77:143–154.
- Tesfaigzi J, Th'ng J, Hotchkiss JA, Harkema JR, Wright PS. 1996b. A small proline-rich protein, SPRR1, is upregulated early during tobacco smoke-induced squamous metaplasia in rat nasal epithelia. *Am J Respir Cell Mol Biol* 14:478–486.
- Thompson RC, Ohlsson K. 1986. Isolation, properties, and complete amino acid sequence of human secretory leukocyte protease inhibitor, a potent inhibitor of leukocyte elastase. *Proc Natl Acad Sci USA* 83:6692–6696.
- Tokieda K, Ikegami M, Wert SE, Baatz JE, Zou Y, Whitsett JA. 1999b. Surfactant protein B corrects oxygen-induced pulmonary dysfunction in heterozygous surfactant protein B-deficient mice. *Pediatr Res* 46:708–714.
- Tokieda K, Iwamoto HS, Bachurski C, Wert SE, Hull WM, Ikeda K, Whitsett JA. 1999a. Surfactant protein-B-deficient mice are susceptible to hyperoxic lung injury. *Am J Respir Cell Mol Biol* 21:463–472.
- Vracko R. 1972. Significance of basal lamina for regeneration of injured lung. *Virchows Arch A Pathol Pathol Anat* 355:264–274.
- Warfel AH, Zucker-Franklin D. 1992. Specific ligation of surface alpha-D-galactosyl epitopes markedly affects the quantity of four major proteins secreted by macrophages. *J Leukocyte Biol* 52:80–84.

Weaver TE, Whitsett JA. 1991. Function and regulation of expression of pulmonary surfactant-associated proteins. *Biochem J* 273:249–264.

Weiland JE, Davis B, Holter JF, Mohammed JR, Dorinsky PM, Gadek JE. 1986. Lung neutrophils in the adult respiratory distress syndrome: Clinical and pathophysiologic significance. *Am Rev Respir Dis* 133:218–225.

Wiener-Kronish JP, Gropper MA, Matthay MA. 1990. The adult respiratory distress syndrome: Definition and prognosis, pathogenesis and treatment. *Br J Anaesth* 65:107–129.

Wilkinson MM, Busuttill A, Hayward C, Brock DJ, Dorin JR, Van Heyningen V. 1988. Expression pattern of two related cystic fibrosis-associated calcium-binding proteins in normal and abnormal tissues. *J Cell Sci* 91:221–230.

Yeaman M, Daggett CW, Lau CL, Byrne GW, Logan JS, Platt JL, Davis RD. 1999. Human complement regulatory proteins protect swine lungs from xenogeneic injury. *Ann Thorac Surg* 67:769–775.

Zhang Q, Kusaka Y, Sato K, Nakakuki K, Kohyama N, Donaldson K. 1998. Differences in the extent of inflammation caused by intratracheal exposure to three ultrafine metals: Role of free radicals. *J Toxicol Environ Health* 53:423–438.

Zhu H, Bunn HF. 1999. Oxygen sensing and signaling: Impact on the regulation of physiologically important genes. *Respir Physiol* 115:239–247.

ABOUT THE AUTHORS

George Leikauf PhD is a professor of environmental health, molecular and cellular physiology, a professor of pulmonary and critical care medicine, and director of the molecular toxicology division at the University of Cincinnati, College of Medicine.

Susan A McDowell (unpaid graduate assistant), **Scott C Wesselkamper** (graduate assistant), and **Clay R Miller** (unpaid graduate assistant) received support from the US Environmental Protection Agency in the form of an individual STAR (U-9157301) graduate fellowship, a Ryan Fellowship, and University of Cincinnati Graduate Assistantships, respectively. This work is in partial fulfillment of their degree requirements at the University of Cincinnati. They each have been first authors on at least one manuscript generated from work on this project as unpaid assistants. Ms McDowell focused her studies on the cDNA microarray in mice during acute lung injury, Mr Wesselka-

mpfer conducted the initial comparisons of responses of inbred mouse strains exposed to NiSO₄ and those exposed to O₃ and PTFE, and Mr (now Dr) Miller examined the role of chemical and morphological properties of combustion aerosols containing submicrometer nickel.

William D Hardie MD (unpaid consultant) is an assistant professor in pulmonary medicine and pediatrics and **Thomas R Korfhagen MD, PhD** (unpaid consultant) is an associate professor of pulmonary biology and pediatrics, both at the Children's Hospital Medical Center in Cincinnati. Dr Korfhagen developed the transgenic mouse lines that express human transforming growth factor and works closely with Dr Hardie in studies examining how these mice are protected from the adverse effects of inhaled materials.

Bruce J Aronow PhD (unpaid consultant) is an associate professor of developmental biology and pediatrics and **Kelly Gammon** (unpaid consultant) is an information sciences specialist, both at the Children's Hospital Medical Center in Cincinnati. Dr Aronow is an expert in bioinformatics and enabled the computational analysis of the microarray data. Ms Gammon provided valuable expertise in the data management that led to the temporal clustering analysis of the cDNA microarray findings.

Pratim P Biswas PhD (coinvestigator) is a professor of civil and environmental engineering and **Klaus Willeke PhD** (coinvestigator) is a professor of environmental health at the University of Cincinnati. Both were consultants in the area of aerosol generation and characterization. Dr Biswas was the doctoral advisor to Clay Miller.

Cindy J Bachurski PhD (unpaid consultant) is an assistant of pulmonary biology and pediatrics at the Children's Hospital Medical Center in Cincinnati and a molecular biologist who aided in the evaluation of the regulation of SP gene expression using S1 nuclease protection assay.

Jonathan S Wiest PhD (unpaid consultant) is an assistant professor of environmental health and **John E Leikauf** (student assistant) is a student helper, at the University of Cincinnati, College of Medicine, and both were involved in the sequencing, annotation analysis, and evaluation of ESTs.

Eula Bingham PhD (coinvestigator) is a professor of environmental health at the University of Cincinnati, College of Medicine and a consultant in macrophage pathophysiology and nickel toxicology.

Daniel R Prows PhD (coinvestigator) was a postdoctoral assistant and is now an assistant professor of environmental health at the University of Cincinnati, College of Medicine. He conducted genomewide quantitative trait

analysis and microarray analyses comparing inbred mouse strains.

OTHER PUBLICATIONS RESULTING FROM THIS RESEARCH

Prows DR, Leikauf GD. 2001. Quantitative trait locus analysis of nickel-induced acute lung injury in mice. *Am J Respir Cell Mol Biol* 24:740–746.

Leikauf GD, Borchers MT, Hardie WD, Korfhagen TR, Wesselkamper SC, McDowell SA, Prows DR. 2000. Susceptibility to air pollution: Genetic determinants and transgenic models. In: *Relationships Between Acute and Chronic Effects of Air Pollution* (Heinrich U, Mohr U, Bates DV, Brain JD, Driscoll KE, Dungworth DL, Grafstrom RC, Harris CC, Heyder J, Koren HS, Maduerly JL, Paulahn J, Samet JM, Utell MJ, eds). ILSI Monograph. ILSI Press, Washington DC, pp 97–111.

Leikauf GD, McDowell SA, Gammon K, Wesselkamper SC, Bachurski CJ, Puga A, Wiest JS, Leikauf JE, Prows DR. 2000. Functional genomics of particle-induced lung injury. *Inhalation Toxicol* 12(Suppl 3):59–73.

McDowell SA, Gammon K, Bachurski CJ, Weist JS, Leikauf JE, Prows DR, Leikauf GD. 2000. Differential gene expression in the initiation and progression of nickel-induced acute lung injury. *Am J Respir Cell Mol Biol* 23:466–474.

Wesselkamper SC, Prows DR, Biswas P, Willeke K, Bingham E, Leikauf GD. 2000. Genetic susceptibility to irritant-induced lung injury in mice. *Am J Physiol Lung Cell Mol Physiol* 279:L575–L582.

Hardie WD, Prows DR, Piljan-Gentle A, Wesselkamper SC, Leikauf GD, Korfhagen TR. Dose-related protection from nickel-induced lung injury in transgenic mice expressing human transforming growth factor- α . *Am J Respir Cell Mol Biol* (in press).

Leikauf GD, McDowell SA, Bachurski CJ, Aronow BJ, Gammon K, Wesselkamper SC, Hardie W, Wiest JS, Korfhagen TR, Prows DR. Functional genomics of oxidant-induced lung injury. In: *Biological Reactive Intermediates. VI: Chemical and Biological Mechanisms of Susceptibility to and Prevention of Environmental Disease* (Synder R et al, ed). Kluwer Academic Plenum Publishers, New York NY (in press).

McDowell SA, Mallakin A, Bachurski CJ, Toney-Earley K, Prows DR, Bruno T, Kaestner KH, Witte DP, Melin-Aldana MD, Degen SJF, Leikauf GD, Waltz SE. Accelerated acute lung injury in mice deficient in the cytoplasmic domain of RON. *Am J Respir Cell Mol Biol* (in press).

Miller CR, Biswas P, Leikauf GD. Combustion generated nickel species aerosols: Role of chemical and morphological properties in lung injury. *Aerosol Sci Technol* (in press).

ABBREVIATIONS AND OTHER TERMS

<i>Aliq1</i>	acute lung injury QTL1
<i>Aliq4</i>	acute lung injury QTL4
ANOVA	analysis of variance
<i>Aqp1</i>	aquaporin-1 gene
ATP	adenosine triphosphate
B6	C57BL/6 mouse strain, common name
BAL	bronchoalveolar lavage
BLAST	Basic Local Alignment Search Tool
BSA	bovine serum albumin
C3	C3H/He mouse strain, common name
CAPs	Concentrated ambient particles
CCSP	Clara cell secretory protein
cDNA	complementary DNA
cm	centimorgans
<i>Col3a1</i>	procollagen type III, α 1 gene
<i>Cyp2b9</i>	cytochrome P450 2b9 gene
dNTP	deoxyribonucleoside triphosphate
EPA	Environmental Protection Agency (US)
<i>Es1</i>	esterase-1 gene
EST	expressed sequence tag
GAPDH	glyceraldehyde-3-phosphate dehydrogenase
<i>Gr1</i>	glutathione reductase-1 gene
<i>Hba-a1</i>	hemoglobin- α , adult chain-1 gene
HEPA	high-efficiency particulate air (filter)
<i>Hmox1</i>	heme oxygenase-1 gene
hTGF- α	human transforming growth factor- α
IARC	International Agency for Research on Cancer
ICDD	International Center for Diffraction Data
ID	internal diameter
LD ₅₀	lethal dose producing 50% mortality
<i>Lgals3</i>	galectin-3 gene (lectin, galactose-binding, soluble 3)
MAP	mitogen-activated protein
MMAD	mass median aerodynamic diameter

mRNA	messenger RNA	QTL	quantitative trait locus
MST	mean survival time	r^2	bivariate coefficient of determination
<i>Mt1</i>	metallothionein-1 gene	rRNA	ribosomal RNA
NAAQS	National Ambient Air Quality Standard (US)	<i>S100a8</i>	S100 calcium-binding protein A8 (calgranulin A) gene
<i>Ndr1</i>	<i>N</i> -myc downstream regulated-1 gene	SD	standard deviation
Ni ²⁺	ionic nickel	SDS	sodium dodecyl sulfate
NiO	nickel oxide	SET	NaCl, Tris-HCl, EDTA buffer
NiSO ₄	nickel sulfate	SMPS	scanning mobility particle sizer
NIOSH	National Institute for Occupational Safety and Health (US)	SP	surfactant-associated protein (SP-A, SP-B, SP-C, SP-D)
NTP	National Toxicology Program (US)	spi2	serine proteinase inhibitor-2
O ₃	ozone	SSLP	simple sequence length polymorphism
PCR	polymerase chain reaction	STAT	signal transducer and activator of transcription protein
PM	Particulate matter	STAT-3	signal transducer and activator of transcription-3
PM ₁₀	PM less than 10 μm in aerodynamic diameter	TGF-α	transforming growth factor-α
PM _{2.5}	PM less than 2.5 μm in aerodynamic diameter	<i>Tgfa</i>	transforming growth factor-α gene
PMN	polymorphonuclear leukocyte	TNF-α	tumor necrosis factor-α
PTFE	polytetrafluoroethylene	σ_g	geometric standard deviation
<i>Ptpn16</i>	MAP kinase phosphatase-1 gene		

INTRODUCTION

Several epidemiologic studies have indicated that short-term, low-level increases in particulate matter, the complex mixture of particles in the atmosphere, are associated with short-term increases in morbidity and mortality (reviewed in Environmental Protection Agency [EPA*] 1996). These findings were obtained in different locations in which the physical and biologic properties (including size and chemical composition) of the particles varied. Epidemiologic studies also indicated that some individuals—in particular, the elderly and persons with cardiopulmonary conditions—may be more vulnerable to the effects of particulate matter than others. The biologic mechanisms linking exposure to low levels of particulate matter and increased morbidity and mortality, however, have not been established. In addition, the components or characteristics of particulate matter responsible for adverse health effects have not been determined. Nonetheless, several studies in humans and other species indicate that exposure to high levels of emissions containing metals, including nickel, can induce adverse changes in the airways and the cardiovascular system (Shirakawa et al 1990; Bright et al 1997; Dreher et al 1997; Watkinson et al 1998).

In 1998, HEI issued RFA 98-1, “Characterization of Exposure to and Health Effects of Particulate Matter,” to address gaps in knowledge about particulate matter effects by identifying factors that enhance susceptibility to particulate matter effects and evaluating particulate matter mechanisms in appropriate animal models. In response, Dr George Leikauf and colleagues at the University of Cincinnati Medical Center proposed to study whether genetically different mice differed in susceptibility to the toxic effects of a nickel aerosol and, if so, which genes might be involved. They also proposed to determine whether the size of the nickel particles influenced toxicity. The HEI Research Committee recommended funding the proposed

* A list of abbreviations and other terms appears at the end of the Investigators’ Report.

+ Dr Leikauf’s 15-month study, *Pulmonary Pathogenetics of Particulate Matter*, began in September 1998. Total expenditures were \$472,000. The draft Investigators’ Report from Leikauf and colleagues was received for review in March 2000. A revised report, received in December 2000, was accepted for publication in February 2001. During the review process, the HEI Health Review Committee and the investigators had the opportunity to exchange comments and to clarify issues in both the Investigators’ Report and the Review Committee’s Commentary.

This document has not been reviewed by public or private party institutions, including those that support the Health Effects Institute; therefore, it may not reflect the views of these parties, and no endorsements by them should be inferred.

research because it thought the study was innovative and would contribute to an understanding of the genetic control of responses to a potentially important component of particulate matter.

Leikauf and colleagues’ draft Investigators’ Report underwent external peer review under the direction of the HEI Health Review Committee, which discussed the report and the reviewers’ critiques and prepared this Commentary. The Commentary is intended to aid HEI sponsors and the public in understanding the study by highlighting its strengths, pointing out alternative interpretations, and putting the report into scientific perspective. During the review of this study, the HEI Review Committee and the investigators exchanged comments and clarified issues in the Investigators’ Report and in the Commentary.

SCIENTIFIC BACKGROUND

Nickel is emitted into the atmosphere from many industrial sources, cigarette smoking, and to a small extent, mobile sources (EPA 2000). Human occupational studies have associated inhalation of high levels of nickel with both acute and chronic effects on respiration, which can lead to death (US National Institute for Occupational Safety and Health 1977; Shirakawa et al 1990; Bright et al 1997). The adverse effects of residual oil fly ash, a nickel-containing emission from power plants, have been particularly well documented in rodents: exposure to high doses resulted in severe inflammation of the airways and in death among animals with cardiopulmonary conditions (Costa and Dreher 1997; Dreher et al 1997; Killingsworth et al 1997; Watkinson et al 1998).

The mechanism or mechanisms by which nickel exerts its inflammatory and toxic effects are not established. Nickel is one of a large group of transition metals found in ambient air particles, which also includes iron (the most abundant of this group in the atmosphere), vanadium, copper, and cobalt. These elements catalyze the reduction of molecular oxygen to generate reactive oxygen species. Formation of reactive oxygen species has been suggested as a mechanism by which these metals, and hence particulate matter, may start a cascade of intracellular events in the airways, ultimately leading to airway inflammatory responses and cardiovascular changes (Stohs and Bagchi 1995; Pritchard et al 1996; Costa and Dreher 1997).

The size of the nickel-containing particle may also play a role in determining the extent of its effects: smaller particles

IDENTIFICATION OF GENES CONTROLLING COMPLEX TRAITS

Definition of Genetic Terms

A *trait* is a genetically determined characteristic. Simple traits are controlled by single genes (as shown in Mendel's classic experiments on pea shape). *Quantitative* or *complex traits*, such as weight or eye color, are controlled by multiple genes.

When a gene exists in multiple stable forms or variants in the population, we say that the gene exists as different *alleles*. In other words, different individuals have slightly different versions of a prototypical gene; genes coding for human leukocyte antigens (HLA; transplantation antigens) and for some cytokines are important examples. The phenomenon of multiple stable forms of a gene existing in the population is known as *genetic polymorphism*.

Quantitative Trait Locus Analysis

A *quantitative trait locus (QTL)* is a chromosomal region associated with expression of a quantitative trait. Typically, a QTL contains several different genes, any of which could be the one associated with the trait. *QTL analysis* is a technique used to identify the positions on different chromosomes of the multiple genes that play a role in expression of a quantitative trait—in this report, the survival time of mice exposed to a toxic nickel aerosol. The underlying principle is genetic linkage: the closer together 2 DNA sequences are on a chromosome, the more likely it is that they will be passed on together.

The analysis begins with 2 parental (P generation) strains of the organism that are each genetically homogeneous but differ from each other in the trait of interest; in the current report, these were A strain mice (sensitive to nickel) and B6 strain mice (resistant to nickel). The 2 strains of mice, A and B6, are then mated (or crossed); their offspring are referred to as the F₁ generation. Because of the many genes inherited in different combinations in individual F₁ mice, the

total F₁ population may show a smooth or continuous variation in the trait of interest. (In the current report, responses of all F₁ animals to toxicants were similar to those of the resistant parental strain B6, suggesting that resistance was dominant or that susceptibility was recessive.) To further analyze the association of genes (*genotype*) with the trait of interest (*phenotype*), F₁ mice are then crossed with one of the parental strains (backcrossed) to generate mice that are either A × F₁ or B6 × F₁. Individual backcross mice are scored for their survival in response to continuous nickel exposure. In the current report, the distribution of survival times in the population of mice backcrossed with the susceptible A strain indicated that multiple genes influenced survival. DNA from individual backcross mice is then analyzed as described below.

To associate specific regions of the genome with a quantitative trait such as survival time, genetic markers called *simple sequence length polymorphisms (SSLPs)* are analyzed. These are specific areas of the genome where a sequence of 2 to 4 nucleotides is repeated; the usefulness of SSLPs as markers is that the number of such repeats differs in different strains of mice. Because the sequences on either side of the repeat (the flanking regions) are constant among strains, the length of the SSLP on a specific chromosome of an individual mouse can be determined with oligonucleotide primers specific for these invariant flanking regions in a polymerase chain reaction (PCR). This helps to identify the mouse strain from which the SSLP was derived. Results are analyzed by a computer program that compares the observed association of each SSLP and the phenotype with the expected association for an unrelated segment of DNA.

For these associations, the log of the ratio of likelihood of linkage to likelihood of no linkage (*log odds ratio* or *lod score*)

are more likely than larger particles to be deposited and to affect the critical air-exchanging regions of the lung alveoli (International Commission on Radiological Protection 1994). The importance of the size of metal-containing particles in inducing inflammatory responses has also been suggested by studies in rodents instilled intratracheally with particles containing another metal, titanium oxide: at the same concentration, ultrafine particles (less than about 0.1 μm mass median aerodynamic diameter [MMAD]) were more effective inducers of pulmonary inflammation than fine particles (between approximately 0.1 and 2.5 μm diameter) (Oberdörster et al 1990, 2000; Ferin et al 1992).

In the current study, Leikauf and colleagues proposed to evaluate the airway inflammatory and toxic effects of exposure to nickel in several inbred strains of mice, including

efforts to identify genes that may be involved in controlling the toxic response to nickel. Their rationale for this study was based on earlier findings suggesting that different strains of mice differed in their airway inflammatory responses to airborne pollutants. For example, Stokinger (1957) and Goldstein and associates (1973) found that the extent of acute lung injury in inbred mouse strains varied in response to the oxidant pollutants nitrogen dioxide and ozone. Subsequently, Kleeberger and colleagues (1997) and Leikauf and colleagues (Prows et al 1997) attempted to identify the genes involved in determining susceptibility versus resistance to developing inflammation and injury in response to ozone exposure. Both groups used an approach known as *quantitative trait locus (QTL)* analysis. (See sidebar titled Identification of

IDENTIFICATION OF GENES CONTROLLING COMPLEX TRAITS (*continued*)

is determined; the higher the lod score, the more likely a marker is associated with the trait. In many studies, a lod score of 3.0 has been used as the significance threshold. While this means the likelihood of linkage would be 1,000 times that of no linkage, false-positive results are extremely common owing to incorrect assumptions and experimental errors. In addition to the lod score, the program estimates the magnitude of effect of the QTL by calculating the percentage decrease in variance among the statistical population when each QTL is held constant (Lincoln et al 1992).

This QTL analysis broadly identifies chromosomal regions implicated in the response of interest. For any region with a high lod score, additional, more closely clustered SSLPs are used to locate the QTL more precisely.

QTLs may act independently or they may interact. Such interactions may be either synergistic or inhibitory. To test for possible genetic interdependence (*epistasis*), a program called Epistat compares the effect of each gene alone on the phenotype and the combined effects of each pair of genes. If the results are not additive, then the 2 genes interact (Chase et al 1997).

While QTL analysis generates important information about the location of genes responsible for a trait, it tends to lead to an oversimplified model. There are important caveats to this approach: First, the endpoint of the analysis is SSLP markers, not specific genes. Second, the SSLP markers used in the QTL analysis may vary in distance from the genes of interest; thus, the lod scores and variance would reflect both the distance of the SSLP from the gene and how strongly the gene affects the phenotype.

Breeding mice and characterizing their phenotypes and genotypes for QTL analysis is time-consuming and costly. After the

current study was completed, a rapid alternative approach for identifying chromosomal regions potentially involved in determining complex traits was published (Grupe et al 2001). The investigators used a computational method—a linkage prediction program—to scan a database of over 3500 single nucleotide polymorphisms (single DNA base differences) among 15 different strains of inbred mice. This technique rapidly predicts the chromosomal regions most likely to contribute to complex traits. The applicability of this approach to toxicology or toxicogenomics remains to be determined.

Haplotype Analysis

The term *haplotype* is commonly used to refer to the set of alleles expressed in one individual, as distinct from the set of alleles of the same genes expressed in another individual. The haplotype analysis described in the current report evaluated the contribution of individual and multiple QTLs to the susceptibility and resistance phenotypes in response to nickel aerosol inhalation. For a single QTL, this was done by comparing the mean survival time (MST) of mice expressing the susceptible-strain allele with that of mice expressing the resistant-strain allele of the same QTL (for example, the QTL identified by the investigators on chromosome 6). To evaluate the effect on survival time of multiple QTLs located on different chromosomes, the investigators performed similar analyses; they compared the MST for groups of mice expressing combinations of susceptible-strain QTL alleles with the MST of mice expressing the “opposite” combination of resistant-strain QTL alleles. This analysis provided an estimate of the number of QTLs that may contribute to susceptibility phenotype versus resistance phenotype as well as a picture of the allelic pattern of the contributing QTLs.

Genes Controlling Complex Traits for further descriptions of QTL analysis and other techniques used in the current study.) Kleeberger and colleagues (1997) showed that one or more genes on chromosome 17 were associated with the elicitation of ozone-induced inflammation, and Prows and coworkers (1997) showed that genes on chromosomes 11 and 13 were associated with the survival time of mice exposed to continuous and high levels of ozone. Leikauf and colleagues proposed to extend this type of genetic approach to identify genes that may play a role in determining susceptibility versus resistance in the acute response to nickel exposure. They also proposed to use other molecular and genetic techniques to address this issue.

TECHNICAL EVALUATION

AIMS and OBJECTIVES

The first aim of the proposal was to determine whether the susceptibility of mice to the acutely toxic effects of high levels of a fine particle nickel aerosol had a genetic basis. To that end, the investigators would assess mean survival time (MST) and lung injury responses (as reflected in inflammatory parameters in bronchoalveolar lavage [BAL] cells and fluid and in lung histopathology) in several inbred strains of mice and in crosses between strains of mice susceptible and resistant to nickel. The investigators performed these studies and also analyzed

MST and lung injury responses after exposure to 2 other toxicants, polytetrafluoroethylene (PTFE) and ozone.

The second aim was to evaluate airway inflammation in a sensitive mouse strain after exposure to nickel aerosol. Leikauf and colleagues originally proposed to correlate the survival time of a nickel-sensitive mouse strain with inflammatory endpoints in BAL cells and fluid: namely, the level and percentage of polymorphonuclear leukocytes (PMNs) or neutrophils and the concentration of lavage protein. They performed these studies and, in addition, used a microarray technique to identify genes in both susceptible and resistant mouse strains whose level of expression changed after exposure to nickel aerosol.

The third aim was to use QTL analysis of MST in backcrosses of susceptible mice and resistant mice to define the genetic regions involved in controlling the response to nickel aerosol. Leikauf and colleagues performed this analysis and also evaluated the effects of exposure to nickel aerosols in mice expressing different levels of a cytokine, human transforming growth factor- α (hTGF- α), which had been inserted as a transgene. These experiments were performed because transforming growth factor- α (TGF- α) is a cytokine that may protect against lung injury (Madtes et al 1994; Liu et al 1996).

METHODS

Atmosphere Generation and Characterization

The investigators generated aerosols of fine nickel sulfate (MMAD, 0.22 μm) in most experiments by placing a nebulizer into a solution of nickel sulfate hexahydrate. In a few experiments, fine nickel sulfate aerosols were generated by combustion in a high-temperature furnace system. Nickel oxide aerosols and powder were produced by pyrolysis of nickel nitrate at 800°C. Particle number concentration and size were determined with a differential mobility analyzer. Aerosol size distribution was measured by a scanning mobility particle sizer.

Using an ultraviolet ozonator, ozone was generated from 100% ultradry oxygen. Levels were monitored continuously with an ozone detector. Ultrafine PTFE particles (MMAD, 0.02 μm) were produced by heating PTFE powder to 420°C. Particle size and concentration were determined with an electrical aerosol analyzer.

Mice and Exposures

The investigators obtained inbred mice from the Jackson Laboratory (Bar Harbor ME). They also used 4 lines of mice transgenic for hTGF- α , which they had generated previously (Korfhagen et al 1994; Hardie et al 1997). These lines

express different levels of hTGF- α in the lung: line 28 > line 2 > line 4 >> line 6108 (see Investigators' Report and Hardie et al 1997, 1999).

For studies of survival, the investigators exposed mice continuously for up to 2 weeks to aerosols of fine particulate nickel sulfate ($150 \pm 15 \mu\text{g}/\text{m}^3$), ultrafine PTFE (particle and gas mixture, 10^7 PTFE particles/ cm^3), or ozone (gas alone, 10.0 ± 0.1 ppm). Control animals were exposed to dry, particle-free air.

In one experiment to assess the effects of different-sized nickel particles on acute lung injury and inflammation, the investigators intratracheally instilled C57BL/6 (B6) mice with insoluble nickel oxide particles over a range from ultrafine to fine particles (MMAD, 40 nm, 130 nm, 300 nm, and 1,000 nm). In an experiment to compare the effects of ultrafine and fine nickel sulfate and nickel oxide particles on acute lung injury and inflammation, the investigators exposed B6 mice to aerosolized particles via inhalation for up to 72 hours.

Evaluation of Survival Time and of Inflammatory and Injury Responses

Survival times of individual mice and MSTs of groups of mice were the main measures of sensitivity versus resistance to a particular toxicant. The investigators also evaluated several parameters of inflammation and injury in BAL fluid (protein levels) and cells (total and differential cell counts, focusing on percentage of PMNs or neutrophils and cell viability) of mice exposed to toxicants for up to 72 hours. In addition, they measured lung wet weights and dry weights and determined the ratio of wet lung weight to dry lung weight. Leikauf and colleagues also evaluated pathologic changes in paraformaldehyde-fixed lungs of mice that died from nickel sulfate exposure.

Evaluation of Gene Expression

The investigators used a number of techniques to assess the level of gene expression during exposure to nickel. They used a microarray approach (see sidebar titled Microarrays to Assess Gene Expression and Zarbl [2001]) to assess simultaneously the changes in expression of multiple genes (that is, the changes in messenger RNA [mRNA] levels) in lung cells after different times of exposure to highly toxic nickel aerosol. Briefly, they prepared fluorescent complementary DNA (cDNA) probes from the mRNA of lung cells derived at different times (0 = control, 3, 8, 24, 48, or 96 hours) during exposure to $150 \mu\text{g}/\text{m}^3$ aerosolized nickel sulfate. Samples from exposed animals were competitively hybridized against samples from unexposed control mice on a microarray containing 8,734 murine cDNAs (derived from both genes and expressed sequence

MICROARRAYS TO ASSESS GENE EXPRESSION

Microarrays, or gene chips, are powerful new tools for examining the level of expression of thousands of genes simultaneously. The microarray comprises thousands of DNA fragments, each with a unique sequence, attached in an ordered arrangement to a glass slide. These DNA fragments, in the form of complementary DNA (cDNA, generally 500 to 5,000 base pairs long) or oligonucleotides (20 to 80 base pairs long), can represent genes from all parts of the genome; alternatively, specialized microarrays can be prepared that use DNA from genes thought to be of particular interest. In addition to fragments of known genes, commercially prepared microarrays usually contain a set of short segments of sequences referred to as *expressed sequence tags* (ESTs). These sequences have been found to be expressed in some cells; some ESTs are *annotated* and correspond to specific known genes, while for other ESTs there is no information, and these are referred to as *nonannotated*.

To perform an experiment, the investigator takes a sample of total messenger RNA (mRNA)—the product obtained from transcription of all active genes—from a cell or tissue and analyzes its binding to the microarray. The samples that are added to the microarray are generally not mRNAs; rather, the total mRNA is reverse transcribed into cDNA, which is then labeled with a fluorescent material (a fluorochrome) or radioactive molecule. Messenger RNAs prepared at different timepoints are labeled distinctly. For example, in the current report, a red fluorochrome labels the control timepoint cDNAs, and a green fluorochrome labels the cDNAs prepared at different timepoints during nickel aerosol exposure. The labeled sample cDNA is washed over the microarray and allowed to hybridize by base pairing with matching fragments.

In the current report, cDNA samples derived from both control samples and samples taken at different timepoints during nickel exposure are added together to the microarray so that they compete for binding to the microarray. Unhybridized material is washed away, leaving pockets of fluorescence where matching has occurred.

At the end of the hybridization reaction, the microarray will contain red, green, or black (or gray or yellow) spots, indicating higher levels of control cDNA, higher levels of cDNA from later timepoints during exposure, or equal levels of DNA in the 2 samples. To interpret the results, a scanning robot examines each spot on the slide for the precise level of fluorescence. Spots are included in the analysis only if the fluorescence from the spot is significantly higher than the background fluorescence and the cDNA covers a large portion of its location on the microarray. Because each timepoint requires a different microarray, and each microarray has a slightly different labeling efficiency, data from all the microarrays must be normalized. The data are then analyzed by a computer program that combines the fluorescence information with a genetic database to determine which genes are overexpressed or underexpressed at different timepoints.

Characterizing the pattern and amount of binding to the microarray has multiple potential uses: clinical diagnosis, drug development, and new gene discovery for examples. In the current report, it is used in toxicogenomics, providing a profile of the genes that change their level of expression at different times in different individuals after exposure of cells or tissue to a toxic agent. What has in the past taken years of work based on educated guesses by countless scientists can now be done in a single experiment.

tags [ESTs]). Using this technique, the investigators assessed which genes were differentially expressed compared with control levels of expression at a particular timepoint. In some analyses of the data, genes were considered differentially expressed if the change was greater than 1.8-fold, and in others, greater than 2-fold. Genes increased in expression relative to the control would appear red, and genes decreased in expression would appear green.

Leikauf and colleagues used additional techniques to evaluate changes in expression of some genes they considered to be of particular interest. Changes in levels of mRNAs for metallothionein-1 and heme oxygenase-1 (both had increased expression in the microarray) were analyzed by Northern blot analysis. Changes in gene expression for surfactant-associated protein A (SP-A), which was not on

the microarray, and for surfactant-associated proteins B and C (SP-B and SP-C), which were decreased in the microarray analysis, were assessed by S1 nuclease protection. In these assays, the investigators used the housekeeping gene, L32, as a control because the expression of this gene should be constant at different times and under different conditions.

Identification of Genes Correlating with Mean Survival Time After Nickel Exposure

Quantitative Trait Locus Analysis The investigators exposed (B6 × A)₁F₁ (F₁) mice and 307 backcross mice, generated by mating F₁ mice to the parental A strain, by inhalation to 150 µg/m³ nickel sulfate aerosol. They recorded the time of death and analyzed DNA from each mouse for the expression of 77 microsatellite markers distributed

throughout the entire genome that differed between the A and B6 strains. (See Identification of Genes Controlling Complex Traits for further details.) They derived the lod score (the log of the ratio of the likelihood of linkage to the likelihood of no linkage) for regions on each chromosome, generating a linkage map for survival time and each of the chromosomes using standard programs. To more closely define the chromosomal region linked with survival, chromosomal regions with lod scores above 1.6 were typed with additional microsatellite markers.

Haplotype Analysis The investigators used this technique to evaluate the contribution of each QTL independently, and of combinations of two or more QTLs, to survival in response to nickel sulfate aerosol exposure. To characterize the effect of a single QTL, they compared the survival time of mice expressing the susceptible-strain allele (A type) with the survival time of mice expressing the resistant-strain allele (B6 type) of the same QTL. To evaluate the effect on survival time of multiple QTLs (the haplotype), the investigators performed a similar analysis for mice expressing combinations of susceptible-strain and resistant-strain QTL alleles.

Locus Number Estimation The investigators used the Wright formula to estimate the number of independent genes associated with survival in response to continuous exposure to nickel (Silver 1995).

Statistical Analysis

Group measurements of lung inflammation and survival in response to different toxic agents were expressed as means \pm SE. To compare differences in means between MSTs of different strains and F₁ crosses exposed to nickel sulfate, PTFE, or ozone, Leikauf and colleagues performed an analysis of variance (ANOVA) followed by a Student-Newman-Keuls multiple comparison test of significance. To compare differences in means of lung wet-to-dry weight ratios and of protein, neutrophils, and PMNs in lavage fluid, they performed a 2-way ANOVA followed by a Student-Newman-Keuls test of significance. The factors for each analysis were strain and exposure. Because the distribution of data for all these parameters (particularly survival times) is skewed rather than normal, however, it would have been more accurate to take logs before performing the ANOVA. For the QTL analysis, the investigators correctly log transformed survival times of backcross mice exposed to nickel.

Analysis of cDNA microarray data was based on information supplied by the manufacturer (Incyte Pharmaceuticals, Palo Alto CA), which showed that 99% of the cDNAs

displayed less than 1.4-fold differential in expression for a single sample hybridized against itself (Braxton and Bedilion 1998). In some analyses of the data, genes were considered differentially expressed if the change was greater than 1.8-fold, and in others, greater than 2-fold. For S1 nuclease protection assays, samples were normalized to L32 and means were compared by 1-way ANOVA followed by Dunnett's method for multiple comparisons. Two means of multiple groups were evaluated by ANOVA in conjunction with Student-Neuman-Keuls test for comparisons among all the groups, or by Dunnett's test when the comparison of treated groups with a control group was of most concern. Values were considered different when a level of significance (*P* value) of less than 0.05 was obtained.

RESULTS

GENETIC BASIS OF SUSCEPTIBILITY TO TOXICANTS

Interstrain Differences in Survival

Leikauf and colleagues found that patterns of susceptibility or resistance to the acute toxic effects of nickel sulfate, PTFE, and ozone were similar in a number of strains of mice. Of 7 strains of mice evaluated, the A strain was the most sensitive and the B6 strain was the most resistant to all the toxicants examined. (See Figure 1 of the Investigators' Report. All references to Figures and Tables are to those found in the Investigators' Report.) The approximate MSTs were as follows: for nickel sulfate, A strain was 70 hours and B6 was 130 hours; for ozone, A strain was 20 hours and B6 was 50 hours; and for PTFE, A strain was 6 hours and B6 was 18 hours. Survival times in the offspring of a cross between A and B6 strains (B6AF₁) exposed to each of the toxicants were similar to those in the resistant parent, B6 (see Figure 2).

The extent of lung pathology (histology and lung wet-to-dry ratios) was comparable in A and B6 mice at the time of death from exposure to nickel (see Figures 3 and 4).

Interstrain Differences in Pulmonary Responses

In addition to MST, the investigators evaluated 2 other endpoints for nickel-induced lung injury: percentage of PMNs in lavage cells and protein concentration in lavage fluid (see Figure 6 and Table 1). The A strain, which was the most susceptible as defined by shortest survival time, had the lowest protein levels in lavage fluid but the highest percentage of PMNs in lavage cells. The B6 strain, which was resistant in terms of survival time, showed the highest levels of protein and a high percentage of PMNs in

BAL. In the strains B6 and C3He and the offspring of their cross, B6C3F₁ mice, the correlation between percentage of PMNs and protein concentration in BAL was very low ($r^2 \leq 0.1$). These differences indicate that distinct genes most likely correlate with different measures of lung injury.

EFFECTS OF PARTICLE SIZE AND SOLUBILITY

Leikauf and colleagues evaluated the inflammatory effects of nickel particles of different sizes and solubility in B6 mice. They showed that inhalation of soluble nickel sulfate as either 60-nm ultrafine particles (420 $\mu\text{g}/\text{m}^3$) or 250-nm fine particles (480 $\mu\text{g}/\text{m}^3$) for up to 72 hours increased lavage protein and neutrophils, especially after 72 hours of exposure. In contrast, inhalation of insoluble nickel oxide as 50-nm ultrafine particles (340 $\mu\text{g}/\text{m}^3$) did not affect any BAL parameter (see Table 4) at any timepoint examined. When nickel oxide particles ranging in size from 40 to 1,000 nm (300 $\mu\text{g}/\text{kg}$ body weight) were instilled intratracheally, only 40-nm particles induced an inflammatory response in BAL after 18 hours. This was observed as an increase in the percentage of neutrophils but not in any other inflammatory parameter that was measured (see Table 2).

MICROARRAY ANALYSIS

Using microarray analysis, Leikauf and colleagues found that inhalation exposure of the resistant B6 mice and the sensitive A mice to 150 $\mu\text{g}/\text{m}^3$ nickel sulfate resulted in multiple and time-dependent changes in gene expression in their lung cells.

Results in B6 Mice

Only a small percentage (less than 4%) of the total 8,734 genes and ESTs evaluated changed expression (either increased or decreased) compared with control levels during exposure of B6 mice to toxic levels of nickel sulfate aerosol (see Table 5 and Figures 7 and 8). The number of genes and ESTs whose expression changed and the magnitude of changes increased progressively during exposure (see Figure 7). Using the criterion of change in gene expression of at least ± 1.8 at 2 or more timepoints, Leikauf and colleagues identified a subgroup of 100 genes. Genes whose expression changed in similar temporal patterns frequently had similar functions (see Figure 8 and Table 5).

To verify that the changes in gene expression noted on the microarray were consistent with results obtained using other methods for identifying such changes, the investigators also measured the expression of a few genes by Northern analysis and by S1 nuclease protection. Figure 9 illustrates that the magnitude of the increases in

metallothionein-1 and heme oxygenase-1 expression at different timepoints were comparable, measured by Northern or microarray analyses. Figure 10 illustrates that the trend of decreased expression of SP-B and SP-C over time of exposure was comparable whether measured by S1 nuclease protection or by microarray. In the S1 assay, however, the magnitude in the change at each timepoint was greater than that detected by microarray.

Comparison of Results in A and B6 Mice

The investigators also performed a microarray analysis with lung mRNA from A mice. Because A mice die earlier than B6 mice during exposure to nickel, comparisons of gene expression between the 2 strains were made only at timepoints during the first 48 hours of exposure (see Table 7). As was noted for B6 mice, relatively few (146) of the cDNAs increased or decreased expression at any of the 4 times (3, 8, 24, and 48 hours) examined during nickel exposure of A strain mice. The number of genes that changed expression in A strain also increased with exposure time, as was found in B6 mice. Table 7 also indicates that 280 genes changed expression in *either* A or B6 mice (3.2% of total cDNAs on the microarray, and comprising 183 known genes and annotated ESTs with 97 nonannotated ESTs). Sixty-six genes showed changes in expression in *both* strains (36 increased and 30 decreased).

To show similarities and differences between the strains' responses to nickel sulfate, the investigators tabulated the genes whose level changed more than 2-fold (either increased or decreased) compared with control in either A or B6 mice at 3, 8, 24, or 48 hours of exposure (see Tables 8 and 9). Leikauf and colleagues also categorized some of the genes and ESTs that changed in both A and B6 by function (see Table 10), and by differences in level of expression between the strains (see Figures 15 through 17).

GENETIC DETERMINANTS OF ACUTE LUNG INJURY

Quantitative Trait Locus Identification

From an initial chromosomal analysis of microsatellite expression in backcross mice that were the most susceptible ($n = 55$) and the most resistant ($n = 54$) to acute nickel toxicity, the investigators identified 6 putative QTLs located on chromosomes 1, 6, 8, 9, 12, and 16. The authors used a previously defined lod score of 1.9 or greater to define suggestive linkage to a trait (Lander and Kruglyak 1995); the QTLs they identified had lod scores in the range between 2.1 and 2.8. Together, these QTLs accounted for more than 62% of the genetic variation in the backcrosses whose responses to nickel were most polarized (see Table 6).

The investigators extended the chromosomal analysis to all backcross mice ($n = 307$) and included an additional 32 microsatellite markers in the regions suggested by the QTLs they had identified (see Figure 13). Using an empirically derived definition of significant linkage (lod score greater than 2.6) and suggestive linkage (lod score between 2.3 and 2.6), the investigators reported that only the QTL they had previously identified on chromosome 6 showed significant linkage to survival. Leikauf and colleagues designated this QTL on chromosome 6 (in the region known as *D6Mit183*) as *Aliq4*, for *Acute lung injury QTL 4*. This QTL contains genes coding for aquaporin-1, SP-B, and TGF- α , all of which may play a role in protecting the lung from injury.

The QTLs on chromosome 1 and chromosome 12 reached suggestive linkage. No significant interactions among the putative QTLs were found. The lod scores for the QTLs on chromosomes 8, 9, and 16, previously identified by analysis of the most sensitive and most resistant mice, were not significant.

Haplotype Analysis

To determine whether the QTLs they had identified contributed individually or as a group to survival, the investigators performed a haplotype analysis (see Identification of Genes Controlling Complex Traits). They found that the single QTL that made the most significant contribution to susceptibility versus resistance was that on chromosome 6; mice expressing the resistant-strain B6 allele survived an average of 12 hours longer than mice homozygous for the sensitive A allele (see Figure 14). Adding the QTLs identified on chromosomes 1, 9, 12, and 16 increased survival time: mice expressing the optimal pattern of alleles at chromosomes 1, 6, 9, 12, and 16 survived 75 hours longer than mice expressing the opposite allelic pattern. Interestingly, the optimal survival time occurred when the QTL on chromosome 9 was of the A type rather than of the B6 type. When the sixth identified QTL, that on chromosome 8, was added to the haplotype analysis, however, the difference in MST between the haplotypes decreased slightly (from 75 hours to 70 hours).

Locus Number Estimation

Using a modified formula of Wright (Silver 1995), Leikauf and colleagues estimated that 5 independently segregating genes correlated with survival in nickel-induced acute lung injury.

FUNCTIONAL EVALUATION OF CANDIDATE GENES

The QTL *Aliq4* contains several candidate genes that may play a role in survival of continuous exposure to nickel. To investigate further the potential role of one of these genes, TGF- α , in survival, the investigators evaluated the effects of continuous exposure to nickel sulfate aerosol in lines of transgenic mice expressing distinct levels of hTGF- α in their lungs. They found the MSTs of transgenic mouse lines expressing the highest levels of hTGF- α (lines 28 and 2) were greater than the MST of the wildtype FVB/N strain mice (see Figure 18). Four of 6 line 28 mice survived until the end of the exposure period, 240 hours.

The investigators also compared the effects of nickel aerosol exposure on multiple parameters of inflammatory injury in line 28 mice, the most resistant to the toxic effects of the nickel aerosol, and in wildtype mice. After 72 hours of exposure, the wildtype mice had edematous and inflamed lungs (see Figure 19), increased wet-to-dry lung weight ratios, and increased percentage of PMNs and protein in BAL. By contrast, all these indicators of inflammation remained at control levels in line 28 mice after 72 hours of exposure. Levels of interleukin 1 β , interleukin 6, and macrophage inflammatory protein-2 were similar in wildtype and line 28 lung homogenates at 0, 24, and 48 hours of exposure, but at 72 hours the levels were considerably higher in homogenates prepared from wildtype mice (see Figure 20). Interestingly, the amount of nickel in the lungs, which was below the limit of detection in both sets of animals before exposure, increased to higher levels in line 28 mice than in wildtype mice at 72 hours of exposure.

Line 28 and wildtype mice also had differences with regard to levels of SP-B, encoded by another positional candidate gene measured in lung homogenates (see Figure 21). Before exposure to nickel aerosol, lungs of line 28 mice expressed approximately 70% lower levels of SP-B than lungs of wildtype mice. After 72 hours of exposure to nickel aerosol, SP-B levels in lungs of line 28 mice remained at preexposure levels, whereas SP-B levels in lungs of wildtype mice decreased by 72%. In contrast, preexposure levels of SP-D were similar in lungs of line 28 and wildtype mice; after 72 hours of exposure to nickel, SP-D levels dropped by similar amounts in these 2 sets of mice.

DISCUSSION

In this study, Leikauf and colleagues have produced a large amount of interesting data about the inflammatory and toxic effects of multiple agents in different mouse strains. Their finding that many strains were either susceptible or resistant to the toxic effects of nickel sulfate, ozone, and

PTFE confirms and extends previous observations about the likely genetic control of mouse responses to toxic agents (Stokinger 1957; Goldstein et al 1973; Kleeberger et al 1990; Holroyd et al 1997; Prows et al 1997). Their finding that individual strains were either susceptible or resistant to *all* these agents is novel, and it suggests that the mechanisms involved in the acute responses to all 3 agents may be the same or at least similar in each strain. Their histopathologic finding that the lungs of both the more susceptible strain and the more resistant strain appeared similar at death indicates that the mechanisms of toxicity are likely to be similar in the 2 strains; presumably, these pathways are accelerated in the susceptible mice or slowed down in the resistant mice. Their finding that markers of lung inflammation (increased protein level and percentage of neutrophils) showed little correlation with survival time in response to nickel exposure may indicate that lung inflammation per se is not linked to survival. Alternatively, the result may be interpreted to suggest that not all inflammatory changes are markers of toxicity.

The main part of the study evaluated the effects on mice of inhaled nickel aerosols at very high levels compared with those in ambient air. The investigators' observation that inhaling fine and ultrafine nickel sulfate particles induced comparable inflammatory responses is the first comparison of the effects of different-sized particles in an inhalation study. Further inhalation studies with different types of particles are needed to confirm whether fine and ultrafine metal particles induce comparable inflammatory responses after exposure via this physiologically relevant route.

Leikauf and colleagues' finding that ultrafine rather than fine particles of nickel oxide induced airway inflammatory responses after intratracheal instillation is consistent with results from other instillation studies of particles containing the metals titanium oxide (Oberdörster et al 1990, 2000; Ferin et al 1992) or nickel oxide (Zhang et al 1998). One possible reason for the differences between the current inhalation results and those of instillation studies is the difference in solubility of the particles used: nickel and titanium oxides are insoluble, whereas nickel sulfate is soluble. In their studies of nickel's effects on mice, the investigators focused on genetic control of the response, which their findings on strain differences in responsiveness had suggested. They used a variety of complementing genetic and molecular approaches to preliminarily identify the set of genes involved in determining susceptibility versus resistance in the responses of mice continuously exposed to toxic levels of a nickel aerosol. The major endpoint measured was the difference in survival time between strains of mice identified as resistant to the toxicant (B6) or sensitive to the toxicant (A).

The investigators' initial results from crossing the resistant and susceptible strains suggested that survival is a simple dominant trait. The finding that backcrossing F₁ mice with the susceptible parent strain yielded a wide range of survival times, however, indicated that survival is a complex trait affected by many genes. To identify the *number* of genes involved in determining the survival phenotype, Leikauf and colleagues extended their genetic analysis in several ways. Using QTL analysis of the survival times of the mice that were most sensitive and the mice that were most resistant to nickel toxicity, they characterized 6 chromosomal regions potentially linked to survival time. The QTL on chromosome 6 appeared significantly linked to survival; the QTLs identified on chromosomes 1, 8, 9, 12, and 16 were only suggestively linked to the trait. Haplotype analysis of backcross mice provided further support for the association of 5 of the 6 identified QTLs with survival. The investigators found that the difference in survival times between mice expressing the QTLs on chromosomes 1, 6, 9, 12, and 16 in an optimal combination of alleles and mice expressing the opposite QTL alleles (a difference of 75 hours in MST) was even greater than the difference in survival times between the resistant and sensitive parental strains (a difference of 50 hours in MST). This finding suggests that the QTLs identified may account completely for the differences in survival time between these 2 strains.

The finding that a small number of genes controlled the difference in response between the strains was corroborated by the Wright formula. Using the formula to analyze the distribution of survival times in F₁ and backcross mice, the investigators showed that 5 independently segregating genes could account for the variation observed. This number matches well the number of genes estimated by QTL analysis.

To begin to define the genes involved in the acute response to nickel toxicity, Leikauf and colleagues further characterized the genes located in the QTL on chromosome 6, which showed the most significant linkage to survival time. This QTL, designated *Aliq4* by the investigators, contained several genes involved in lung injury responses to a number of stimuli. These include aquaporin-1, which forms a water channel in the lungs (Matthay et al 1998), SP-B, involved in maintaining surface tension in the lung (Weaver and Whitsett 1991), and TGF- α , which has been shown to stimulate epithelial cell proliferation and wound healing and may protect against lung injury (Konturek et al 1992; Hardie et al 1999). Thus, it is likely that these genes play some role in the response to toxic levels of nickel aerosols. Even after identifying a QTL or QTLs associated with a particular trait, however,

identifying the specific gene or genes responsible for the trait is a lengthy and complex task (see recent review by Nadeau and Frankel 2000).

The investigators provided intriguing functional evidence that genes within the QTL on chromosome 6, TGF- α and SP-B, may be involved in resistance to the toxic effects of nickel. In contrast to control mice, transgenic mice expressing high levels of hTGF- α were resistant to nickel-induced lung injury (no pathologic changes in the lungs at 48 hours, and no changes in levels of inflammatory cytokines at 72 hours). In addition, after 72 hours of nickel exposure, SP-B levels in lungs of the resistant hTGF- α transgenic mice were unchanged, whereas SP-B levels in exposed control mice were substantially decreased. The microarray (and S1 nuclease protection) studies also implicated the gene for SP-B as one that may play a role in the response to nickel. At all timepoints during exposure, the SP-B gene showed one of the largest decreases in level of expression of the genes in B6 mice examined by microarray.

Taken together, these findings suggest that both TGF- α and SP-B play a role in resistance to nickel exposure, but precisely how is not clear. Some of the findings implicating SP-B in the response to nickel are difficult to reconcile: in resistant hTGF- α transgenic mice, levels of SP-B protein did not change during nickel exposure, but microarray analysis of resistant B6 mice (and sensitive A mice) indicated that SP-B gene levels decreased early after exposure and remained low.

The investigators' microarray analysis indicates the potential utility of this approach for analyzing multiple gene expression changes over time as well as for characterizing differences in gene expression between sensitive and resistant strains during exposure to a toxicant. Leikauf and colleagues' finding that the number of genes with changed expression in both sensitive and resistant mice increased with duration of nickel exposure suggests that the initial stimulus triggered a cascade of responses, most likely involving more and more cell types. Some genes showed changed expression only in resistant mice or only in susceptible mice. At least some of these genes probably contribute to determining degrees of susceptibility or resistance to nickel toxicity; other genes may shed light on the mechanism of the toxic response to nickel. Studies with transgenic mice that overexpress these genes (similar to the studies performed by Leikauf and colleagues in the current report), or with the genes knocked out, may provide evidence for the involvement of genes and their products in resistance to nickel aerosol exposure. Because some of the unique gene expression changes were detected in nonannotated ESTs (ie, in sequences not matching those of any currently known gene), some unknown genes likely play a role in determining susceptibility to nickel exposure.

The finding from the microarray experiments that many genes changed expression in both the resistant strain and the sensitive strain suggests that exposure to a toxicant triggers common pathways of response. Further, this finding suggests that susceptibility or resistance may be determined by the expression of different levels of the same genes. Some of the changes in gene expression common to both strains are involved in injury responses to a number of stimuli and are not specific to nickel. For instance, metallothionein-1 and heme oxygenase-1, which Leikauf and colleagues found to change during the response, are general oxidative stress response genes (Chen et al 2001; Minamino et al 2001; Penkowa et al 2001; Yet et al 2001).

Leikauf and colleagues' use of the microarray approach has some major limitations. One general limitation of the method is that the microarray does not provide information about the level of expression of protein, so it is not clear how detected changes in gene expression, or lack thereof, correlate with protein levels. In addition, the microarrays used in these experiments did not contain sequences from all genes in the mouse genome (currently estimated to contain approximately 30,000 genes), and as the investigators noted, several genes of potential interest were not represented.

The nature of differences detected by the microarray is limited: a small difference in a regulatory sequence that changes the expression level of the attached gene will be detected easily, while a difference in the coding region of a gene (ie, that changes how the protein functions) will not be evident. Conversely, changes in the expression of many genes may not represent genetic polymorphisms, but rather downstream effects of changes in the expression of other genes. Thus, these downstream genes may not play a role in determining susceptibility.

Furthermore, the microarray system used by Leikauf and colleagues cannot distinguish cells in which gene expression changes are occurring from among the many cell types present in the lung. It is probable that some of the gene expression changes detected at later timepoints in the response occurred in cells that migrated into the lung as a consequence of the inflammatory or injury response, rather than in lung cells per se. In addition, only one set of microarray experiments was performed in the current study, and it is not clear how repeatable the findings are. Repetition of the experiments would certainly reduce the possibility of artifacts.

One of the strengths of the study is that Leikauf and colleagues used multiple approaches to provide information about the genes involved in the response to nickel. This multifaceted approach was important because many of the genes that a priori may be considered relevant to responses in the lung (including SP-A and TGF- α) were missing from

the microarray. Indeed, very few genes associated with inflammation, lung injury, or cytokines were present on this particular microarray. However, the results of the microarray experiments did show some overlap with the results of the genetic analysis. For example, SP-B, a candidate gene located within the QTL on chromosome 6, was differentially expressed in the 2 strains that differed in their sensitivity to nickel, as were procollagen type III, $\alpha 1$ (located within the QTL on chromosome 1), and several genes within the QTL on chromosome 8. Other than these few, the candidate genes within the QTLs did not change or were not on the microarray. Many genes that changed or differed in expression on the microarray were not mapped in the genome so no comparison could be made.

Kleeberger and colleagues have identified QTLs controlling susceptibility to ozone (Kleeberger et al 1997, 2000) and to acid-coated particles (Ohtsuka et al 2000); none of these QTLs overlaps with those found by Leikauf and colleagues in either the current or previous study (Prows et al 1997). Kleeberger's studies compared responses in strains different from those used in Leikauf's current and previous studies, and differences in the strains evaluated may lead to different conclusions about the nature of the genes determining susceptibility. In addition, the ozone studies of the 2 groups evaluated different endpoints of ozone effect (lung hyperpermeability and percentage of PMNs in the Kleeberger studies and survival time in the Leikauf studies). In the current study Leikauf and colleagues showed that not all measured endpoints of a toxic agent's effect are correlated. Thus, in future investigations of genetic control of inflammatory or injury responses to a toxic agent, the endpoint selected is likely to be a critical determinant of the outcome.

Leikauf and colleagues' QTL findings concerning the genes potentially implicated in determining susceptibility versus resistance in the response to the acute toxic effects of nickel exposure differ from those identified in their QTL study of the genetic control of mice susceptible or resistant to the acute toxic effects of ozone (Prows et al 1997). (The ozone study used the same sensitive [A] and resistant [B6] strains that were used in the current study.) This finding may be expected, perhaps, because the pollutants were different in the 2 studies. Nonetheless, results from the current study, indicating that strain patterns of susceptibility and resistance in A and B6 mice were similar for exposure to nickel and to ozone, suggest that genes identified as candidates in determining susceptibility and resistance to ozone might overlap with those determining susceptibility and resistance to nickel exposure. Other techniques, such as the use of microarrays, may help to determine whether ozone and nickel up-regulate or down-regulate identical or overlapping sets of genes.

SUMMARY AND CONCLUSIONS

In this interesting study, Leikauf and colleagues have shown that mice respond to nickel and other airborne pollutants by altering gene expression. Further, the investigators showed that differences in 5 chromosomal regions, and one in particular on chromosome 6 may account for a large portion of the variation in survival time of mice exposed continuously to toxic levels of aerosolized nickel sulfate. Leikauf and colleagues identified candidate genes in the implicated chromosomal region on chromosome 6 which they thought might play a role in influencing susceptibility to nickel exposure. These genes included aquaporin-1, TGF- α , and SP-B, which have known roles in lung function. The involvement of TGF- α and SP-B in protecting mice from the toxic effects of nickel was also confirmed by experiments in mice transgenic for hTGF- α .

Findings from microarray analysis of lung cells derived from mice sensitive to nickel and mice resistant to nickel provided support for a role of some of these candidate genes, and SP-B in particular, in the response to nickel. The microarray analysis also revealed that many other genes changed levels of expression during the exposure to nickel (approximately 200 of the more than 8,000 examined). Some of the genes whose expression changed may be important in determining susceptibility to nickel; in particular, genes whose activity changed more in one strain than another. It will be interesting to determine whether similar patterns of gene expression would be seen in response to levels of nickel lower than the high, toxic concentrations used in this study.

Overall, Leikauf and colleagues have shown that mice respond to high toxic levels of inhaled nickel particles by altering gene expression. They have also preliminarily identified a small number of genes involved in susceptibility to this response. Similar genes may be involved in human responses to nickel particles in high concentrations. Additional studies are required to determine whether similar genes are involved in responses to low ambient levels of nickel and other airborne pollutants. Further characterization of the genes involved in these responses will assist in efforts to understand the mechanisms by which pollutants act, characterize similarities and differences in gene expression among individuals' responses to a stimulus, and ultimately identify individuals who may be particularly susceptible to pollutant effects.

ACKNOWLEDGMENTS

The Health Review Committee thanks the ad hoc reviewers for their help in evaluating the scientific merit of

the Investigators' Report. The Committee is also grateful to Lucia Somberg and Geoffrey Sunshine for their assistance in preparing its Commentary, and to Sally Edwards, Genevieve MacLellan, Ruth Shaw, and Jenny Lamont for their roles in publishing this Research Report.

REFERENCES

- Braxton S, Bedilion T. 1998. The integration of microarray information in the drug development process. *Curr Opin Biotechnol* 9:643–649.
- Bright P, Burge PS, O'Hickey SP, Gannon PF, Robertson AS, Boran A. 1997. Occupational asthma due to chrome and nickel electroplating. *Thorax* 52:28–32.
- Chase K, Adler FR, Lark KG. 1997. Epistat: A computer program for identifying and testing interactions between pairs of quantitative trait loci. *Theor Appl Genet* 94:724–730.
- Chen H, Carlson EC, Pellet L, Moritz JT, Epstein PN. 2001. Overexpression of metallothionein in pancreatic beta-cells reduces streptozotocin-induced DNA damage and diabetes. *Diabetes* 50:2040–2046.
- Costa DL, Dreher KL. 1997. Bioavailable transition metals in particulate matter mediate cardiopulmonary injury in healthy and compromised animal models. *Environ Health Perspect* 105 (Suppl 5):1053–1060.
- Dreher KL, Jaskot RH, Lehmann JR, Richards JH, McGee JK. 1997. Soluble transition metals mediate residual oil fly ash induced acute lung injury. *J Toxicol Environ Health* 50:285–305.
- Environmental Protection Agency (US). 1996. Air Quality Criteria for Particulate Matter. Document EPA/600/P95/001. Office of Research and Development, Washington DC.
- Environmental Protection Agency (US). 2000. Draft Technical Support Document: Control of Emissions of Hazardous Air Pollutants from Motor Vehicles and Motor Vehicle Fuels. EPA420-D-00-003. Office of Air and Radiation, Washington DC.
- Ferin J, Oberdörster G, Penney DP. 1992. Pulmonary retention of ultrafine and fine particles in rats. *Am J Respir Cell Mol Biol* 6:535–542.
- Goldstein BD, Lai LY, Ross SR, Cuzzi-Spada R. 1973. Susceptibility of inbred mouse strains to ozone. *Arch Environ Health* 27:412–413.
- Grupe A, Germer S, Usuka J, Aud D, Belknap JK, Klein RF, Ahluwalia MK, Higuchi R, Peltz G. 2001. In silico mapping of complex disease-related traits in mice. *Science* 292:1915–1918.
- Hardie WD, Bruno MD, Huelsman KM, Iwamoto HS, Carrigan PE, Leikauf GD, Whitsett JA, Korfhagen TR. 1997. Postnatal lung function and morphology in transgenic mice expressing transforming growth factor-alpha. *Am J Pathol* 151:1075–1083.
- Hardie WD, Prows DR, Leikauf GD, Korfhagen TR. 1999. Attenuation of acute lung injury in transgenic mice expressing human transforming growth factor-alpha. *Am J Physiol* 277:L1045–L1050.
- Holroyd KJ, Eleff SM, Zhang LY, Jakab GJ, Kleeberger SR. 1997. Genetic modeling of susceptibility to nitrogen dioxide-induced lung injury in mice. *Am J Physiol* 273:L595–L602.
- International Commission on Radiological Protection. 1994. Human Respiratory Tract Model for Radiological Protection. A Report of Committee 2 of the ICRP. Pergamon Press, Oxford, England.
- Killingsworth CR, Alessandrini F, Krishna Murthy GG, Catalano PJ, Paulauskis JD, Godleski JJ. 1997. Inflammation, Chemokine expression, and death in monocrotaline-treated rats following fuel oil fly ash inhalation. *Inhalation Toxicol* 9:541–565.
- Kleeberger SR, Bassett DJ, Jakab GJ, Levitt RC. 1990. A genetic model for evaluation of susceptibility to ozone-induced inflammation. *Am J Physiol* 258:L313–L320.
- Kleeberger SR, Levitt RC, Zhang LY, Longphre M, Harkema J, Jedlicka A, Eleff SM, DiSilvestre D, Holroyd KJ. 1997. Linkage analysis of susceptibility to ozone-induced lung inflammation in inbred mice. *Nat Genet* 17:475–478.
- Kleeberger SR, Reddy S, Zhang L, Jedlicka AE. 2000. Genetic susceptibility to ozone-induced lung hyperpermeability: Role of toll-like receptor 4. *Am J Respir Cell Mol Biol* 22:620–627.
- Konturek SJ, Brzozowski T, Majka J, Dembinski A, Slomiany A, Slomiany BL. 1992. Transforming growth factor alpha and epidermal growth factor in protection and healing of gastric mucosal injury. *Scand J Gastroenterol* 27:649–655.
- Korfhagen TR, Swantz RJ, Wert SE, McCarty JM, Kerlakian CB, Glasser SW, Whitsett JA. 1994. Respiratory epithelial cell expression of human transforming growth factor-alpha induces lung fibrosis in transgenic mice. *J Clin Invest* 93:1691–1699.

- Lander E, Kruglyak L. 1995. Genetic dissection of complex traits: Guidelines for interpreting and reporting linkage results. *Nat Genet* 11:241–247.
- Lincoln SE, Daly MJ, Lander ES. 1992. Mapping Genes Controlling Quantitative Traits with MAPMAKER/QTL 1.1. Technical Report, 2nd ed. Whitehead Institute, Cambridge MA.
- Liu JY, Morris GF, Lei WH, Corti M, Brody AR. 1996. Up-regulated expression of transforming growth factor-alpha in the bronchiolar-alveolar duct regions of asbestos-exposed rats. *Am J Pathol* 149:205–217.
- Madtes DK, Busby HK, Strandjord TP, Clark JG. 1994. Expression of transforming growth factor alpha and epidermal growth factor receptor is increased following bleomycin-induced lung injury in rats. *Am J Respir Cell Mol Biol* 11:540–551.
- Matthay MA, Flori HR, Conner ER, Ware LB. 1998. Alveolar epithelial fluid transport: Basic mechanisms and clinical relevance. *Proc Assoc Am Physicians* 110:496–505.
- Minamino T, Christou H, Hsieh CM, Liu Y, Dhawan V, Abraham NG, Perrella MA, Mitsialis SA, Kourembanas S. 2001. Targeted expression of heme oxygenase-1 prevents the pulmonary inflammatory and vascular responses to hypoxia. *Proc Natl Acad Sci USA* 98:8798–8803.
- Nadeau JH, Frankel WN. 2000. The roads from phenotypic variation to gene discovery: Mutagenesis versus QTLs. *Nat Genet* 25:381–384.
- National Institute for Occupational Safety and Health (US). 1977. Criteria for a Recommended Standard: Occupational Exposure to Inorganic Nickel. DHEW-NIOSH Document 77-164. Government Printing Office, Washington DC.
- Oberdörster G, Ferin J, Finkelstein G, Wade P, Corson N. 1990. Increased pulmonary toxicity of ultrafine particles? II. Lung lavage studies. *J Aerosol Sci* 21:384–387.
- Oberdörster G, Finkelstein JN, Johnston C, Gelein R, Cox C, Baggs R, Elder ACP. 2000. Acute Pulmonary Effects of Ultrafine Particles in Rats and Mice. Research Report 96, Health Effects Institute, Cambridge MA.
- Ohtsuka Y, Brunson KJ, Jedlicka AE, Mitzner W, Clarke RW, Zhang LY, Eleff SM, Kleeberger SR. 2000. Genetic linkage analysis of susceptibility to particle exposure in mice. *Am J Respir Cell Mol Biol* 22:574–581.
- Penkowa M, Espejo C, Martinez-Caceres EM, Poulsen CB, Montalban X, Hidalgo J. 2001. Altered inflammatory response and increased neurodegeneration in metallothionein I+II deficient mice during experimental autoimmune encephalomyelitis. *J Neuroimmunol* 119:248–260.
- Pritchard RJ, Ghio AJ, Lehmann JR, Winsett DW, Tepper JS, Park P, Gilmour MI, Dreher KL, Costa DL. 1996. Oxidant generation and lung injury after particulate air pollutant exposure increase with the concentrations of associated metals. *Inhalation Toxicol* 8:457–477.
- Prows DR, Shertzer HG, Daly MJ, Sidman CL, Leikauf GD. 1997. Genetic analysis of ozone-induced acute lung injury in sensitive and resistant strains of mice. *Nat Genet* 17:471–474.
- Shirakawa T, Kusaka Y, Fujimura N, Kato M, Heki S, Morimoto K. 1990. Hard metal asthma: Cross immunological and respiratory reactivity between cobalt and nickel? *Thorax* 45:267–271.
- Silver LM. 1995. *Mouse Genetics: Concepts and Applications*. Oxford University Press, New York NY.
- Stohs SJ, Bagchi D. 1995. Oxidative mechanisms in the toxicity of metal ions. *Free Radic Biol Med* 18:321–336.
- Stokinger HE. 1957. Evaluation of the hazards of ozone and oxides of nitrogen: Factors modifying toxicity. *Arch Ind Health* 15:181–190.
- Watkinson WP, Campen MJ, Costa DL. 1998. Cardiac arrhythmia induction after exposure to residual oil fly ash particles in a rodent model of pulmonary hypertension. *Toxicol Sci* 41:209–216.
- Weaver TE, Whitsett JA. 1991. Function and regulation of expression of pulmonary surfactant-associated proteins. *Biochem J* 273:249–264.
- Yet SF, Tian R, Layne MD, Wang ZY, Maemura K, Solovyeva M, Ith B, Melo LG, Zhang L, Ingwall JS, Dzau VJ, Lee ME, Perrella MA. 2001. Cardiac-specific expression of heme oxygenase-1 protects against ischemia and reperfusion injury in transgenic mice. *Circ Res* 89:105–107.
- Zarbl H. 2001. DNA microarrays: An overview of technologies and applications to toxicology. In: *Current Protocols in Toxicology* (Maines MD, Costa LG, Hodgson E, Reed DJ, Sipesy IG, eds), Suppl 9, pp 1.4.1–1.4.16. John Wiley & Sons, New York NY.
- Zhang Q, Kusaka Y, Sato K, Nakakuki K, Kohyama N, Donaldson K. 1998. Differences in the extent of inflammation caused by intratracheal exposure to three ultrafine metals: Role of free radicals. *J Toxicol Environ Health A* 53:423–438.

RELATED HEI PUBLICATIONS: PARTICULATE MATTER

Report Number	Title	Principal Investigator	Publication Date*
Research Reports			
104	Inhalation Toxicology of Urban Ambient Particulate Matter: Acute Cardiovascular Effects in Rats	R Vincent	2001
100	Respiratory Tract Toxicity in Rats Exposed to Mexico City Air	OR Moss	2000
99	A Case-Crossover Analysis of Fine Particulate Matter Air Pollution and Out-of-Hospital Sudden Cardiac Arrest	H Checkoway	2000
97	Identifying Subgroups of the General Population That May Be Susceptible to Short-Term Increases in Particulate Air Pollution: A Time-Series Study in Montreal, Quebec	M Goldberg	2000
96	Acute Pulmonary Effects of Ultrafine Particles in Rats and Mice	G Oberdörster	2000
95	Association of Particulate Matter Components with Daily Mortality and Morbidity in Urban Populations	M Lippmann	2000
94	The National Morbidity, Mortality, and Air Pollution Study <i>Part I. Methods and Methodologic Issues</i>	JM Samet	2000
	<i>Part II. Morbidity and Mortality from Air Pollution in the United States</i>		
93	Effects of Concentrated Ambient Particles in Rats and Hamsters: An Exploratory Study	T Gordon	2000
91	Mechanisms of Morbidity and Mortality from Exposure to Ambient Air Particles	JJ Godleski	2000
86	Statistical Methods for Epidemiologic Studies of the Health Effects of Air Pollution	W Navidi	1999
83	Daily Changes in Oxygen Saturation and Pulse Rate Associated with Particulate Air Pollution and Barometric Pressure	DW Dockery	1999
75	Ozone Exposure and Daily Mortality in Mexico City: A Time-Series Analysis	DP Loomis	1996
68	Pulmonary Toxicity of Inhaled Diesel Exhaust and Carbon Black in Chronically Exposed Rats <i>Part I. Neoplastic and Nonneoplastic Lung Lesions</i>	JL Mauderly	1994
	<i>Part II. DNA Damage</i>	K Randerath	1995
	<i>Part III. Examination of Possible Target Genes</i>	SA Belinsky	1995
45	The Effects of Exercise on Dose and Dose Distribution of Inhaled Automotive Pollutants	MT Kleinman	1991
40	Retention Modeling of Diesel Exhaust Particles in Rats and Humans	CP Yu	1991
10	Predictive Models for Deposition of Inhaled Diesel Exhaust Particles in Humans and Laboratory Species	CP Yu	1987

* Reports published since 1990, with exceptions.

Copies of these reports can be obtained from the Health Effects Institute and many are available at www.healtheffects.org.



BOARD OF DIRECTORS

Richard F Celeste *Chair*

Ambassador of the United States of America (Retired)

Donald Kennedy *Vice Chair*

Editor-in-Chief, *Science*; President (Emeritus) and Bing Professor of Biological Sciences, Stanford University

Archibald Cox *Chair Emeritus*

Carl M Loeb University Professor (Emeritus), Harvard Law School

HEALTH RESEARCH COMMITTEE

Mark J Utell *Chair*

Professor of Medicine and Environmental Medicine, University of Rochester

Melvyn C Branch

Professor and Associate Dean, College of Engineering and Applied Science, University of Colorado

Peter B Farmer

Professor and Section Head, Medical Research Council Toxicology Unit, University of Leicester

Helmuth Greim

Professor and Chairman of Toxicology, Technical University Munich and GSF–National Research Center for Environment and Health

Rogene Henderson

Senior Scientist and Deputy Director, National Environmental Respiratory Center, Lovelace Respiratory Research Institute

HEALTH REVIEW COMMITTEE

Daniel C Tosteson *Chair*

Professor of Cell Biology, Dean Emeritus, Harvard Medical School

Ross Anderson

Professor and Head, Department of Public Health Sciences, St George's Hospital Medical School, London University

John C Bailar III

Professor Emeritus, The University of Chicago

John R Hoidal

Professor of Medicine and Chief of Pulmonary/Critical Medicine, University of Utah

Thomas W Kensler

Professor, Division of Toxicological Sciences, Department of Environmental Sciences, Johns Hopkins University

Brian Leaderer

Professor, Department of Epidemiology and Public Health, Yale University School of Medicine

OFFICERS & STAFF

Daniel S Greenbaum *President*

Robert M O'Keefe *Vice President*

Jane Warren *Director of Science*

Howard E Garsh *Director of Finance and Administration*

Sally Edwards *Director of Publications*

Richard M Cooper *Corporate Secretary*

Aaron J Cohen *Principal Scientist*

Maria G Costantini *Senior Scientist*

Debra A Kaden *Senior Scientist*

Geoffrey H Sunshine *Senior Scientist*

Alice Huang

Senior Councilor for External Relations, California Institute of Technology

Purnell W Choppin

President Emeritus, Howard Hughes Medical Institute

Richard B Stewart

Professor, New York University School of Law

Robert M White

President (Emeritus), National Academy of Engineering, and Senior Fellow, University Corporation for Atmospheric Research

Stephen I Rennard

Larson Professor, Department of Internal Medicine, University of Nebraska Medical Center

Howard Rockette

Professor and Chair, Department of Biostatistics, Graduate School of Public Health, University of Pittsburgh

Jonathan M Samet

Professor and Chairman, Department of Epidemiology, School of Public Health, Johns Hopkins University

Frank E Speizer

Edward H Kass Professor of Medicine, Channing Laboratory, Harvard Medical School and Department of Medicine, Brigham and Women's Hospital

Clarice R Weinberg

Chief, Biostatistics Branch, Environmental Diseases and Medicine Program, National Institute of Environmental Health Services

Thomas A Louis

Senior Statistical Scientist, The Rand Corporation

Edo D Pellizzari

Vice President for Analytical and Chemical Sciences, Research Triangle Institute

Nancy Reid

Professor and Chair, Department of Statistics, University of Toronto

William N Rom

Professor of Medicine and Environmental Medicine and Chief of Pulmonary and Critical Care Medicine, New York University Medical Center

Sverre Vedal

Professor, University of Colorado School of Medicine; Senior Faculty, National Jewish Medical and Research Center

JoAnn Ten Brinke *Staff Scientist*

Annemoon MM van Erp *Staff Scientist*

Terésa Fasulo *Senior Administrative Assistant*

Gail A Hamblett *Office and Contracts Manager*

L Virgi Hepner *Senior Scientific Editor*

Jenny Lamont *Scientific Copy Editor*

Francine Marmenout *Senior Executive Assistant*

Teresina McGuire *Accounting Assistant*

Jacqueline C Rutledge *Controller*

Ruth E Shaw *Senior DTP Specialist*



HEALTH
EFFECTS
INSTITUTE

Charlestown Navy Yard
120 Second Avenue
Boston MA 02129-4533 USA
+1-617-886-9330
www.healtheffects.org

RESEARCH
REPORT

Number 105
December 2001

